KTH Information and
Communication Technology

Multihop Wireless Networks with Advanced Antenna Systems

An Alternative for Rural Communication

MARVIN SÁNCHEZ GARACHE

Doctoral Thesis in
Radio Communication Systems
Stockholm, Sweden 2008

TRITA–ICT–COS–0801
ISSN 1653-6347
ISRN KTH/COS/R--08/01--SE

KTH Communication Systems
SE-100 44 Stockholm
SWEDEN

Akademisk avhandling som med tillstånd av Kungl Tekniska Högskolan framlägges till offentlig granskning för avläggande av teknologie doktorsexamen i radiosystemteknik fredagen den 30 maj 2008 klockan 14.00 i sal N1, Electrum, Kungl Tekniska Högskolan, Isafjordsgatan 28, Kista.

Tryck: Universitetsservice US AB

Abstract

Providing access to telecommunication services in rural areas is of paramount importance for the development of any country. Since the cost is the main inhibiting factor, any technical solution for access in sparsely populated rural areas has to be reliable, efficient, and deployable at low-cost. This thesis studies the utilization of Multihop Wireless Networks (MWN) as an appealing alternative for rural communication. MWN are designed with a self-configuring capability and can adapt to the addition or removal of network radio units (nodes). This makes them simple to install, allowing unskilled users to set up the network quickly.

To increase the performance and cost-efficiency, this thesis focuses on the use of Advanced Antenna Systems (AAS) in rural access networks. AAS promise to increase the overall capacity in MWN, improving the link quality while suppressing or reducing the multiple access interference. To effectively exploit the capabilities of AAS, a proper design of Medium Access Control (MAC) protocols is needed. Hence, the results of system level studies into MAC protocols and AAS are presented in this thesis. Two different MAC protocols are examined: Spatial Time Division Multiple Access (STDMA) and Carrier Sense Multiple Access Collision Avoidance (CSMA/CA) with handshaking. The effects of utilizing advanced antennas on the end-to-end network throughput and packet delay are analyzed with routing, power control and adaptive transmission data rate control separately and in combination.

Many of the STDMA-related research questions addressed in this thesis are posed as nonlinear optimization problems that are solved by the technique called "column generation" to create the transmission schedule using AAS. However, as finding the optimal solution is computationally expensive, we also introduce low-complexity algorithms that, while simpler, yield reasonable results close to the optimal solution. Although STDMA has been found to be very efficient and fair, one potential drawback is that it may adapt slower than a distributed approach like CSMA/CA to network changes produced e.g. by traffic variations and time-variant channel conditions. In CSMA/CA, nodes make their own decisions based on partial network information and the handshaking procedure allows the use of AAS at the transmitter and the receiver. How to effectively use AAS in CSMA/CA with handshaking is addressed in this thesis. Different beam selection policies using switched beam antenna systems are investigated.

Finally, we demonstrate how the proposed techniques can be applied in a rural access scenario in Nicaragua. The result of a user-deployed MWN for Internet access shows that the supported aggregated end-to-end rate is higher than an Asymmetric Digital Subscriber Line (ADSL) connection.

Acknowledgements

I am grateful to the many people whose support was indispensable to this work. Foremost I would like to express my gratitude to my wife Ana Cristian and my daughters, Cristiancita and Fátima Lucia, whose support at home was extraordinarily helpful, and to my supervisor Prof. Jens Zander, for giving me the opportunity to join the COS group and whose wisdom, guidance and encouragement have helped me achieve the seemingly impossible. I would like also to express my never-ending appreciation to my co-advisor, Dr. Bo Hagerman from Ericsson; his enthusiasm, feedback and practical way of thinking has broadened my perspectives. I would like to express special thanks to Dr. Tim Giles who was my co-advisor for the Licentiate.

The financial support from the Swedish Agency for Research with Developing Countries (SAREC) and the National University of Engineering (UNI) is gratefully acknowledged.

Special thanks to Assistant Professor Slimane Ben Slimane for their valuable reviews and discussions. Also thanks to Dr. Robert Karlsson and Pietro Lungaro for providing important reviews of the contents of this thesis. Also I would like to thank to Prof. Mikael Johansson, Dr. Alexandre Proutiere, Dr. Magnus Linström, Oscar Somarriba, Bogdan Timus, Luca Stabellini, Saltanat Khamit, Johan Hultell, Dr. Kai-Erik Sunell, Dr. Anders Furuskär, Dr. Klass Johansson, Prof. Dongwoo Kim, Leonel Plazaola, Marvin Arias, and former PhD students at COS who have contributed to my work in several ways too long to be listed here. Special thanks to Dr. Eva Englund and Dr. Jan Nilsson, reviewers of my Licentiate and PhD proposal, correspondingly, and to the members of the Swedish Defense Research Agency for their valuable comments and discussions. The review and feedback from the opponent, Prof. Martha Steenstrup (Edmonton, AB, Canada), on the preliminary version of the thesis was also very valuable.

I am particularly indebted to Irina Radulescu, Ulla Eriksson and Lise-Lotte Wahlberg for their assistance with all practical issues regarding my work and Niklas Olsson for his help with everything regarding computer issues.

Last but not least, I want to express my gratitude to my mother and to my brothers and sisters, all of whom have been an example to follow.

Contents

Chapter 1

General Background

1.1 Introduction

The research and development of wireless technologies in general is driven by its potential success on attractive markets where users are wealthy enough to pay for the required handset, infrastructure and services. However, "over 40 % of the world's population lives in rural and remote areas of developing countries and have difficult or no access to even basic telecommunications service" [1]. Providing access to telecommunications services plays an important role stimulating economic and social development, which is of major concern to governments and telecom regulators and may constitute a very important market opportunity for equipment manufacturers and operators. However, any technological solution to be implemented has to face the fact that potential users are spread out over a wide area (meaning a low user density/km^2) and come from low income groups, which establish very important cost constraints.

The general objective of this thesis is to support understanding and provide guidance for the development of remote area communication systems. The understanding and guidance will be addressed from a technological point of view subject to low cost limitations. As a means to provide low cost services the technological solution should not rely on any existing infrastructure while targeting system reliability, efficiency, and easy and fast deployment.

Many possible candidate technologies exist that can be used to provide communication means in rural areas, for instance expanding the cellular network coverage. Economical methods to stimulate cellular coverage in rural areas is one possibility that some countries like Bolivia, Nicaragua and Peru have applied through the Universal Service Fund administered by governments [2]. Coverage extension for cellular infrastructure can be done, for instance utilizing lower frequency bands e.g. 450MHz. The use of wireless relays as a method to extend coverage in cellular systems is also considered to be potential low cost solution [3]. Relays do not have a wired connection to the backhaul. Instead they store the data received from a base

station and forward them to the user terminal and vice versa. The planning cost and hardware requirement are expected to be significantly reduced compared to systems deployed by using only base stations. The store and forward functionality of relays in cellular systems is an extension of another technological solution called Multihop Wireless Networks (MWN), the main subject of this thesis.

1.2 Multihop Wireless Networks Overview

Multihop Wireless Networks(MWN) have been studied in many different communication scenarios where simplicity, self-configuring, speed in setting up the network, i.e. quick deployment, as well as the ability to function without any wired infrastructure are of primary importance [4–14]. These characteristics make multihop wireless networks particularly attractive as a potential candidate to provide communication services in rural areas.

In this document the term multihop wireless network is used to indicate that the information is conveyed through the network using data packets that may be forwarded through a number of intermediate nodes (transceivers with router functionalities), between their source node and destination node. The network is self-configuring and setup without requiring planning and interaction of wireless expertise. Fig.1.1 illustrates a typical MWN scenario. For instance in this case, communication between node 3 and node 5 is enabled by using first node 2 and then node 4 as relaying nodes.

MWN were formerly known as multihop packet radio networks, having their origins in the early 1970s with the establishment of the ALOHA network in Hawaii. Driven by the technological advances in personal computing, there has been a surge of renewed interest in MWN within the last few years [4, pages 1-14] . There are several reasons for using MWN in practical communication applications:

1) *Radio Range extension*
   Mutihop allows the radio range of a terminal that may be limited by power/battery limitations and poor radio propagation conditions to be extended, since every

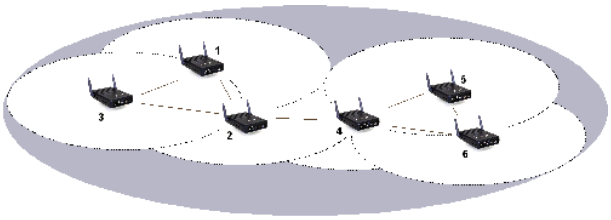

Figure 1.1: Example illustrating a multihop wireless network scenario. Here node 3 can communicate with node 5 using node 2 and then node 4 as relaying nodes.

node (or a subset of them) in the network may be utilized as router nodes to relay packets from a source node to a destination node.

2) *Simplify Installation*
Through a self routing mechanism, multi-hopping permits simplified installation requiring no site survey or costly planning or involvement of wireless experts.

3) *Resiliency and Self-healing*
The potential existence of redundant routes ensures resiliency and self-healing in case of offline nodes or broken links through self routing mechanism.

4) *Transmission Power Saving*
Multihop may reduces the total maximum transmission power (sum of transmission powers over multiple hops) required to transmit a packet between a source node and a destination node. Then, a multihop network, if used properly, may save battery power by handing off data from node to node rather than utilizing a higher-power RF signal.

The addition or removal of network nodes is a critical feature, for instance in military and emergency applications. In fact, one of the original motivations for MWNs comes from the military need for battlefield survivability [4, Chapter 2], i.e. to survive in the battlefield a wireless communication system is needed to coordinate distributed group actions without relying upon any centralized administration, which could be the first target for the enemy. Similar demands may exist for rescue operations whenever a natural disaster severely affects the fixed infrastructure.

In the civilian arena, there are many other potential applications of MWNs including Wireless Local Area Network (WLAN), home networking, personal area networking (PAN) [8] and Wireless Metropolitan Area Networks (WMAN). Another important application can be found in developing countries where long distances, difficult terrain and poverty limit the availability of land-based communication infrastructure. The deployment of multihop wireless rural-area networks could provide a cost-effective solution to their needs.

In spite of the advantage provided by MWNs there is, however, a capacity limitation. As the number of nodes increases in a MWN we can expect an increase in the external traffic but this also creates an increase in the internal traffic needed for store-and-forward of the information transmitted from each source node to the destination nodes. Gupta and Kumar in [15,16] have shown that when n identical nodes randomly located, each capable of transmitting at W bits per second and using an omnidirectional fixed radio range, form a wireless network, the throughput $\lambda(n)$ obtainable by each node for a randomly chosen destination is $O(W/\sqrt{(n \log n)}$ bits per second under a non-interference protocol. Therefore, as the number of nodes increases the gain provided by spatial reuse would not be enough to compensate the increase of the internal traffic for a given traffic demand.

Mulihop wireless networks are expected to increase their capacity by utilization of Advanced Antenna Systems (AAS) [17, 18]. In this document we use the term

advanced antenna systems to indicate utilization of several antenna elements (array) whose signals are processed adaptively by a combining network (similar definitions are used for Smart Antenna Systems in [19], Adaptive Arrays in [20], [21] and MIMO systems in [22]). In fact, the adaptation method utilized defines the type of AAS.

The use of AAS within multihop wirless networks are expected increase the hardware cost per node (compared with the use of a single omnidirectional antenna systems) to some extent but promises to significantly increase the capacity if they are appropriately used. This increase in capacity may allow, for instance, the addition of more nodes, making effective use of the scarce and generally expensive radio spectrum. This justifies the assumption that the additional hardware cost of AAS is considered to be low compared with the additional capacity gain that they may provide. In addition, recent development shows that AAS are expected to be built cost-effective in the near future [20, 23].

Consequently, AAS constitute a very interesting research area that introduces yet another dimension, the spatial dimension, to the traditional radio resource allocation in MWNs (e.g. power, frequency and time). • This raises the general research question addressed in this thesis: how can effective use be made of this additional dimension in multihop wireless networks? The effective use of advanced antenna systems is studied integrally linked to the radio resource management done in MWN through the Medium Access Control (MAC) protocol and subject to traffic demands.

1.3 Medium Access Control Protocols

The type of multihop wireless network considered in this thesis assumes utilization of half-duplex transmission on the same carrier frequency (common channel) for the whole network. Utilization of half-duplex transceivers can be found in many practical communication systems, for instance in Wireless LAN (IEEE 802.11b/g/a [24]), in Wireless Personal Area Networks (e.g. IEEE 802.15.4 Low-Rate WPAN) [5] and in TDD operation of IEEE 802.16 [25].

In order to share the common channel, a Medium Access Control (MAC) protocol has to be utilized. The MAC moderates access to the radio channel by defining a set of rules that allows nodes to communicate to each other in a relatively efficient manner. Under half-duplex operation, the MAC protocol must deal with the fact that a node can not transmit and receive at the same time and furthermore we assume that nodes cannot receive simultaneously from more than one of their neighbors (nodes within their radio range at a single hop) [26]. Simultaneous transmission over the same channel is commonly referred as packet *collision* [27]. Packets involved in a collision may survive provided that the Signal-to-Interference plus Noise Ratio (SINR) at the receiver site is high enough for error-free reception. This phenomenon referred to as *capture effect* was observed in the early seventies [7]. The capture effect allows simultaneous transmission and reception by node

pairs separated enough in space, creating the general concept of multihop wireless networks.

Wireless MAC protocols have been studied intensively since the 1970s and different ways exist to classify them including if they are *distributed* or *centralized* [28]. Our classification is presented in Fig.1.2 as *conflict-free* MAC protocols (Centralized, Scheduled) or *contention* MAC protocols (Random, Distributed) and is based on the definitions in the book "*Multiple Access Protocols*" written by Rom and Sidi [29].

In *contention* MAC protocols nodes compete for access to the channel. When only one node makes a transmission attempt the packet is received successfully. When multiple nodes transmit simultaneously a collision results and a contention resolution algorithm is used to try to resolve the conflict. This resolution process does consume resources but for bursty and relatively low traffic load the small loss of resources is usually worthwhile for the benefit of a distributed implementation [29, page 4].

Within the class of contention MAC protocols we can find the first MAC protocol proposed for packet radio networks, called ALOHA [7, 28]. ALOHA is a straightforward based contention MAC protocol where a node transmits randomly without verifying if the channel is idle or busy. Due to this completely uncoor-

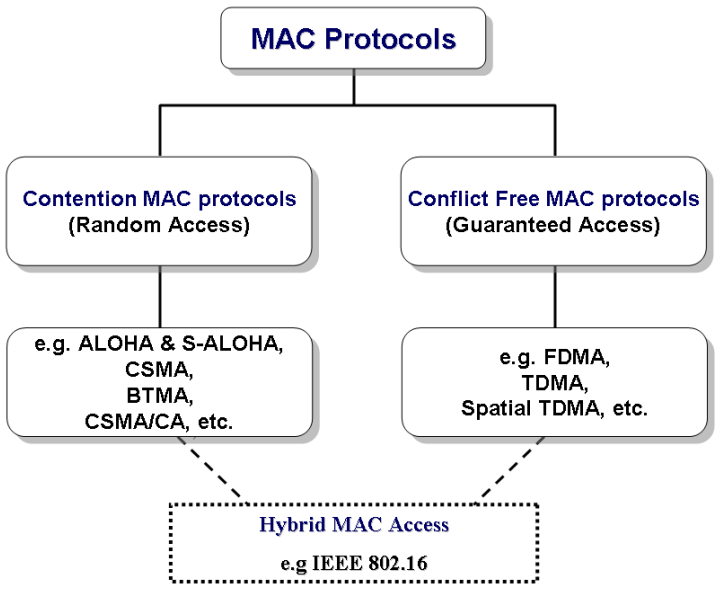

Figure 1.2: Multiple Access Protocols

dinated functionality packet collisions on the channel may occur frequently under moderate traffic loads resulting in relatively poor channel utilization. An improved version of ALOHA is called Slotted-ALOHA where the time space is divided into slots and nodes randomly decide whether to transmit or not during each slot. By this mechanism the vulnerability period of a packet to be successfully received is reduced to a single slot, doubling the capacity with respect to ALOHA [7]. An attempt to avoid collisions by listening to the channel to detect other users' transmissions is done with Carrier Sense Multiple Access (CSMA) [30]. By this way a local estimation of the multiple access interference is done, resulting in increased channel utilization compared to Slotted ALOHA, provided that all nodes are able to detect other nodes transmissions. However, the performance of CSMA starts to degrade in MWN due to the *hidden* terminal problem, i.e. the lack of a node to be able to hear all other nodes in the network. A possible solution for this problem was presented by Kleinrock and Tobagi in [31] where the receiving node broadcasts (on a different channel) a tone to indicate to its neighbors that the channel is busy, thus potentially improving the performance with respect to CSMA in MWNs; this MAC protocol was denominated the Busy Tone Multiple Access (BTMA). In order to provide a solution to the hidden terminal problem without the need of a separate channel, Carrier Sense Multiple Access Collision Avoidance (CSMA/CA) with handshaking has been proposed [32]. In CSMA/CA with handshaking the data transmission is preceded by transmitting a short Request-To-Send (RTS) packet to the intended receiver which in turn answers with a short Clear-To-Send (CTS) packet if the channel is idle at the receiver site. This procedure reduces the probability of collision but does not eliminate them. In addition, the handshaking mechanism creates what is called the *exposed* terminal, i.e. nodes that restrain themselves from transmitting although they don't produce harmful interference. Several variants of CSMA/CA with handshaking can be found in the literature, for instance MACA [32], FAMA [10, 11], MACAW [12, 33] and last but no least, the Distributed Coordination Function (DFC) with optional use of Request-to-Send (RTS) and Clear-to-Send (CTS) frames as part of the IEEE 802.11 standards [9].[1]

On the other hand, *conflict-free* MAC protocols are those ensuring that a transmission, whenever made, is a successful one, i.e. not impaired by another transmission. Conflict-free transmissions can be achieved by allocating the channel to the user either statically or dynamically[2]. The channel resources can be viewed, for this purpose, from a time, frequency, or mixed time-frequency standpoint.

[1]The architecture of the MAC sublayer in IEEE802.11 also includes the (optional) Point Coordination Function (PCF) and the hybrid coordination function (HCF) access methods (single hop network configurations). In PCF transmission rights are given to stations by a polling master. HCF uses both a contention-based channel access, for contention-based transfer, and a controlled channel access, for conflict-free transfer. [24, pag.251-278]

[2]Usually, the request for dynamic allocation of the channel requirers utilization of a separated channel. For instance, the frame structure of the OFDM PHY operating in Time Division Duplex(TDD) of the IEEE 802.16 standards consists of a Downlink subframe followed by an Uplink subframe. The uplink subframe starts with contention intervals scheduled for request purposes following a Slotted-ALOHA principle [25]. We refer to this as a hybrid MAC access.

Examples of conflict-free MAC protocols are:

- *Time Division Multiple Access* (TDMA)
  Interference is controlled by separating transmission in time. The time axis is divided into time intervals of equal length called *slots* or *timeslots* and each node receives its own timeslot.
- *Frequency Division Multiple Access* (FDMA)
  The radio spectrum is divided into orthogonal channels. Each node is assigned a unique frequency channel to transmit.
- *Code Division Multiple Access* (CDMA)
  Reduction of interference is performed by the use of a unique spreading code assigned to a node for transmission.

TDMA can be utilized in multihop wireless networks by assigning to each node a conflict-free transmission on the common channel for a fraction of time. During that fraction of time (timeslot) a node can transmit to any of its neighboring nodes, ensuring the packet will be received since it will not be interfered by other node transmissions.

However, TDMA does not take advantage of the spatial separation that may exist between nodes in a sufficiently large network or when utilizing AAS. In order to take advantage of the spatial separation that may exist between nodes in large networks and increase efficiency by spatial reuse of timeslots in TDMA, Spatial Time Division Multiple Access (STDMA) has been proposed in [34].

STDMA is a MAC protocol where conflicts are avoided by assigning node (or link) transmissions into a repetitive pattern of slots of finite length called a *schedule*. This characteristic makes STDMA worthy of selection for further investigation in this thesis to better exploit the spatial dimension provided by advanced antenna systems.

Similarly, within contention MAC protocols, CSMA/CA with handshaking provides an interesting mechanism to be integrated with the use of AAS that is further investigated in this thesis.

1.4 Research Overview and Related Work

In this section we review the work dealing with utilization of directional antennas and MAC protocols for MWN.

Within the area of contention MAC protocols, there have been several papers related to utilization of AAS in MWN. One of the earliest works showing that significant performance gain can be achieved by utilizing directional antennas in Slotted-ALOHA multihop packet radio networks was presented by Zander in [35]. Yum and Hung in [36] introduced a protocol to be used with sector antennas based on utilization of busy tones for transmission coordination called Simple Tone Sense (STS), and Variable Power Tone Sense (VPTS). Better improvement, in terms of

throughput-delay, was achieved with VPTS compared to Busy Tone Multiple Access (BTMA) using omnidirectional antennas. The performance gain with VPTS was larger for densely located nodes with better connectivity (from 40 nodes with 5.45 average number of neighbors to 80 nodes with 8.38).

Utilization of Multiple Beam Adaptive Array (MBAA) in single hop packet radio systems with a central base station to achieve multiple packet captures in Slotted-ALOHA was proposed by Ward and Compton in [37]. The adaptation method used maximizes the Signal to Interference plus Noise Ratio (SINR). Two important factors were identified limiting the performance of an adaptive array: the number of degrees of freedom and the angular resolution. The angular resolution is very important since if the desired packet and an interfering packet are angularly too close, the array cannot be adapted to simultaneously null the interference and form a pattern maximum to the desire packet. The angular resolution is much less than the beamwidth between the first nulls because of the array gain. To be able to perform the beam adaptation, omnidirectional reception was used at the beginning of each slot. Three periods of a Pseudo Noise (PN) sequence were used as preamble at the beginning of each packet and an uncertainty interval (less than the period of the PN sequence to have all the interfering packet at least during the second period of a preamble) is added to the slot size to randomize the starting of packet transmissions. Their results show that even with modest MBAA capabilities significant improvement can be achieved in both packet delay and throughput (with a single beamformer the throughput achieved is similar to CSMA without hidden terminal problem).

Utilization of MBAA in multihop wireless networks has been thoroughly investigated by Bao and Garcia-Luna-Aceves in [38] by introducing a distributed (hybrid) MAC protocol called ROMA. In ROMA the time domain is divided into slots and T_{sched} timeslots are used for scheduled access, followed by T_{nbr} timeslots used for random access in order to exchange two hops neighborhood information using omnidirectional antennas. The performance of ROMA was compared to a centralized minimum frame length schedule called UxDMA (found by applying graph coloring). It was shown that significant improvements on network throughput can be achieved by using MBAA for multiple simultaneous communication sessions. However the study didn't consider the aggregated interference caused by transmission of nodes that are more than two hops away.

A significant number of papers have addressed the integration of AAS with some variations of the Distributed Coordination Function (DFC) with the Request-to-Send (RTS) and Clear-to-Send (CTS) frames of the IEEE 802.11 standard. In [39] Ko, Shankarkumar, and N. Vaidya introduced a MAC protocol using directional antennas showing that the capacity increases for a network using Global Positioning System (GPS) to activate the appropriate antenna sector. Nasipuri, You and Hiromoto in [40] used RTS/CTS exchanges to determine which of the sectors should be used. In [41] equipped nodes using Electronically Steerable Passive Array Radiator (ESPAR) antennas keep the locations of others in what is called an Angle-SINR Table and directional routing was proposed. Reference [42] studied directional an-

tennas and co-channel interference generated by antenna sidelobes. Both adaptive beamforming and switched-beam were considered together with directional neighbor discovery and power control, showing an extended range advantage provided by AAS. Another related work is the one in [43] which the author proposed a distributed link scheduling and compare its performance to a redesigned CSMA/CA MAC protocol for directional antennas. Recently, R. Ramanathan, J. Redi, C. Santivanez, D. Wiggins, S. Polit, in [44] presented a real-life prototype called Utilizing Directional Antennas for Ad hoc Networking (UDAAN) that utilize a mechanism for adaptive control of steered or switched-beam antenna systems utilizing a MAC protocol called D-MAC. Their results show that AAS (switched-beam and beamforming) can produce a very significant improvement in throughput over omnidirectional communications.

On the other hand, transmission scheduling has been suggested since the beginning of the 80s. Robertazzi and Sarachik in [26] described the concepts, benefits and general problem of self-organizing communication networks. A hierarchical network structure using time synchronous transmissions was proposed. Utilization of slotted TDMA frame allowing individual stations to be paired with individual slots was described. A self-organization procedure to determine the neighbor local connectivity was exemplified. By monitoring the wireless channel, nodes over a large geographical area could select locally unused slots. Review of proposed methods using ordinary stations (nodes), gateways and cluster head was also done. Addressing only the selection of a minimum number of cluster heads was described as a computationally untractable problem as the network size increases. However that does not prevent the use of sub-optimal techniques, which provide reasonable results. A distributed Link Activation Algorithm (LAA) was described. The limitation of LAA is that it does not take into account either the aggregated power of nearby transmissions (interference) or the differences in link traffic. Utilization of a centralized heuristic scheduling algorithm called Distributed Evolutionary Algorithm (DEA) was suggested as a way to include interference and differences in link traffic. However, the algorithm concentrates on distributing the topology and traffic information throughout the network (not really addressing the interference problem). Scheduling and routing were identified as two interrelated problems needing further research.

The term Spatial TDMA was first introduced and analyzed by Nelson and Kleinrock in [34] as an alternative to the use of fixed wire lines. Nodes were assumed to be fixed with known locations. The allocation of timeslots (scheduling transmission) was addressed by considering each link traffic (from one node to its neighbors) as different classes of traffic and assigning link transmissions to timeslots in a TDMA frame. A method to approximate the end-to-end packet delay was also presented. The concept of compatibility matrix for link assignments was introduced and the link capacity assignment was formulated. The analysis didn't consider the interference, which is an additional problem in a single carrier frequency channel. The time allocation and traffic flow constraints were used to minimize the end-to-end delay formulated as a convex optimization problem (using time allocation as a con-

tinuous approximation). By demonstrating that the flexibility region was convex, the time allocation vector for all links was then formulated as a linear programming problem assuming that a set of compatible links (called cliques) was given covering all links in the network at least once (the clique maximization was excluded). It was highlighted that the "optima" capacity assignment (in the sense of minimizing the delay) is very difficult to find due to the dependency of the time allocation and the ordering of the slots assigned to the set of compatible links. The order of the slot allocation, size, and number of periods from the frame allocated to internal arrival and service periods was observed to have a great influence on the mean system delay. It was suggested to do the slot allocations uniformly distributed over the duration of a frame to reduce the waiting time.

Shor and Robertazzi in [45] introduced scheduling algorithms to assign node transmissions on a centralized base. The centralized scheduling algorithm considered the relative traffic load passing through a node assigning a number of slots proportional to the node's traffic. To our knowledge, the Shor and Robertazzi algorithm is the first one that tried to integrate the routing and scheduling through the relative traffic load information by using the Most Forward Routing (MFR) and uniform unicast traffic (from a source node to a destination node). MFR was used to determine the relative traffic load through a node. However, in their analysis the interference from other node transmissions was assumed to be negligible. A distributed algorithm was also proposed. The algorithm is a modification of a previously suggested algorithm by Ephremides and Truong in [46] referred to as the Degree Algorithm. Nodes assignment priorities were based on the number of incoming links. The number of incoming links was shown to be a relative measure of the traffic that can pass through a node, therefore improving the performance with respect to the Ephremides and Truong algorithm in terms of the number of allocation slots needed. However, the single network used for a case study was fairly well connected.

Most of these early contributions on the field of Spatial TDMA neglect the interference from other node transmissions by describing the network as a binary graph; i.e. two nodes are either connected holding a reliable communication or disconnected with infinite path loss (producing no interference) [27, 34, 45, 47–49]. Relaxation of this assumption has been investigated in [50–58] utilizing omnidirectional antennas and realistic terrains to create the scheduling based on the received Signal-to-Interference plus Noise Ratio (SINR). In [57] both node assignment and link assignment scheduling methods were investigated showing that for unicast traffic, link assignment result in higher achievable end-to-end throughput but node assignment results in lower end-to-end Delay.

Lal, Joshi, and Agrawal in [59] investigate the used of switched-beam antennas modeling the network as a binary graph to create link scheduling (edge) and multiple transmitters (one per beam) and multiple receptions were assumed. No routing was considered only one hop traffic demands were addressed.

Utilization of AAS by beamforming antennas and beamforming with null steering in STDMA with fixed data rate has been investigated by Dyberg, Farman et

al. in [60] by utilizing the Minimum Hop Algorithm (MHA) as routing method and the proposed Traffic Controlled Scheduling Algorithm (TCSA) by Grönkvist in [51]. Performance evaluations with network size of 20 nodes and circular antennas array of 6 and 8 elements were presented. The results show that both beamforming and beamforming with null steering produce a very significant lower end-to-end packet delay and throughput with respect to the use of single omnidirectional antennas. The best capacity gain was obtained by utilizing beamforming at the transmitter and beamforming with null steering at the receiver compared to utilizing beamforming at both the transmitter and the receiver. The study indicates that the benefit of AAS with respect to the use of omnidirectional antennas is higher in flat terrain that in rough terrain because of the reduction of the connectivity and interference.

Constant transmission power and constant bit rate have been generally assumed in all the mentioned previous works, i.e. node transmissions where scheduled using a constant maximum power and a fixed data rate. Therefore, only time and space allocation of the channel were exploited. Better spatial reuse can be achieved if power control is used together with the scheduling algorithm. Somarriba and Giles in [53] introduced a heuristic algorithm called Power-Sensitive TC Scheduling (PSTCS) using minimum hop routing with SINR balancing power control to achieve a given SIR target at a fixed data rate, constrained by the maximum transmission power and using omnidirectional antennas. A removal procedure based on the set of feasible power allocation vectors and link traffic priorities was used to create the link schedule in STDMA.

However, it is known that the optimal solution to *interference-based* scheduling is computational hard to solve even for fixed rate systems [48]. Exhaustive search has been one method utilized for performance evaluations in many studies [56, 61]. Elbatt and Ephremides in [56] analyzed the issue of joint scheduling and power allocation in single hop request ad hoc networks using a single carrier frequency by adopting an approach similar to cellular systems and omnidirectional antennas. Even in this reduced single hop scenario, where routing was not considered, finding an optimal scheduling for power allocation was a hard computational problem motivating utilization of heuristic methods.

Utilization of variable data rates has been included in standards, for instance in IEEE 802.11 [24]. However, the literature on variable power and transmission data rate in multihop wireless networks is limited. Farman, Stern and Tronar have addressed the impact of variable data rate in multihop wireless networks with TDMA and generalized TDMA as MAC protocol utilizing omnidirectional antennas in [62]. In generalized TDMA, a node's transmission rights are given in a number of slots proportional to its traffic needs. The impact of route selections on the throughput-delay performance was also analyzed by using the minimum cost routing (solved by e.g. Dijkstra algorithm [63]). Two different cost metrics were used: I) setting the cost of all links equal to one, resulting in the minimum hop routing and II) setting the cost to inverse of the data rate on the link, referred as $1/R$ routing. The results show that $1/R$ routing makes better use of the variable data

rate capability in multihop wireless networks compared to minimum hop routing. This work can be seen as a joint routing and TDMA scheduling approach done by transferring information between separated layers.

Joint routing and scheduling has received some attention recently in [49, 54, 58] [64]. These studies have included the power allocation within the schedule to either get higher spatial reuse, higher data rates or both simultaneously, utilizing omnidirectional antennas. Nonlinear optimization using the technic called "column generation" [65] applied to the interferenced-based scheduling problem has been proposed recently [55, 58]. Johansson and Xiao have formulated the problem of joint routing, scheduling and power allocation in STDMA using that technic in [58]. Their proposed method is to find a numerical "optimum" solution in terms of throughput and fairness. In their studies constant transmission power, SINR balance and variable data rates were addressed with omnidirectional antennas. However, their proposed optimization method has a computational bottleneck that limits the network size that can be addressed by this approach, but it can be used as a good benchmark for heuristics approaches.

1.5 Thesis Contributions

In this thesis we present how to analyze and design multihop wireless networks for rural areas when utilizing advanced antenna systems with spatial time division multiple access and also with CSMA/CA with handshaking. The utilization of AAS is here studied integrally linked to the MAC protocol, the transmission power adjustment, and the modulation and coding scheme that allows utilization of fixed or variable transmission data rates. In the realm of conflict-free MAC protocols the main focus is on the utilization of AAS in STDMA. We also include Generalized TDMA in order to evaluate the order of magnitude in performance gain that STDMA provides. The main contributions are summarized as follows:

I. Scheduling algorithm design and performance evaluation methodology. This has been done through this monograph by:

   - Derived methods for finding numerical bounds for STDMA with AAS based on the nonlinear optimization method proposed in [58].
   - We propose a methodology for evaluating the performance of heuristic algorithms that are designed to do max-min fair allocation to users.
   - Through case studies of test networks, we have evaluated the "optimum" performance gain that can be achieved utilizing different physical layer capabilities of the nodes that comprise the network.
   - We introduce novel heuristic algorithms for STDMA with power control and/or with rate control. Their performances are evaluated against the numerical bound found by the nonlinear optimization method.

II. Investigation and evaluation of possible performance gain from using advanced antenna systems in spatial time division multiple Access. This has been done by:

- Evaluation of the performance gain of STDMA with respect to the utilization of generalized TDMA
- Performance evaluation for different physical layer capabilities of the nodes that comprised the network including power control as well as rate control

III. Joint routing & scheduling analysis and design for the utilization of AAS in STDMA systems:

- We analyze the impact of routing and scheduling showing that, depending on the network topology, there may be a significant improvement in performance by combined routing and scheduling. As a proposal for a better network design we introduce a combined routing and scheduling procedure that improves the performance of STDMA.

IV. Throughput-delay performance estimations. When evaluating wireless networks by different algorithms, packet level simulations require a significant amount of time. Therefore, having an accurate model for estimating the throughput-delay performance is very important for allowing reduced simulation requirements. By stochastic simulations we have found that a reasonable estimation can be obtained by applying Kleinrock's independence approximation assumption commonly used for modeling fixed-point-to-point packet switching networks.

V. Investigation and evaluation of possible performance gain from using low complexity switched-beam antenna systems as AAS technology with CSMA/CA with handshaking. Four different beam selection policies were evaluated.

VI. Finally, we demonstrate how the proposed techniques can be applied in a rural access scenario in Nicaragua

Most of these contributions have been published in the following list of publications:

P1. M. Sánchez, J. Zander, B. Hagerman, "On the Performance of Power and Rate Control in STDMA Multihop Networks with Advanced Antennas," in *Proc. International Conference on Networking (ICN2008)*, Cancun, Mexico, April 2008 [66].

P2. M. Sánchez, J. Zander, B. Hagerman, "A Reuse-Greedy Algorithm for STDMA Multihop Networks With Advanced Antennas & Rate Control," in *Proc. International Symposium on Wireless Pervasive Computing 2008 (ISWPC2008)*, Santorini, Greece, May 2008 [67].

P3. M. Sánchez, J. Zander, B. Hagerman, "Radio Resource Allocation in Spatial TDMA Multihop Networks with Advanced Antennas," in *Proc. of IEEE Conference on Wireless Rural and Emergency Communications (WRECOM2007)*, Rome, Italy. October 2007 [68].

P4. M. Sánchez, M. Munguía, "On the Integration of Adaptive Antenna Systems in Multihop Ad hoc Networks Utilizing Generalized TDMA as MAC protocol," in *Proc. XX Congreso COPIMERA 2005*, Havana, Cuba, October 2005 [69].(Originally written in spanish)

P5. B. Shrader, M. Sánchez, T. Giles, "Throughput-delay Analysis of Conflict-free Scheduling in Multihop Ad-hoc Networks," in *Proc. Swedish workshop on Wireless Ad hoc Networks 2003*, Stockholm, Sweden, May 2003 [70].

P6. M. Sánchez, J. Zander, T. Giles, "Combined Routing and Scheduling for Spatial TDMA in Multihop Ad hoc Network," in *Proc. Of the 5th International Symposium on Wireless Personal Multimedia Communications (WPMC 2002)*, Honolulu, USA, October 2002 [71].

P7. M. Sánchez, "Multiple Access Protocols with Smart Antennas in Multihop Ad Hoc Rural-Area Networks," Technical Licentiate Thesis in Radio Communication Systems. Royal Institute of Technology, Stockholm, Sweden, June 2002 [72].

P8. M. Sánchez, T. Giles, J. Zander, "CSMA/CA with Beam Forming Antennas in Multihop Packet Radio Network," in *Proc. Swedish workshop on Wireless Ad hoc Networks 2001*, Stockholm, Sweden, March 2001 [73].

P9. M. Sánchez, O. Somarriba, J. Zander, "User-deployed and Capacity Evaluation of Multihop Wireless Networks: A Case Study for Nicaragua," in *Proc. Swedish workshop on Wireless Ad hoc Networks 2008*, Stockholm, Sweden, May 2008 [74].

There are some other works done during my research studies related to the previous listed publications. Among those the most relevant to be mention here are:

P10. M. Sánchez, J. Zander, T. Giles, "Combined Routing and Scheduling for Spatial TDMA in Multihop Ad hoc Network," in *Proc. Swedish workshop on Wireless Ad hoc Networks 2002*, Stockholm, Sweden, March 2002 [72].

P11. M. Sánchez, J. Zander, "Adaptive Antennas in Spatial TDMA Multihop Packet Radio Network," in *Proc. Radio Scientific Conference , RVK99*, Karlskrona, Sweden, June 1999 [75].

The original ideas for publications [P1-P10] were developed by the author of this work under the main advising and valuable feedback of Prof. Jens Zander [P1-P3,

P6, P8-P10], Dr. Bo Hagerman [P1-P3] and Dr. Tim Giles [P5, P6, P8, P9].

The second author of paper [P4] was responsible for conducting the numerical evaluations with the simulation tools and analysis developed by the first author.

The first author in paper [P5] wrote the scheduling algorithm utilized and was the responsible editor of the paper. The second author built the discrete event simulator (stochastic), the underlying models and network topologies to be utilized. Both authors worked together to do the numerical evaluations.

The original idea for paper [P11] was developed by Prof. Jens Zander while the modeling, simulation and performance evaluation was done by the first author.

Finally, the content on chapter 2 and [P9] has been done in collaboration with Oscar Somarriba at the Dept Communication System. We worked together under the assessment and valuable contributions of Prof. Jens Zanders.

1.6 Thesis Outline

This thesis is written as a monograph composed of eleven chapters and appendixes. In chapter 2 we discuss the main issues related to the problem of providing rural communications using as case study the telecommunication development process followed by Nicaragua. In chapter 3 the system model, assumptions, and performance evaluations utilized in the thesis are described. In chapter 4 we investigate the integration of AAS in MWN utilizing generalized TDMA and compare the potential gain that STDMA may provide in terms of throughput and packet delay (these findings were published in [69]). In chapter 5 we present a general overview of STDMA for fixed rate systems, analyze the benefit of combining routing and scheduling, and introduce an approach called RA-MHA for exploiting this potential benefit (this chapter is based on publication [72]). In chapter 6 we present the nonlinear optimization method applied to fixed rate STDMA systems with AAS and introduce a methodology to analyze the performance of heuristic schemes using constant transmission power as well as power control (these results have been published in [68]). In chapter 7 we extend the utilization of nonlinear optimization to variable rate systems to analyze the performance of STDMA with AAS (published in [66]). In chapter 8 we introduce a novel scheduling algorithm for AAS and variable rate systems called Greedy-RS (the results have been published in [67]). Utilization of AAS for contention based MAC protol is addressed in chapter 9. In that chapter we investigate the utilization of low complexity switched-beam antenna systems as AAS technology with CSMA/CA with handshaking. Next, in chapter 10 an example of deployment analysis applied to rural communities in Nicaragua is presented. Finally, the conclusions of the thesis are presented in chapter 11.

Chapter 2

Rural Area Communications: The case of Nicaragua

In this chapter we discuss the main issues that, from the authors' point of view, are related to the problem of providing rural communications in a particular developing country, Nicaragua. We explore the roll-out process of telecommunication infrastructure by studying the development of voice and data services over the last twenty years. Together with the historical evolution we analyze the positive impact that *regulatory policies* have had in fostering this development. In this discussion we also present some related issues that seems to be correlated with the introduction and usage of new technologies, provide small business opportunities, and have had an important impact on the Nicaraguan society to reducin the *digital divide*.

We also present some of the applied methods (and technologies) carried out by he Nicaraguan regulatory body to provide communication means to communities in rural and low income areas. Then we present our view of the roll-out process of telecommunication infrastructure and its relation to the selection of potential technologies. In this context, self-organizing technologies like multihop wireless networks are very appealing technologies to provide rural area communication means. We think that this type of technologies could also influence important changes to the current mechanisms used regarding the financial support for services in rural areas done through Nicaragua *fund for investment in telecommunications*. We believe that by taking advantage of self-organizing technologies, the communities themselves or even new potential local players can take an active part in the solution to their own needs by deploying multihop wireless networks.

2.1 Introduction

Nicaragua is a country located midway across Central America. With its 130,373.40 square kilometers [76], it is the largest in area but one of the most sparsely populated nations of the region. Roughly triangular in shape with approximately 500

kilometers to a side, it is bordered by Honduras to the north and Costa Rica to the south. The Pacific Ocean lies to the west of the country, while the Caribbean Sea lies to the east [76] (Fig. 2.1).

Nicaragua experienced high economic growth during the 1960s and 1970s largely as a result of industrialization, and became one of Central America's most developed nations [77]. However within the last four decades the country has been subjected to numerous events that have severely affected its development. One of the most devastating natural events occurred in December 1972 when an earthquake destroyed much of its capital, Managua. It destroyed much of Nicaragua's industrial infrastructure, most government offices, the financial district of Managua, and thousands of small shops engaged in manufacturing and commercial activities [77]. Legacies of the earthquake were government budget deficits, inflation, and the highest level of foreign indebtedness in Central America.

The above event was followed by an insurrection intensified in 1978 and finishing in July 1979, toppling more than forty years of a dictatorship. However, from 1981 to 1990 Nicaragua was subjected to a continuous war and an imposed trade embargo starting in 1985, which lasted 5 years. These damaged most of its industries, undermined the communications infrastructure and seriously affected the country's economy.

Nevertheless, since the end of the war in 1990 Nicaraguans have been, step by step, rebuilding the country and a lot of progress has been achieved regarding its economical growth as compared to the status in 1990.

In particular, in the telecommunication sector important policy reforms were done during the 1990s. The reforms have fostered private sector investment in telecommunication services and infrastructure. This has been translated into benefit to Nicaraguan citizens who now, at least in urban areas of the country, have access to several telecommunication services with good quality and at affordable prices.

Although we have observed tremendous growth in the telecommunication infrastructure and services (voice and data) that includes the Public Switching Telephone Network (PSTN), mobile telephony, cable TV and Fixed Wireless Access (FWA) networks, it seems to be economically difficult to extend these benefits can be extended to rural areas without the financial support of the government. So far, the rural areas far from the main cities have been unattractive to private investors due to low population density, long distance, and difficult terrain together with low or seasonable incomes. This problem has been a challenge to a Nicaraguan government, whose ultimate goal is to eliminate the digital divide.

In a country with so many needs one may think that investment in telecommunications might have a low priority level. However, the Nicaraguan government recognizes that the development of and access to telecommunication means is a key enabler [78] in promoting job creation, knowledge-based growth, business innovation, access to valuable information, and improve education and health-care assistance.

Figure 2.1: Map of Nicaragua

2.2 Reforms and Regulatory Regime

Today, the main players in the telecommunication market of Nicaragua are the private sectors. However, the government has played a vital role in the process of this development. As in many other countries, Nicaragua has followed the stages in the liberalization process illustrated in Fig.2.2.

The reform process started in 1995 separating the state telecom monopoly from the regulation of the sector. This was done first creating the Nicaraguan Institute of Telecommunications and Postal Services (TELCOR). TELCOR is an independent regulatory body created by the General Law of Telecommunication and Postal Services (Ley No.200) published in December 1995 [1]. Next the privatization of the state telecom monopoly approved by law (Ley No.210) creating the still state-

[1]TELCOR is responsible for telecommunications, radiocommunications, broadcast transmission and postal regulation. However it is not responsible for content regulation.

owned operator ENITEL S.A. in 1996. Law No.210 also established the set of rules to conduct the beauty contest in order to sell 40% of ENITEL's stock. The actual privatization of the 40% of ENITEL was effective by the end of 2001. Later, in December 2003, the remaining state-owned shares were sold, completing the privatization process.

Besides creating TELCOR, the Law of Telecommunication and its regulatory law, presidential decree 19-96 and its reforms, establish the licensing regimes, the general rules to introduce and guarantee fair competition in the telecom market, rules to guarantee interconnection arrangements, tariff, spectrum management, numbering and user rights complementary to the general law for consumer's protection (Ley No.182).

Privatization of the state monopoly by itself does not guarantee the introduction of competition and it is known that in fact there is a high risk that may create a "private monopoly" vertically integrated in related services. Such high market dominance can delay interconnection and can use cross-subsidy to gain competitive advantages. These aspects are prevented by the law and the regulator has the

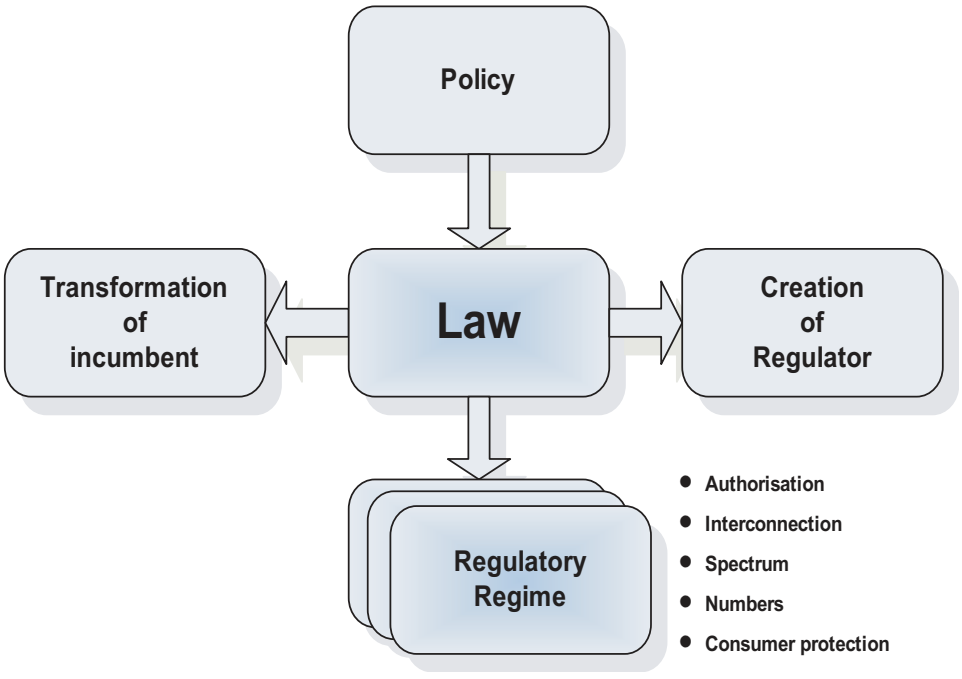

Figure 2.2: Common stages of the liberalization process.
(Source: Telecommunications Regulatory Master Class 2006.)

empowerment to intervene when needed. In addition, to protect the free markets a relatively new law, similar to an antitrust law, has been introduced in 2006.

Transparency of the regulatory acts and decisions are also part of the regulatory regime now in place. The regulatory acts and decisions once known by the administered (users and operators) can be appealed to the president and after that to the Supreme Court. Rules, acts and decisions taken by the regulator are also published in its web site www.telcor.gob.ni.

The above described legal framework with a transparent regulatory pro-competitive regime seems to be a success attracting foreign and local investors in the telecommunication market. This success is highly visible, in particular looking at the evolution of the PSTN and the mobile telephony market as shown in the following section.

2.3 The Evolution of Fixed and Mobile Telecommunication Infrastructure in Nicaragua

During the 80's the PSTN and private radio communications were the prevailing utilized two-way communication means. As shown in table 2.1, during that period the teledensity[2] of the fixed telephony was rather low. However, it is worth recognizing that even under a war and a trade embargo, Nicaragua managed to sustain and even have an small improvement in the PSTN capacity. As shown in the table, the number of subscribers increased from 32,844 in 1983 to 46,169 by the end of 1989 (24% teledensity improvement).

By the end of the war in 1990, Nicaragua had a population of 3.6 million and the teledensity was only 1.26. With such a low rate it is not difficult to realize that the lack of telecommunication services was very strong even in the capital, Managua. Even in the main cities, Nicaraguan citizens had to register in a waiting list for years to maybe get a fixed line. Then the lack of service was not only in areas considered to be rural but also in urban and suburban areas.

Together with the need to increase the available capacity there was the need to upgrade the already obsolete analog technology and it was in 1990 that the migration to an Integrated Digital Network was started. By the time of the creation of the telecommunication law and the law to sell the state-own incumbent, ENITEL, the teledensity had increased up to 2.22 (almost double with respect to the one by the end of the war in 1990); and by the time that was actually sold in 2001, the teledensity was already 3.09. From table 2.1 and Fig.2.3 we can observe that even after the privatization of ENITEL, the growth rate of the PSTN has been almost linear. Until now, the high expectations of improvement that private investment could have in fostering the services on the PSTN has not been fulfilled yet. Several reasons may influence this. However we think that the strongest reason is that there is still a "private monopoly" in the fixed telephone market even though the temporary exclusive period established by law expired at the beginning of 2005.

[2]Teledensity is defined as the the number of telephone lines per one hundred inhabitants

Table 2.1: Evolution of Fixed and Cellular services (Period 1983 to June 2006)

YEAR	INHABITANTS	Suscriptions PSTN	Suscriptions Cellular	Teledensity	
				PSTN	Cellular
1983	3,212,000	32,844	0	1.02	
1984	3,309,000	33,905	0	1.02	
1985	3,400,000	43,364	0	1.28	
1986	3,485,000	44,118	0	1.27	
1987	3,565,000	45,921	0	1.29	
1988	3,644,000	45,483	0	1.25	
1989	3,729,000	46,169	0	1.24	
1990	3,676,000	46,328	0	1.26	
1991	3,816,000	48,305	0	1.27	
1992	3,962,000	54,280	0	1.37	
1993	4,114,000	66,810	324	1.62	0.01
1994	4,275,000	85,254	2,284	1.99	0.05
1995	4,357,099	96,611	3,660	2.22	0.08
1996	4,519,240	111,397	5,100	2.46	0.11
1997	4,660,663	122,817	7,911	2.64	0.17
1998	4,806,727	141,233	18,710	2.94	0.39
1999	4,957,596	150,258	45,023	3.03	0.91
2000	4,956,964	162,484	102,860	3.28	2.08
2001	5,058,644	156,457	164,509	3.09	3.25
2002	5,162,275	171,632	237,248	3.32	4.60
2003	5,267,715	205,004	466,706	3.89	8.86
2004	5,374,820	214,480	738,624	3.99	13.74
2005	5,483,447	226,634	1,119,379	4.13	20.41
Jun-06	5,483,447	232,299	1,446,467	4.24	26.38

The introduction and protection of competition has shown to be a key factor in the Nicaraguan telecom market. On the contrary, the "legal private monopolies" appears to be a delaying factor in translating the benefit of better service offers to the citizens. We cannot conclude the above from our observations on the fixed telephony since in practice the market is still not open to competition. However, we have observed the effect of introducing competition on the growth of the cellular market illustrated in Fig.2.3.

In Nicaragua, the first cellular system was introduced in 1992 when TELCOR (the state-owned operator at that time), through a competitive process [79], gave a ten-year term license to the private operator "Telefonía Celular de Nicaragua, S.A. (TCN)" [80]. Later, in 1997, TCN was acquired by BellSouth and since 2004 belongs to Telefonica. In November 2003 the coverage area extension to the rest of the country was authorized to TCN [81]. The first license gave five years exclusive

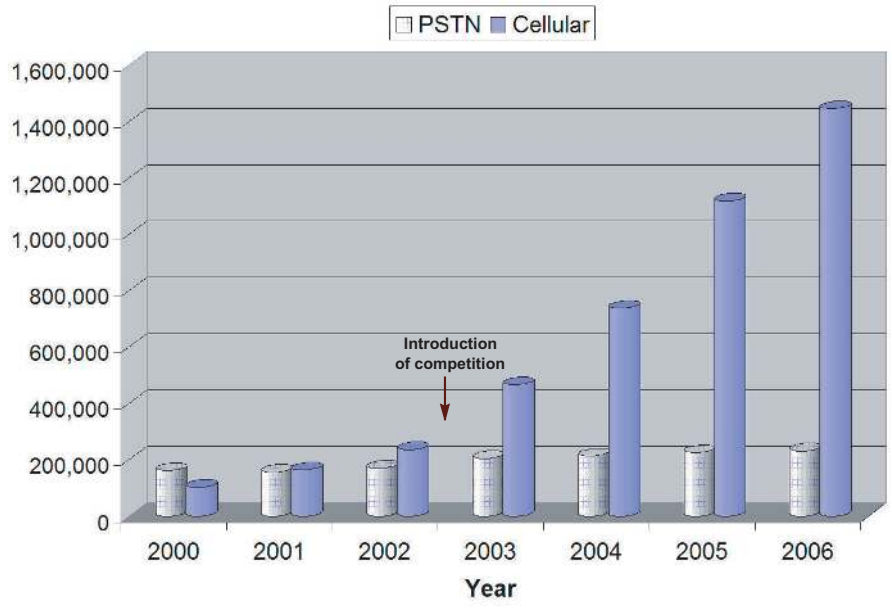

Figure 2.3: Number of PSTN and cellular subscribers.

rights to provide cellular services on the 850MHz along the Pacific region[3] of the country operating on the 850MHz frequency band. That is, given the conditions at that time, the first cellular operator was a *legal private monopoly* until the end of 2002. As shown by the data in table 2.1, the growth of subscribers was almost linear until the year 2000. However, just before the start of competition, TCN made changes regarding tariff and service offers and evolved its network to CDMA technologies creating that triggered the start of an exponential growing as shown in Fig.2.3.

Two new operators, SERCOM and ENITEL, started operations after the end of the exclusive period on the 1900MHz frequency band in the whole country. ENITEL's license for cellular services was part of the privatization incentive together with three-year exclusive rights for fixed telephony given by law. On the other hand, SERCOM won the beauty contest carried on by the regulator, as commanded by Nicaragua Telecommunication Law for the cellular license.

The introduction and protection of fair competition in the cellular market together with the effective application of the regulatory regime, in particular interconnection agreements and tariffs have been of paramount importance to produce

[3]The Pacific region is the most populated and includes the departments of Managua, Chinandega, León, Granada, Masaya, Carazo and Rivas

the tremendous growth in the number of subscribers. As a result, the cellular service has emerged as a substitute to the demand for the traditional fixed telephony service.

In addition, as described in the next section, the cellular system has been an important mechanism to provide universal access.

2.4 Universal Access

Universal access refers to the ability of all people to have equal opportunity and access to a service or product from which they can benefit, regardless of their social class, ethnicity, background or physical disabilities. It is a vision, and in some cases a legal term, that spans many fields, including education, disability, telecommunications, and healthcare. Regarding telecommunications, it is of paramount importance for our society to provide affordable communication access to all the people in the country, including remote rural areas.

In the traditional regulatory approach, the government endowed monopoly status to a state-owned telecommunication company and, in exchange, required the monopoly to provide universal access. Universal access obligations in terms of providing public telephony and services were included in the license issue to ENITEL during the privatization. For the three-year exclusive period the obligation was to install a minimum of 220,000 lines and 1,000 new public telephones [82]. Also obligations regarding the time to provide service to formal request in the cities where the service is available were included (six months for the first three years and reduction by one month per year until reducing to one month after that). In addition, regarding the service area, by the end of the exclusive period ENITEL had the obligation to guarantee that at least 90% of the communities with more than 1,000 inhabitants would have at least one public telephone in service (they have to be in service during the concession period). The number of localities to be considered per department are listed in table 2.2.

The license for the cellular operators have also included universal access obligations, significantly improving the access to services in rural and low incomes areas.

For instance, the license contract to TCN [80] includes what it can be considered universal access obligations. TCN assumed the obligation to install at least 5% of their fixed public cellular telephones in rural, remote or low-income areas selected together with the regulator. In addition, the coverage expansion to the rest of the country [83] includes a clause oriented to provide Information and Communication Technologies (ICT) to 100 elementary or high school centers. TCN has to provide 700 computers distributed among the centers with free internet access through their cellular network for a period of two years. Fig.2.4 shows one of such centers located in the small town called “Niquinomo”. Additionally TCN has had to install 5,000 fixed public cellular telephones along the period 2004 to 2008.

The universal access obligations for private operators has been limited to 90% of the communities with over 1,000 inhabitants. By the free market rule itself, there is

Table 2.2: Number of communities with more than 1,000 inhabitants

	RURAL	**URBAN**	**TOTAL**
Madriz	5	5	10
Estelí	4	25	29
Nueva Segovia	11	19	30
León	12	28	40
Chinandega	15	42	57
Managua	5	101	106
Carazo	3	20	23
Rivas	2	8	10
Masaya	18	27	45
Granada	3	21	24
Boaco	2	9	11
Chontales	1	14	15
Matagalpa	21	41	62
Jinotega	15	8	23
RASS	39	19	58
RAAN	18	20	38
Río San Juan	6	3	9
TOTAL	**180**	**410**	**590**

little incentive for private operators to provide expensive network to remote areas under severe financial constraint. The attracted private investment mainly focuses on the urban areas where most of the commercial demand exists [78]. Thus universal access to telecommunication means to all Nicaraguan people has been hard to achieve without government support. The government support is provided through the Universal Access Fund of Nicaragua, referred to as the Fund for Telecommunication Investment (FITEL by its name in spanish).

The Universal Access Fund in Nicaragua: FITEL

Guaranteing universal access to telecommunications to all citizens of the country requires reducing what is called by the regulator the *market efficiency gap* and the *real access gap*. Fig. 2.5 shows the regulator's vision to address this issue illustrating how this can be seen related to the *geographical isolation* and the *level of poverty* (the arrow pointing toward poorest level).

As expressed before, the regulatory reforms have improved the universal access by including *expansion plans* to extend the service area in both fixed and cellular services as part of the operators' obligations. The *market efficiency gap* has also been addressed by the regulator based on the transparent application of the regulatory regime now in place. This has also attracted private investment in other services like radio broadcasting, broadcast television, cable TV and internet service

Figure 2.4: School telecenter, Niquinomo community. (Source: TELCOR)

providers. Important regulatory rules regarding the available radio spectrum for unlicensed frequency bands, 700 MHz and 3.4GHz frequency band, has been set as part of the regulation strategy to reduce the *market efficiency gap*.

However, as illustrated in Fig.2.5, poverty exist even in main cities and close to it such that the geographical isolation is not the only parameter that prevents access to services. Both poverty and geographical isolation are important in preventing access to services to all people even in a perfect competitive market. This is the general

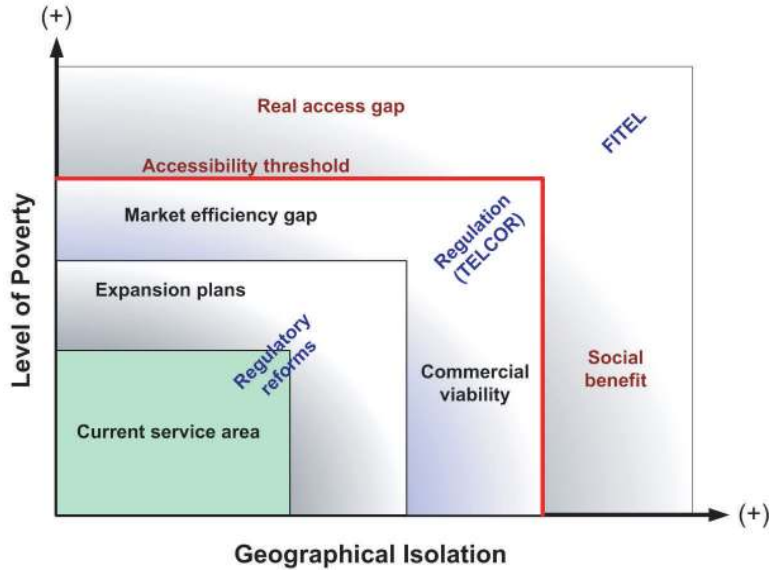

Figure 2.5: The general vision of the Nicaraguan Regulator regarding universal access (version of the original written in spanish).

criterion to identify what is called the *accessibility threshold* by TELCOR through FITEL, in order to reduce the *real access gap* for a social benefit. The final aim is to guarantee that all citizens of the country, independently of their geographical location, have access to information and telecommunication technologies [78].

FITEL was created in 2003 through presidential decree number 84-2003, superseded in 2006 by decree number 05-2006. The fund is financed by the 20% percent of the total income to TELCOR collected through the license fees and spectrum fees. This fund is exclusively for financial support to provide telecommunication services and information technologies[4] to rural areas and low-income citizens.

The general FITEL objectives are oriented to promote:

- access to ICT to rural areas or low-income areas of the country
- social and economical development of rural areas or low-income areas through access to ICT.

[4]Information technology (IT), as defined by the Information Technology Association of America (ITAA), is "the study, design, development, implementation, support or management of computer-based information systems, particularly software applications and computer hardware".

- private sector participation to provide ICT in rural areas or low-income areas through access to special credit or complementary subsidizes to the private investment
- involvement of the population of the rural or low-income areas to identify their own needs as a way to guarantee collaboration and citizens' participation

The administration of this fund is done by the Regulator, TELCOR, through a financial independent direction called FITEL ("Fondo de Inversiones en Telecomunicaciones"). FITEL designs and implements strategies oriented to guarantee ICT access to rural and low-income citizens. The main method designed and implemented up today has been through subsidy in a competitive manner.

Subsidy Scheme in Nicaragua

In many countries one innovative way utilized to address the subsidy issue through Universal Access Fund (UAF) is Negative Competitive Bidding (NCB) for rural access. Through the negative bidding process, the government invites private operators to bid for a license to provide service to certain remote un-served areas, providing such licensees with a one-time subsidy from the Fund as an incentive. The government selects the operator that required a minimum amount of subsidy from the government [84].

Following a similar scheme, with some variants, by the end of 2005 FITEL carried out its first competitive bidding process called project "FITEL I". FITEL I included the coverage extension of cellular service and public telephony to defined rural areas. The two local cellular companies presented their offers and the winner was ENITEL. The cellular coverage has been extended to 30 rural municipalities along the Pacific and center of the country improving cellular coverage up to 72% of the municipalities of the country. In addition, the project has provided access to public telephony to at least 350 rural communities with more than 400 inhabitants. Fig. 2.6 shows the distribution of the communities as well as locations of the base stations installed as part of the project. Fig.2.7 shows one citizen in a rural community utilizing the system. The sign that identifies the availability of public telephony in one of the benefited communities called "San Roque" is shown in Fig.2.8.

Although there are no publicly available details regarding the utilization of the installed system yet, the project is considered to be a success exceeding the estimated traffic. There are several factors that influence the acceptance and utilization of the system generating traffic beyond expected. As illustrated in Fig.2.7 the fixed cellular public telephony is easy to use by all people since it is a well known technology. Also, we have observed that in some of the communities some people have installed fixed cellular phones and rent them to rest of the community. Another factor could have been created by subsidy terminals which allows to get cheap second-hand cellular phones utilized in the rural area now covered by the cellular system together with one dollar prepaid cards.

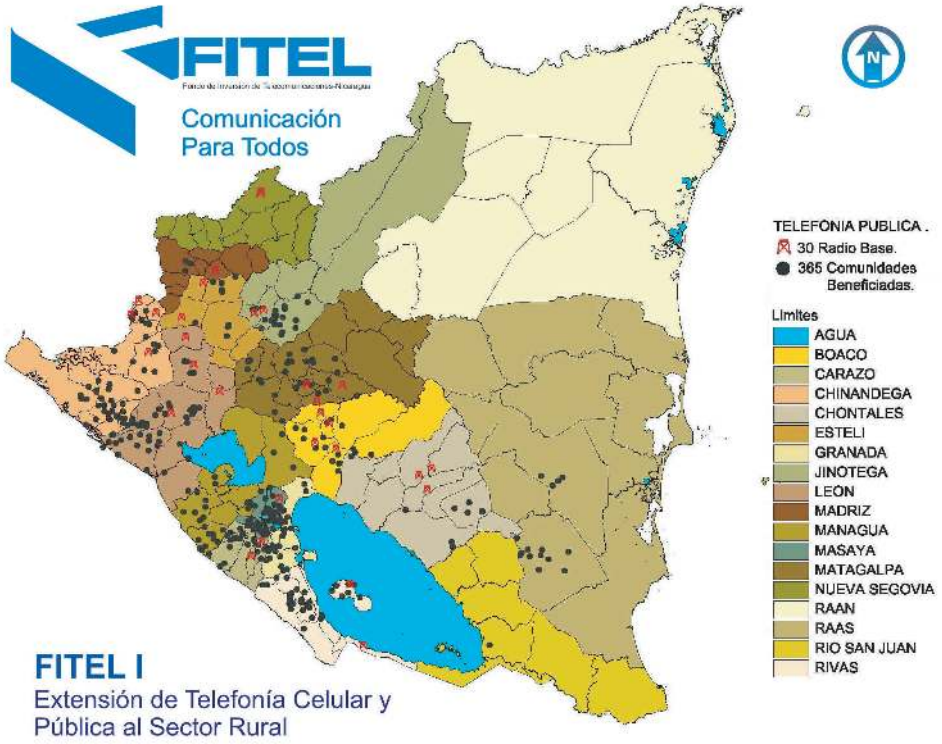

Figure 2.6: Cellular coverage extension and rural public telephony map of project FITEL I.

2.5 Small Business Opportunities: CyberCafes and Telecenters

In the rural areas of Nicaragua, besides the problem of no access to telecommunications means there is no access and education on the usage of "information technologies" (IT). The lack of education and access to IT has been a problem in the whole country, i.e. including main cities. The gap between people with effective access to digital and information technology, and those without access to it is commonly referred as *digital divide*. However, over around the last ten years, access to IT is possible in the main cities of the country with the introduction of CyberCafes.

The success of the CyberCafes didn't start by *data applications* as one may think. In our opinion, the main driving force has been the value of long distance communications for people with relatives and friends overseas. Since the beginning of the civil war in 1978 a large number of Nicaraguans left the country and live

Figure 2.7: Rural public telephony allows utilization of a commonly used technology (source: TELCOR).

Figure 2.8: FITEL's sign for Public Telephony, San Roque community. (source: TELCOR)

abroad. The high price for International Long Distance calls (ILDC) on the Public Switching Telephone Network (PSTN) has been the main incentive for people to use the Internet. Similar to other countries, the VoIP is not included in the regulatory regimes of the law for Telecommunication and Postal Service ("Ley No.200"). Under that precept VoIP for ILDC are provided at low prices over the Internet. However, under the constitutional precept [85] argument, until now, the local operators of telephony (PSTN and cellular) do not have *Interconnection* with the Internet Access

Providers for VoIP calls to terminate in the Nicaraguan telephony network[5].

Nevertheless, this in fact has created a positive domino effect since, through the CyberCafes, young people have access to computer use at reasonable prices (between $0.5-$1.0 per hour) and this way they are "digitally educated".

The idea of extending small business like CyberCafes to rural areas (commonly refer to as telecenters) has been the subject of pilot projects by several governmental and nongovernmental organizations (NGOs) in several countries.

As described in section 2.6, with modern technologies building a wireless network is possible, but making it financial sustainable in rural and low-income areas continuous to be a hard-to-solve business problem. A payment model that considers re-investment and risk is a necessity, or eventually the network may fail. The experienced resulting from projects carried out in several rural communities in [86] (many of them were carried out on developing countries in Africa) suggest that the community itself should be involved in the project from its early planning and installation. Also the payment model has to conform to fiscal cycles of the potential clients as well as their social expectations. For instance, the income of citizens in rural areas is more seasonal than monthly. When performing a proper risk analysis the monthly payment may have an important impact regarding sustainability [86] .

2.6 The Selection of Technologies to Provide Rural Telecommunications

Rural connectivity requires a backbone transmission media and technologies to connect to individual end users (last mile). The connectivity may be provided for instance by utilizing the combination of wire and wireless technologies. However, how can we asses the selection of cost-effective technology to provide rural telecommunications? In [87] the Communications Research Centre Canada (CRC), an agency of Industry Canada, had conducted studies in order to assess the various broadband access technologies, based on population density and looking at their merits in relation to their perceived complexity and cost. Fig.2.9 shows the CRC findings for Optical fiber, ADSL, Cable modem, microwave wireless, satellite and new wireless technologies. The figure shows that in the range below 1.5 person/km^2 only satellite technologies make sense and above 60 person/km^2 wired technologies, such as ADSL and cable modem, become cost-effective. Service to rural areas between these two population density limits requires the development of new wireless broadband access technologies that will extend the reach to allow cost-effective coverage of rural areas.

[5]According to the Nicaraguan Constitution, Art.32, nobody is obligated to do what the law does not order, nor prevented from doing what the law does not prohibit (translation from Spanish of the Cn. Art.32: "Ninguna persona está obligada a hacer lo que la ley no mande, ni impedida de hacer lo que ella no prohibe.")

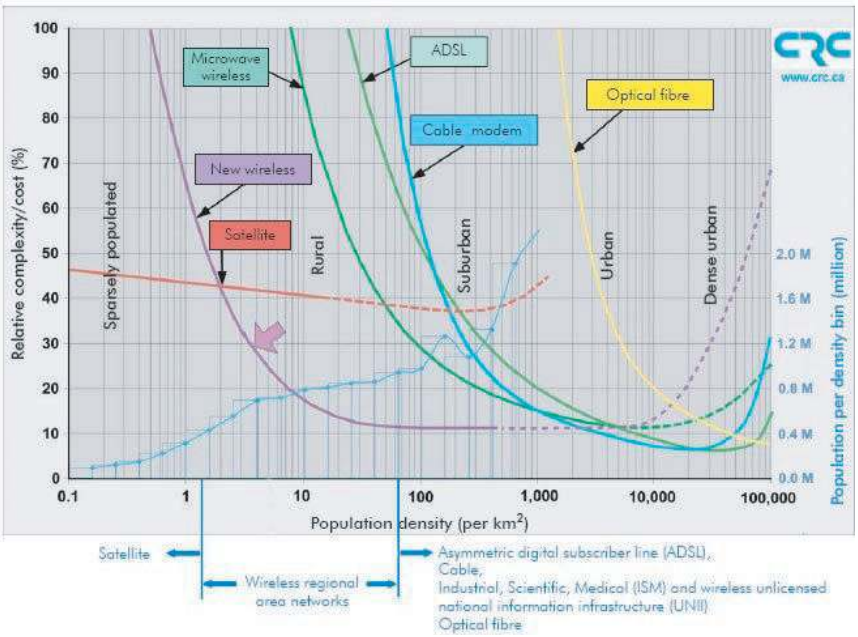

Figure 2.9: Suitable broadband access technologies as a function of population density (source: ITU News magazine [87])

Within the category of wireless technologies we can consider the use of terrestrial (land-based) wireless communications technologies include LMDS (Local Multipoint Distribution Service)and MMDS (Multiple Multipoint Distribution Service), as well as technologies operating on the Industrial, Scientific and Medical frequency band (ISM) like WiFi (Wireless Fidelity based on the family of standards IEEE 802.11x) and even WiMax (Worldwide Interoperability for Microwave Access, standard IEEE 802.16) technologies.

Another important factor related to the perceived cost and complexity is the frequency of operation when trying to extend the radio range. Fig.2.10 shows the relevant factors to be considered in the selection of the recommended carrier frequency. We can see that for rural communication frequency ranges between 300MHz and 1GHz are more suitable for long-range communications. The use of radio frequencies in this range can extend the reach of wireless broadband access systems, allowing for a larger subscriber base in sparsely populated areas. Regarding availability of frequencies, by the end of 2005 the Nicaraguan regulator decided to allocate part of the 700MHz to data communications as exclusive primary use. The spectrum usage fees were also utilized as part of the incentive. To promote the private sector investment, average income and population densities were used to set the annual fees and several ISPs are offering wireless internet on this frequency

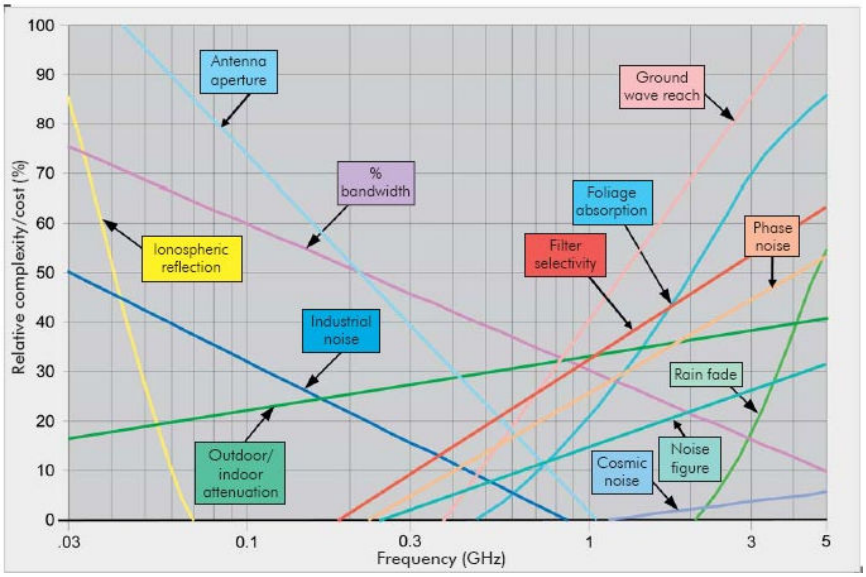

Figure 2.10: Factors to be considered in the choice of the best frequency for wireless broadband access technologies to serve sparsely populated rural areas (source: ITU News magazine [87])

band.

However, the economy of scale has been a driving force regarding rural communication. WiFi technologies have shown to be a popular alternative used in many rural projects extending the total radio range by multi-hopping together with directional antennas and minor modifications to the multiple access protocol to extend the one-hop radio range.

Even though the CRC findings were conducted for rural areas of Canada we can use them to identify and geographically map the potential dominant technology selection applicable to the rural Nicaraguan environment. Table 2.3 shows our vision for the dominant wireless technology solution for the 17 political divisions of the country. Geographical population density[6] has been used as a main criteria. For most of the Central and Pacific regions cellular systems, as decided and implemented by the regulator, seem to be the most promising solution. The central region located in the Nicaraguan savanna and the Caribbean regions are the most promising ones to deploy "new Wireless Technologies", such as Multi-hop Wireless Networks.

Combination of Very Small Aperture Terminal (VSAT) for Internet connection and WiFi technologies for "local" access could be utilized mainly in the rural areas of Rio San Juan, RAAN and RAAS (Atlantic Coast of Nicaragua). In spite of that,

[6]The population density is based on the census 2005 in [88].

Table 2.3: Potential dominant wireless technologies for rural areas of Nicaragua as a function of population density by political division.

Population density 2006 vr. Wireless Technologies				
NICARAGUAN REGION	Population density (per km^2)	Dominant Alternative Wireless Technology		
		Satellite	New Wireless	Cellular
Chinandega	78.6			√
León	69.2			√
Managua	364.5			√
Masaya	474.8			√
Granada	161.8			√
Carazo	163.6			√
Rivas	72.3			√
Nueva Segovia	59.7			√
Jinotega	35.9		√	
Madriz	77.5			√
Estelí	90.4			√
Matagalpa	69.0			√
Boaco	36.1		√	
Chontales	23.8		√	
Río San Juan	12.7		√	
RAAN	9.5	√		
RAAS	11.2		√	

as presented in section 2.5, financial sustainable in rural and low-income areas continues to be a hard-to-solve business problem. The satellite system solution even combined with MWN has a relatively high monthly cost. The cost could range between $400 to $700 just for the VSAT internet service. The experience from many IT development projects is that this expensive monthly cost is difficult to manage. Typically these projects can purchase equipment and pay for the establishment of a wireless network (for instance from donors), but most are not able to pay for the cost of the network after a short period of time (including the recurring Internet costs and operational costs). It is necessary to find a model where the monthly costs for a network can be met by those who use it. For most community telecenters, this is simply too expensive. Often, the only potentially feasible plan is to share the costs with other users. To make the Internet more affordable, this site could use multihop wireless network technologies to share the Internet access to the community, allowing a greater number of organizations to access the Internet while reducing the cost per client. In such case an adequate site selection should

considered together with the shared cost approach.

Regulation could also stimulate this to occur. One such regulation has been implemented in Nicaragua by reducing the spectrum usage fees for VSAT stations whenever their intended usage is to provide rural communication to the people. We think that another possible incentive could be to extend the benefit for private deployed VSAT networks if they share their infrastructure with the communities where located.

Regarding other rural areas along the Pacific and Central region of the country, MWN combined with land-based infrastructure could be utilized with already affordable existing technologies. In applications like Internet access for telecenters, extensions of fixed land-based telecommunication infrastructure could be possible. For this type of applications, the Internet service cost is much more lower than the combined VSAT and WMN solution. For instance, at the moment of writing this thesis, the ADSL Internet service for 512kbps cost $40 per month and a similar price is offered for Internet over cable modem available in main cities on the Pacific and Center region. The regulation actions are reducing the market efficiency gap and increasing the possibilities for this potential alternative to be considered viable.

Chapter 3

System Models and Performance Measure

In this chapter the models utilized for our performance evaluation of multihop wireless networks are introduced. Selection of the models is done to provide a reasonable level of abstraction of the way that the real system operates while at the same time producing easy to analyze results. The physical and link layer operation is modeled through the link quality model and the multiple access interference is influenced by the terrain, MAC protocol, and the type of advanced antenna system utilized. Additionally, the information source attached to a node is analyzed through the traffic model and routing as part of the upper layer functionality. The definition of the performance measures employed are also presented in this chapter.

3.1 Link Quality Model

The MWN is composed of N identical nodes, i.e. all nodes in the network have the same capability (homogeneous configured nodes). It is assumed that the only way to communicate between nodes is through the wireless medium utilizing half-duplex transceivers on the same carrier frequency (common channel). A particular node in the network is uniquely identified by its number $i, (i = 1 \ \ldots \ N)$.

The radio-propagation conditions of the surrounding environment where the network is deployed attenuates the transmitted signal and some nodes may not be within the radio range of each other.

Received Power

We represent the received power level on link (i, j) by P_{ij}, resulting from node i's transmissions with power level P_i at node j; $\forall$ node $j \neq i$. The radio propagation properties of the terrain where the network is deployed are captured by the radio propagation losses. We represent the path losses on link (i, j) by L_{ij}. The inverse

of this quantity is commonly referred as the link *path gain*, $G_{ij} = 1/L_{ij}$, and constitute the elements of the *path gain* matrix, $\mathbf{G}$.

The antenna gain is utilized to find the relation between the received power (at the receiver site) and the transmitted power. The *antenna gain* is one of the most important parameters to describe the radiation properties of an antenna that takes into account its efficiency and its directional capabilities [89]. If the geometrical orientation of the transmitting antenna of node i is such that the receiving antenna of node j is seen in the angular direction θ_{ij} and the receiving antenna of node j is oriented such that the transmitting antenna of node i is seen in the angular direction θ_{ji}, the received power P_{ij} is given by

$$P_{ij} = \frac{P_i A_{ij}(\theta_{ij}) A_{ji}(\theta_{ji})}{L_{ij}} = P_i G_{ij} A_{ij}(\theta_{ij}) A_{ji}(\theta_{ji}). \tag{3.1}$$

$A_{ij}(\cdot)$ denotes the (azimuthal) antenna patterns used by node i to transmit to node j.

To generate easily analyzed results the simple distance dependent propagation model is used. In addition, influence of the terrain irregularity (e.g. mountains) is evaluated using artificial terrains to recreate a more realistic scenario. The terrain model is a modification of the one used in [90] and is described in Appendix B. In this case, the path gains are then computed according to [91] whereby the radio propagation loss is split into three components: a distance dependent path loss, a plane earth propagation loss and a (multiple knife-edge) diffraction loss due to the mountains in the terrain model.

When using the distance dependent model only, equation 3.1 is given by

$$P_{ij} = \frac{P_i A_{ij}(\theta_{ij}) A_{ji}(\theta_{ji})}{d_{ij}^{\alpha}}, \tag{3.2}$$

where d_{ij} is the distance between node i and node j and α is the path loss exponent. A value of $\alpha = 3$ that may correspond to the rural scenario [92, 93] will be used to evaluate performance.

Advanced Antenna System Models

If AAS are properly used in wireless communication systems, they help improve the system performance by increasing channel capacity and spectrum efficiency. They can be used to extend the radio range coverage, and/or also to steer multiple beams to receive from more that one transmitter [19, 21].

AAS can help reduce the Multiple Access Interference (MAI) and improve the system capacity but the cost per node will be higher. Switch-beam technologies can provide cost-effective implementations [1] of AAS in multihop wireless networks.

[1] There are many ways to implement Fixed beamforming Networks (FBN) using off the shelf components (e.g. Butler Matrix)[[19], page 91].

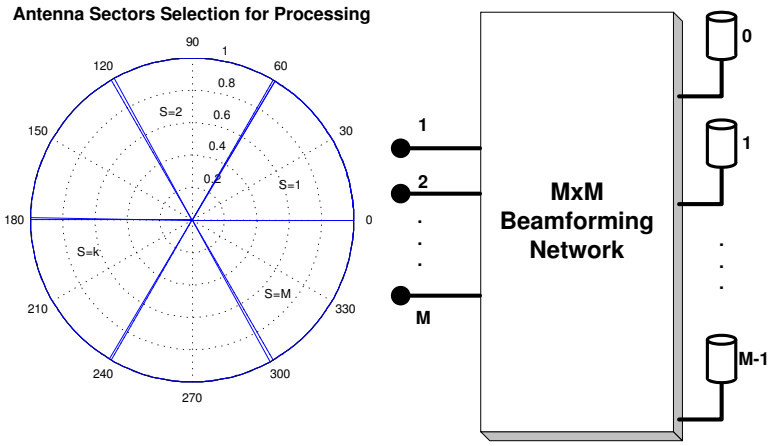

Figure 3.1: Switched-beam method using flat-top antenna model.

On the other hand, Adaptive Beamforming Antennas (ABF) provide electronically controlled steerable beam flexibility, but at higher price.

Switched-beam Antenna Systems Model

As previously mentioned, the switched-beam AAS method is one of the simplest approaches that can be used. For the case when using orthogonal beams, a linear RF network, called a Fixed Beamforming Network (FBN) combines M antenna elements to form up to M directional beams.

In order to obtain easily analyzed and general results, the flat-top antenna radiation pattern model [[19], page 137] has been used in several studies [35,42,94]. When this model is used for switched-beam systems, it is assumed that each node uses a FBN to cover 360^o with M sectors. The antenna pattern for each sector s, $s = 1 \ldots M$ utilized by node i, $A_i(\theta, s)$ is given by (3.3) and is illustrated in Fig.3.1.

$$A_i(\theta, s) = \begin{cases} \frac{2\pi}{\phi_h}; & (s-1)\phi_h < \theta < s\phi_h \\ \\ \frac{1}{a_{sl}}; & Otherwise \end{cases} \tag{3.3}$$

where ϕ_h is the horizontal antenna beamwidth (BW) and a_{sl} is the side lobe attenuation.

Beam-Steering Antenna System Model

To model Adaptive beamforming Antenna Systems, Beam-Steering has been selected as the Adaptation method, i.e. the objective function of the combining network for the antenna system maximizes the Signal-to-Noise Ratio (SNR) for the communication link. The result is that the main lobe of the receiving and transmitting antenna array are pointed toward the strongest signal path. We use realistic as well as simplified antenna models in our studies. As the simplified model we use a Steerable flat-top model. In this case, the antenna pattern $A_{ij}(\theta_{ij})$ used by node i while transmitting to node j is given by (3.4). The antenna radiation pattern of the receiving antenna in node j is computed in the same manner.

$$A_{ij}(\theta_{ij}) = \begin{cases} \frac{2\pi}{\phi_h}; & \theta_{ij} - \frac{\phi_h}{2} \leq \theta \leq \theta_{ij} + \frac{\phi_h}{2} \\ \\ \frac{1}{a_{sl}}; & Otherwise \end{cases} . \tag{3.4}$$

The above model has been relaxed in our analysis in chapters 6, 7 and 8 by utilizing beam-steering circular array antenna systems. In that case, the antenna pattern is computed using a phase mode excitation beamformer according to eq. (4.190) in [95], using as design parameter the halfpower beamwidth (HPBW). In addition, a Schenkunoff-factor is applied for null-filling. Table 3.1 shows a summary of the circular array geometry utilized in our performance evaluations.

Although more complex digital processing techniques are possible (e.g. creation of nulls in the radiation pattern to limit the interference coming from neighboring nodes even further) they are not covered in this thesis. However the methodology and algorithms proposed in our framework can be utilized with that type of AAS as well.

Target Antenna HPBW (φ_h)	15°	30°	45°	60°
No. of Elements	20	10	6	4
Radius (Wavelength)	1.5915	0.7958	0.4775	0.3183
Array Gain (dBi)	13	10	8	6

Table 3.1: Circular Array design parameters.

3.2 Multiple Access Interference Model

In the radio environment the probability of a packet arriving error free is dependent on the modulation, coding, Multiple Access Interference (MAI) and background noise. For the purpose of network modeling it is assumed that a packet survives if the Signal-to-Interference plus Noise Ratio (SINR) during the transmission period of the packet is above a specified threshold γ_k as defined by

$$\Gamma_{ij} = \frac{P_i G_{ij} A_{ij}(\theta_{ij}) A_{ji}(\theta_{ji})}{\sum_{\forall \text{ link } (r,k) \neq \text{ link } (i,j)} P_r G_{rj} A_{rk}(\theta_{rj}) A_{ji}(\theta_{jr}) x_{rk} + P_{Noise}} > \gamma_k \ . \quad (3.5)$$

Γ_{ij} is the Signal-to-Interference plus Noise Ratio for a packet sent from node i to node j and $P_{Noise} = kT_0BF_{sys}$ is the background noise power level at node j, $k = 1.38 \times 10^{-23}$ J/K is the Boltzmann constant, $T_0 = 290K$, F_{sys} is the receiver Noise Factor and B is the receiver equivalent noise bandwidth. x_{rk} is a random variable defined as

$$x_{rk} = \begin{cases} 1 & \text{if } r \text{ transmit to node } k \\ 0 & otherwise \end{cases} \quad (3.6)$$

The random variable x_{rk} depends on the MAC protocol being used and on whether or not a node r has a packet to transmit to node k. When simulating CSMA/CA with RTS and CTS (see Chapter 9) this equation is used to determine if the packet survives in the presence of other node transmissions.

When using STDMA as MAC protocol (see Chapter 5) a *link transmission schedule* is created in advance. The time domain is divided into slots, each long enough to contain one data packet transmitted at rate R_0. In this case the link schedule is created by adding one link at a time to test if all links assigned to transmit in a given slot satisfy their required SINR (3.5) with $x_{rk} = 1$, i.e. considering the worst case when a node r always has a packet to be transmitted to node k.

3.3 Network Topology

It is common to represent networks as composed of two types of objects: nodes and arcs. We let N denote the number of nodes that comprises the network and $\mathcal{N}$ represent the set of nodes (N is the cardinality of the set $\mathcal{N}$). The nodes are connected by arcs and arcs are assumed to be directed. This means that an arc connecting node i to node j is not the same as an arc connecting node j to node i.

For MWN, rather than using the term arc we find it more meaningful to use the term directed link or just link. The link from node i to node j is denoted simply by the ordered pair (i, j). The number of all potential links is $N(N-1)$ since there are $N-1$ possible links outgoing from each node.

However, as stated before, the radio-propagation conditions of the surrounding environment where the network is deployed attenuates the transmitted signal. The

existence of good received signal quality between two nodes defines if they are directly connected. Since nodes have limited transmission power, only a subset of the total possible links may have enough received power to be *feasible*. A link (i, j) is said to be *feasible* if a sufficiently low bit error rate (BER) can be achieved in the absence of MAI.

The set of feasible links define the logical network topology, i.e. how the different nodes in the network are connected to each other. Let L denote the number of all feasible links. We let $\mathcal{A}$ denote the set of all feasible links in the network. In typical MWNs, the set $\mathcal{A}$ is smaller than the set of all links, that is:

$$\mathcal{A} \subset \{(i, j) : i, j \in \mathcal{N}, i \neq j\}.$$

The pair $\mathcal{G} = (\mathcal{N}, \mathcal{A})$ is called a directed network [96, page 24] [2]. In network flow problems it is common to utilize the so-called *node-arc incidence matrix* to define the logical network topology in compact form[3]. By using the labels $l = 1 \ldots L$ $(L \leq N(N-1))$ for the set of feasible links in the network, the entries of the $N \times L$ *node-arc incidence matrix* $\boldsymbol{A}$ are given by:

$$a_{il} = \begin{cases} +1 & \text{if node } i \text{ is the transmitter on link } l \\ -1 & \text{if node } i \text{ is the receiver on link } l \\ 0 & \text{otherwise} \end{cases} \tag{3.7}$$

The use of the above terms and concepts are better explained by the following example.

Example 3.3.1 Consider a simple network, $\mathcal{G} = (\mathcal{N}, \mathcal{A})$, composed of 3 nodes, $\mathcal{N} = \{1, 2, 3\}$ with transmission power enough for good signal quality in absence of MAI for the set of feasible links $\mathcal{A} = \{(1, 3), (3, 1), (2, 3), (3, 2)\}$, then the *node-arc incidence matrix* is given by:

$$\boldsymbol{A} = \begin{pmatrix} +1 & -1 & 0 & 0 \\ 0 & 0 & +1 & -1 \\ -1 & +1 & -1 & +1 \end{pmatrix}$$

■

The *connectivity* is commonly used as an important network parameter to characterize the network topology [57, pag.]. Connectivity is defined as the ratio between the average number of *node's neighbors* to the total number of potential neighbors, as follows:

$$\mathcal{C} = \frac{E\left[\text{node's neighbors}\right]}{(N-1)}. \tag{3.8}$$

[2] It is also sometimes called a directed graph or a digraph (to emphasize the fact that the arcs are directed).

[3] Another common representation is the *Node-Node Adjacency matrix* that stores the network as an $N \times N$ matrix with entries a_{ij} equal to 1 if $(i, j) \in \mathcal{A}$ and equal 0 otherwise

We say that node j is a neighbor of node i if a feasible link exists between them; this also means that node i is at a single hop from node j. Since we only consider bidirectional links, the number of neighbors of a node correspond to one-half of its *degree*. The *degree* of a node is the sum of the number of its incoming links (*indegree*) and the number of its outgoing links (*outdegree*) [96, page 25]. Therefore, if the total number of neighbors to node i is L_i, the average number of neighbors is given by

$$E[neigbors] = \frac{1}{N}\sum_{i=1}^{N} L_i = \frac{L}{N}. \tag{3.9}$$

Note that in a single hop network, all nodes are reachable from any other node and all links are feasible yielding

$$E[neigbors] = N - 1 = L_i \ ; \ \forall \ i.$$

The connectivity parameter can be interpreted as the probability of reaching a randomly selected node in a single hop from another randomly selected node, that is

$$\mathcal{C} = \sum_j P(i, i \neq j/j)P(j) = \sum_j \frac{L_j}{N-1}P(j) \tag{3.10}$$

$$= \sum_j \frac{L_j}{N(N-1)} = \frac{E[neigbors]}{N-1} = \frac{L}{N-1} \tag{3.11}$$

$$\tag{3.12}$$

Another parameter considered important is the average number of hops, since it indicates on average how many relaying nodes a packet has to visit before reaching its final destination. If the minimum number of hops needed to reach node j from node i is h_{ij}, then the average number of hops is given by

$$E[hops] = \frac{1}{N(N-1)}\sum_{i=1}^{N}\sum_{j=1}^{N} h_{ij} \ . \tag{3.13}$$

Note that $h_{ii} = 0$ in the above equation since the packet does not need to be forwarded.

By varying the transmission power utilized by a node the network topology can be changed. The required transmission power to achieve a given SNR (γ_0) while at the same time overcoming a maximum propagation path loss, L_{max}, using isotropic antennas is computed by

$$P_i = \gamma_0 P_{Noise} L_{max} \tag{3.14}$$

Fig.3.3 shows three network realizations using this procedure with a distance dependent model ($\alpha = 3$ is considered typical for the rural scenario [92, 93]) to achieve a maximum radio range of 40 km.

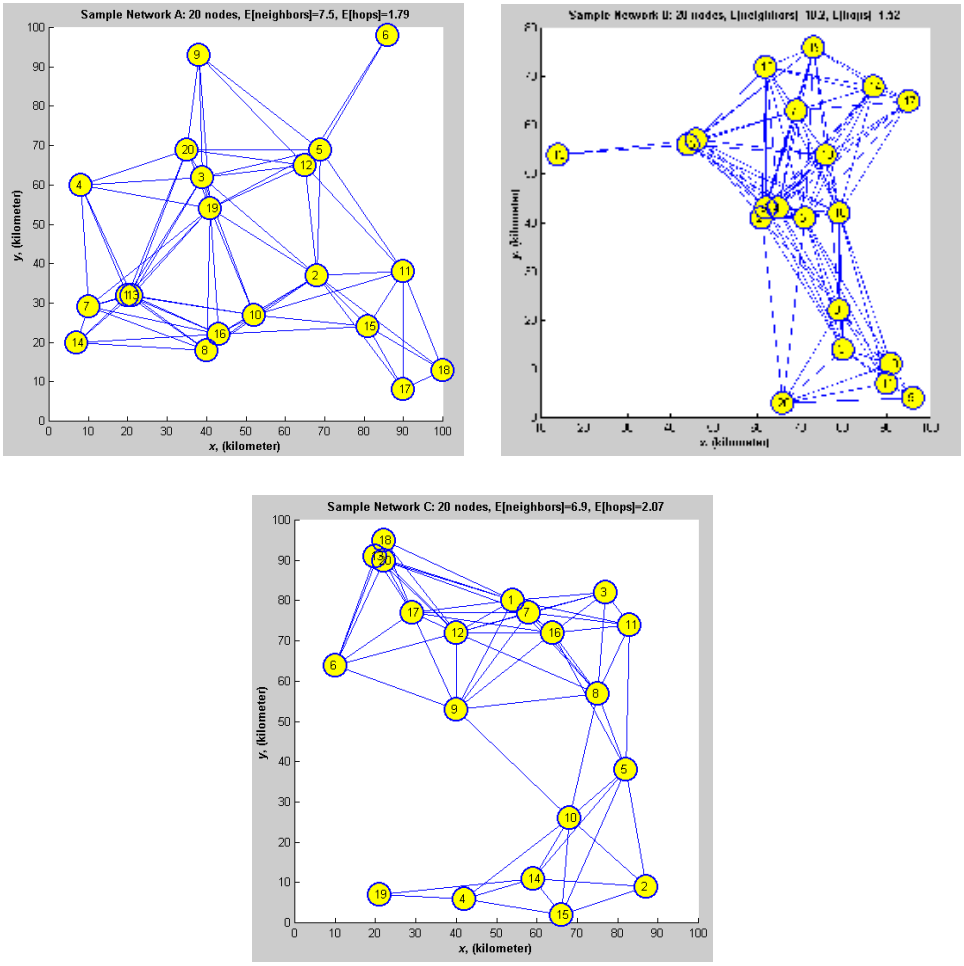

Figure 3.2: Sample networks (Network A, B, C) with N=20 nodes. It can represent static or nomadic behavior simulated by random location over an area of 100x100 km. Lines indicate *feasible* (or reliable) bi-directional communication links in absence of Multiple Access Interference. The average number of neighbors and the average number of hops needed to reach other nodes is indicated.

When using AAS, the radio transmission range can be increased compared to that achieved by using omnidirectional antennas with the same transmission power at the antenna system input. In that case the network topology resulting from utilization of omnidirectional antennas will very likely be changed due to the increased radio range (a different set $\mathcal{A}$ will result). When evaluating in this way, the system performance includes the interference suppression capability and also the

radio range extension benefit but under different network topologies.

In order to analyze the impact of AAS as a function of the network connectivity and topology, the transmission power is reduced to keep the same network topology as for the omnidirectional case. This allows us to evaluate separately the spatial filtering advantage provided by AAS from the radio range extension. Note that for a given connectivity a finite set of logical topologies and an infinite set of physical topologies exist since nodes could be located randomly in a geographical area.

3.4 Traffic Model and Routing

The multihop wireless network conveys information by mean of short bit strings called packets. If a message generated by an information source attached to a node is larger than the packet size, this is broken into several packets to be transmitted through the network as individual entities. From a user perspective these messages are usually a reaction to a particular event (e.g. replying to the source after receiving an email). However, under the network perspective, messages or packets arrive as a random process [63]. It is assumed that the information source attached to a node sends different information to all other nodes in the network (unicast traffic). If we label the set of source-to-destination traffic pairs (S, D) by $p = 1 \dots N(N-1)$, the average external traffic load transported by the network is given by

$$\lambda = \sum_{S=1}^{N} \sum_{\forall D \neq S} \lambda_S^D = \sum_{p=1}^{N(N-1)} \lambda_p \tag{3.15}$$

where λ_p denotes the average traffic load between source to destination pair p (packet/timeslot) . We use the term source to destination rate when λ_p is measured in bits per second. In chapters 4, 6 and 9 we analyze the throughput-delay characteristics of MWNs under variable traffic loads. In that case, for simplicity, it is assumed that packets are of constant length and arrive according to a Poisson process [4] with total external traffic load of λ packets per packet duration.

Due to the store-and-forward mechanism, packets between (S, D) pairs may travel through intermediate nodes selected by the routing mechanism. Routing approaches are generally classified in two categories: Reactive and Proactive routing. Reactive routing is also called on-demand routing since routes between (S, D) pairs are discovered only when they are needed. When a source node needs to send data packets to some destination, it checks its route table to determine whether it has a route. If no route exists, it performs a route discovery procedure to find a path to the destination [97, pag. 281] . On the other hand, in proactive routing each node in the network maintains a route to every node in the network at all times. Route

[4] This model does not capture the reactive property experienced by users over real networks (for instance traffic generated by http or ftp sessions). However, it could be a suitable model for short messages (e.g. short e-mails among users) and help us to analyze the main network design trade-off.

creation and maintenance is accomplished through some combination of periodic and event-triggered routing updates [97, pag. 277]. Proactive approaches have the advantage that routes are available the moment they are needed [5].

By using proactive routing a path is found to route the traffic from source-to-destination. Related to the route selections and the external traffic we can find the average traffic load going through link l, Π_l, by using (3.16).

$$\Pi_l = \sum_{p=1}^{N(N-1)} r_{lp}\lambda_p \tag{3.16}$$

where r_{lp} are the entries of the *link-route incident matrix* $\boldsymbol{R} \in \Re^{L\times N(N-1)}$, given by:

$$r_{lp} = \begin{cases} 1 & \text{if } (S,D) \text{ pair } p \text{ is routed through link } l \\ 0 & \text{otherwise} \end{cases}$$

We use the Dijkstra algorithm [96, pag.108-111] to find the routes from a source node to a destination node.

By defining the vectors $\boldsymbol{\Lambda} = [\ \lambda_1 \quad \dots \quad \lambda_{N(N-1)}\ ]^T$ and $\boldsymbol{\Pi} = [\ \Pi_1 \quad \dots \quad \Pi_L\ ]^T$, (3.16) can be written in a compact matrix form as:

$$\boldsymbol{\Pi} = \boldsymbol{R}\boldsymbol{\Lambda}. \tag{3.17}$$

Furthermore, it is assumed that the traffic load is evenly distributed (3.18).

$$\lambda_p = \frac{\lambda}{N(N-1)} \qquad p \in \{1, 2, \cdots, N(N-1)\}\ , \tag{3.18}$$

Λ_i is the external traffic load on node i.

Therefore, the average traffic load Π_l going through a link (i,j), labeled l, is the result of external and internal traffic [[50], page 25] (3.19).

$$\Pi_l = \sum_{\substack{\forall(S,D) \text{ routed} \\ \text{through link } (i,j)}} \frac{\lambda}{N(N-1)} = \frac{\lambda}{N(N-1)} T_{ij}\ , \tag{3.19}$$

where T_{ij} are the ij-th entries of the *Relative Traffic Load* matrix $\boldsymbol{T}$ given by

$$T_{ij} = \sum (S,D) \text{ routed through link } (i,j) = \sum_{p=1}^{N(N-1)} r_{lp}\ . \tag{3.20}$$

[5] In proactive routing, "the amount of routing state maintained at each node scales as $O(n)$, where n is the number of nodes in the network. Proactive protocols tend to perform well in networks where there is a significant number of data sessions within the network. In these networks, the overhead of maintaining each of the paths is justified because many of these paths are utilized" [97, pag. 277].

As revealed by this equation, route selections have a strong influence on the network performance. Commonly, while doing route search for a particular (S, D) pair, the number of hops are used to select between different possible paths. This may result in uneven traffic distribution. Besides that the MAI is also affected by routing, for instance nodes at the center of the network are highly likely to be selected as part of the shortest path to reach other nodes, resulting in higher interference.

3.5 Performance Measure

Two primary parameters are used to evaluate performance in this thesis, the *end-to-end throughput* and the average *end-to-end packet delay.*

The *end-to-end packet delay* is defined as the time between the arrival of a packet at the buffer of the source node and its successful reception at the destination node. The end-to-end packet delay allows us to evaluate the service quality under low, moderate and high traffic loads.

In general, a randomly selected packet transmitted from node S to node D experiences a random delay D_{SD} that is the sum of the delays on every link utilized to route the packet (selected path). Assuming that (S, D) pairs are equally likely, the expected end-to-end delay is given by

$$E[D] = \frac{1}{N(N-1)} \sum_{\forall (S,D)} \left[\sum_{\substack{\forall \text{ link } (i,j) \text{ in path} \\ \text{selected to route } (S,D))}} E[D_{ij}] \right] \tag{3.21}$$

$E[D_{ij}]$ is the expected packet delay over link (i, j) and is a function of the external traffic load, internal traffic load, MAC protocol and multiple access interference. An exact analysis for $E[D_{ij}]$ in the wireless scenario appears to be very difficult [34, 63]. Nevertheless, the above equation can be rewritten in terms of the relative traffic load and is given by

$$E[D] = \sum_{\forall \text{ link } (i,j)} \frac{T_{ij}}{N(N-1)} E[D_{ij}]. \tag{3.22}$$

Computer simulations are commonly used to measure $E[D_{ij}]$, however as the number of nodes in the network increases, the computer time required simulating MWN significantly increases as well. Since coordination among nodes exists when utilizing STDMA, it is possible to estimate the relative link capacity assigned to each link. This makes it possible to do a reasonable estimation of $E[D_{ij}]$ for the case of fixed transmission rate systems,(see section 5.3).

As mentioned before, the end-to-end packet delay is a function of the traffic generated by users in the network. The total external traffic could not be higher

than the network capacity, otherwise the buffer queue at some nodes grows without bounds, making the system unstable [[98], page 4]. To avoid unstable conditions the external traffic load, λ, must be equal to the end-to-end throughput, i.e. the number of packets that reach their final destination per time period in the entire multihop wireless network and it is a measure of the resource utilization. The term end-to-end throughput is used in this thesis to indicate the total external traffic measured under stable conditions. We are particularly interested in the maximum end-to-end throughput, λ^*, that is here defined as the upper bound limit to the maximum total external traffic load that produces finite $E[D_{ij}]$; $\forall$ existing feasible links in the network.

In STDMA this upper bound can be estimated (see chapter 6). On the other hand, for random MAC protocols estimation of the maximum end-to-end throughput in multihop wireless scenario seems to be very complex. In that case computer simulation is the only method used in chapter 9 to estimate $E[D_{ij}]$ and λ^* for CSMA/CA with handshaking. In order to find an estimation of λ^* with this protocol the external traffic load λ is increased until a buffer overflow occurs in any node of the network.

Chapter 4

Generalized TDMA Multihop Wireless Networks with AAS

4.1 Introduction

In this chapter we study the integration of advanced antenna systems in multihop wireless networks to increase the overall network performance, in terms of throughput and packet delays, utilizing Generalized TDMA (GTDMA) as MAC protocol. The utilization of GTDMA simplifies the overall system design as compared to STDMA in the sense that no estimation of the interference is needed. This is because in GTDMA slot transmission rights are given to individual nodes (no spatial reuse). In addition, when utilizing omnidirectional antennas in small size networks both interference and half-duplex operation may be limiting factors for the spatial reuse. In this chapter we verify the above conjecture and also show that, for the same networks, it does not hold true when AAS are used even with moderated antenna beamwidths.

Our original contribution in this subject is related to the performance analysis and system design when utilizing AAS with GTDMA and its performance comparison with STDMA. The system design is done in order to maximize end-to-end throughput for unicast traffic (i.e. from a source node to a destination node). The throughput-delay characteristic is evaluated by discrete event simulations.

4.2 Generalized Time Division Multiple Access

In the traditional view of the time division multiple access (TDMA) scheme the time axis is divided into time slots, and each slot is preassigned to a different node. During its assigned slot the node is allowed to transmit freely, i.e. during the assigned slot all of the system's resources are devoted to that node. The slot assignments follow a predetermined pattern that repeats itself periodically; each such period is called a cycle or a frame. In the most basic TDMA schemes every

user has exactly one slot in every frame. More general TDMA schemes are adapted to traffic demands and several slots may be assigned to one node within a frame, referred to as Generalized TDMA [29]. The term has been used in the context of single hop networks in [29, pag. 20] for the case when user demands in a system are unequal. The shared wireless channel may be utilized more efficiently if, whenever possible, users with greater traffic demands receive more slots allocated within each frame than users with light traffic. This is done in the generalized TDMA scheme in which a user might be allocated more than one slot within a frame, with arbitrary distances between successive allocated slots.

We use the same term in the context of multihop wireless networks whenever no spatial reuse is exploited. Fig.4.1 shows the concept with a simple 4 node network. The network is defined by $\mathcal{N} = \{A, B, C, D\}$ and 6 links corresponding to the cardinality of the set of links $\mathcal{A} = \{(A,B),(B,A),(B,C),(C,B),(C,D),(D,C)\}$. Node A and D use node B and C as relaying nodes. Therefore the links between nodes B and C have more relative traffic than the links between node AB and CD. The number of (S,D) pairs routing traffic through each link is also indicated. To try to compensate for this difference in traffic in the example we decided to assign 1 slot for nodes A and D and 2 slots for nodes B and C. During its slot a node can transmit to any of its neighbors. For instance in slot 2 if node C has a packet for either node B, A or D it may forward the packet to node B or to node D according to the buffer type of rule. Note that this is not the only possible ordering and scheduling. Changing the ordering and scheduling in general results in different performance for the throughput-delay characteristics of the network.

As expounded by Rom and Sidi in [29, pag.31], the analysis of the system performance in a GTDMA scheme is much more complicated than the analysis for regular TDMA scheme. Even in the single hop scenario and fixed transmission data rate, no closed form expression exists for the throughput-delay characteristic due to the slot distribution. An important observation done by the authors for the single hop case is that, for the arrival pattern under consideration, the evenly spaced allocation of slots to users is better. They reported that "the evenly spaced allocation gives the minimal expected delay and the contiguous allocation gives the maximal expected delay for all values of arrival rate".

Adaptive Bit Rate in Generalized TDMA

In order to increase the transmission data rate, modern wireless technologies are able to utilize multilevel modulation and coding according to the channel quality conditions. Let us assume that the physical layer of the GTDMA system has a set of r discrete transmission rates, $\mathcal{R}_{set} = \{R_0, R_1, \ldots, R_{(r-1)}\}$, selected depending on the achieved SNR, that is the transmission from node i to node j utilizes the transmission rate R_{ij} such that:

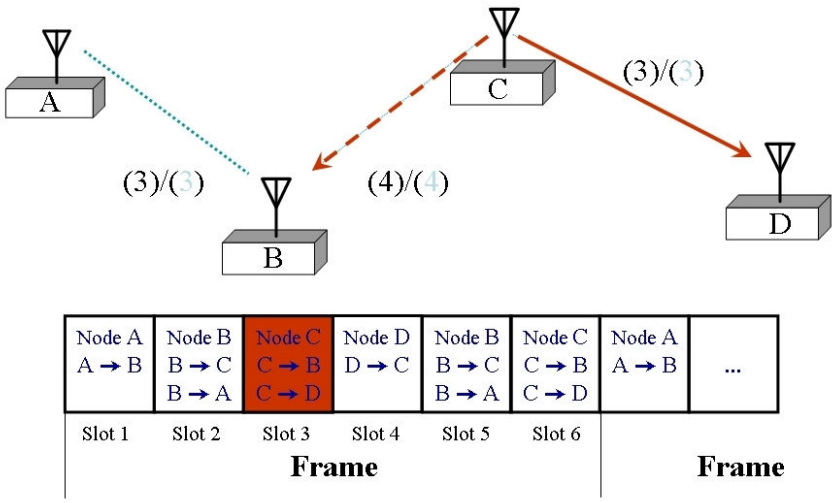

Figure 4.1: Simple example for GTDMA scheduling when four nodes comprise the network. Nodes A and D use nodes B and C as relaying nodes.

$$R_{ij}(\Gamma_{ij}) = \begin{cases} R_0\ , & \gamma_0 \leq \Gamma_{ij} < \gamma_1 \\ R_1\ , & \gamma_1 \leq \Gamma_{ij} < \gamma_2 \\ & \vdots \\ R_{(r-1)}\ , & \Gamma_{ij} \geq \gamma_{(r-1)} \end{cases} \tag{4.1}$$

where Γ_{ij} is the SNR at node j.

The above enhanced physical layer capability gives rise to the question: how does one account for both the differences in traffic and the adaptive bit rate capability of the nodes in an efficient way for the slot assignment in GTDMA with AAS? As illustrated in Fig.4.2, since a node can transmit at a higher data rate it may be possible that some nodes transmit more than one packet in their assigned slots.

As explained in section 3.4, the link traffic demand in a multihop radio network depends on both the external traffic and internal traffic due to the forwarding mechanism associated to the routing.

4.3 Slot Assigment Strategy

In unicast traffic, we use AAS with GTDMA to maximize the SNR by directional transmission and reception. The slot assignment is done to satisfy the relative traffic demand. Although in GTDMA the slot allocation is done in node basic,

to determine the number of slots allocated to each node we determine the relative traffic load passing though each link given by (3.19).

We define t_i as the number of slots assigned to node i and t_{ij} as the fraction of t_i used for packet transmissions on link (i, j), that is:

$$t_i = \sum_{\forall j \neq i} t_{ij} \ . \tag{4.2}$$

Note that $t_{ij} = 0$ for unfeasible links and $K_f = \sum_{\forall i} t_i$ is the frame length.

Under stable traffic conditions the traffic flow law must hold, that is

$$\Pi_l < \frac{t_{ij}}{K_f} R_{ij},$$

substituting (3.19) we get the following set of constraints for the assignment:

$$\frac{\lambda}{N(N-1)} T_{ij} < \frac{t_{ij}}{K_f} R_{ij}, \forall \text{ link } (i, j). \tag{4.3}$$

From (4.3) we observe that the maximum end-to-end throughput occurs when the above bound is achieved by at least one of the links, that is:

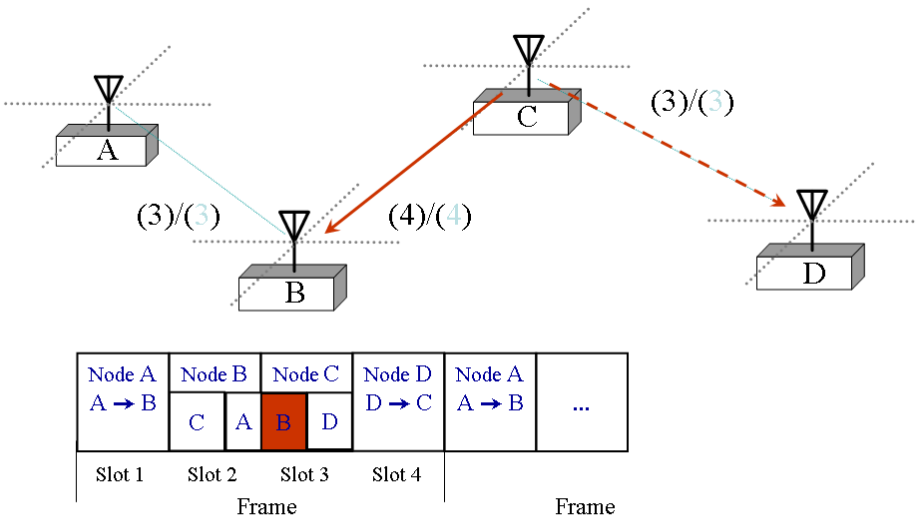

Figure 4.2: Simple example for GTDMA scheduling with variable transmission rate and AAS. Shorter frame length may result as compared to Fig.4.1.

$$\lambda^* = \min_{\forall(i,j)} \left(\frac{t_{ij}}{K_f} \frac{N(N-1)}{T_{ij}} R_{ij} \right) . \tag{4.4}$$

Since N and K_f are the same for the set of above inequalities the throughput is maximized by assigning t_{ij} such as:

$$t_{ij} \propto \frac{T_{ij}}{R_{ij}} \Rightarrow t_{ij} = \frac{T_{ij}}{R_{ij}} \max_{\forall(i,j)}(R_{ij}) , \tag{4.5}$$

where we have selected the maximum achievable rate as the proportionality constant. Therefore

$$t_i = \sum_{\forall j \neq i} t_{ij} = \max_{\forall(i,j)}(R_{ij}) \sum_{\substack{\forall j \neq i \\ R_{ij}>0}} \frac{T_{ij}}{R_{ij}} . \tag{4.6}$$

Finally, by doing this slot assignment, the maximum end-to-end throughput is given by:

$$\lambda^* = \frac{\max_{\forall(i,j)}(R_{ij}) N(N-1)}{K_f} = \frac{N(N-1)}{\sum_{i=1}^{N} \sum_{\substack{\forall j \neq i \\ R_{ij}>0}} \frac{T_{ij}}{R_{ij}}}. \tag{4.7}$$

Based on the above derivation the Generalized TDMA assigment is as follows:

Slot Assignment Procedure for GTDMA

Step 1: Compute the transmission rate for the set of feasible links on the network.

Step 2. Find the link relative traffic loads, $\boldsymbol{T}$.

Step 3. For each node i, assign $t_i = \sum_{\forall j \neq i} t_{ij} = \max_{\forall(i,j)}(R_{ij}) \sum_{\substack{\forall j \neq i \\ R_{ij}>0}} \frac{T_{ij}}{R_{ij}}$ slots.

Step 4. Distribute the slots uniformly in the frame by pseudo-random permutation.

The last step is in order to reduce the waiting time in queue that results from continuous slot allocations to each node. In our simulations we have observed a meaningful increase of the end-to-end delay for low traffic loads if step 4 is omitted.

4.4 Numerical evaluation

In this section we start by evaluating how close the system can approach the bound provided by (4.7) through discrete-event simulation. Since the slot assignment

relies on the statistical average for the time used for transmitting on a link, t_{ij}, a proper queue management has to be used. In our simulations we have implemented a modified FIFO (First In, First Out) Buffer operation for variable transmission rate. A node at the start of its slot begins transmitting the first packet in the buffer to the corresponding forwarding node at the allowed link bit rate; if the transmission rate is higher than the lowest rate there will be a remaining time that may be utilized to transmit another packet from the queue. In that case the next packet is examined and if the corresponding link bit rate to the forwarding node allows its transmission in the remaining time the transmission proceeds, otherwise the next packet in queue is examined and the procedure continues until reaching the end of the buffer or until the end of the slot-time. In our simulation we also relax our assumption of infinite buffer capacity to Buffer size of 500 packets for each node.

Regarding the SNR boundaries for rate selection in (4.1), they depend on several factors, including the background noise and the type of modulation scheme and coding utilized at the physical layer (PHY) of the system. In our numerical evaluations we use the Shannon capacity limit to establish the corresponding relation between the SNR and the transmission bit rate selected at the PHY, that is:

$$R(\gamma) < W \log_2 (1 + \gamma) \text{ bps}, \tag{4.8}$$

where W is the channel bandwidth (Hz) and γ is the SNR at the receiver site. We assume that the limit can be reached with equality. Hence, if the lowest data rate is R_0 and requires at least an SNR γ_0, the SNR boundaries can be found along the shannon capacity curve by:

$$\gamma_i = (1 + \gamma_0)^{\frac{R_i}{R_0}} - 1. \tag{4.9}$$

We use the node distribution of the sample networks shown in Fig.3.3 for numerical examples. We assume that $\gamma_o = 10$dB, therefore $\gamma_1 = 20.79$dB and $\gamma_2 = 41.66$ dB. The noise background at the receiver is computed by $P_{Noise} = kT_0BF_{sys}$, where $k = 1.38 \times 10^{-23}$ is the Boltzmann constant, $T_0 = 290$K, B is the noise equivalent bandwidth(assumed to be equal to the transmission bit rate) and a receiver Noise Figure $F_{sys} = 15$dB is assumed. The SNR for link (i, j) is computed by:

$$\Gamma_{ij} = \frac{P_i G_{ij} A_{ij} (\theta_{ij}) A_{ji} (\theta_{ji})}{kT_0BF_{sys}}$$

Fig.4.3 shows the increase in connectivity as a function of the antenna beamwidth when $P_i = 30$ dBm and flat-top switched-beam antennas are used. In our following evaluation and discussion is important to observe that multihopping is required from omni to 90^o antenna beamwidth with this setup.

Fig.4.4 shows the simulation result for the throughput-delay for network A when omni, 120^o, 90^o, 60^o, and 10^o antenna beamwidths are utilized. The traffic load

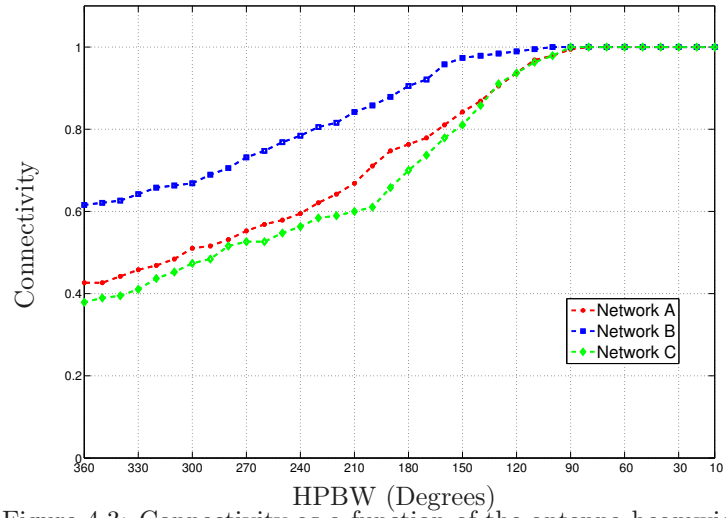

Figure 4.3: Connectivity as a function of the antenna beamwidth.

in the network was simulated by Poisson arrivals with mean from $0.1\lambda^*$ to $0.95\lambda^*$ evenly distributed among nodes; the average delay was found within 95% confidence interval. As the results show, the bound provided by (4.7) can be closely reached since it still provides a bounded end-to-end packet delay.

Before moving to our discussion about the improvement you may get by utilizing spatial reuse it is interesting to discuss which factors contribute to the main gain observed in GTDMA with AAS. Fig.4.5, 4.6 and 4.7 show the impact of using variable transmission rate (VR) as compared to Constant transmission Rate (CR). The maximum end-to-end throughput as a function of the antenna beamwidth is shown in Fig.4.5. For the multihop region, as the connectivity increases and the antenna beamwidth decreases, the throughput increases for both cases. Observe that if constant transmission bit rate is used only the increase in connectivity is exploited by the system. This is clearly shown in the figure by the use of constant transmission rate for antenna beamwidth narrower than 90^o.

The relative gain achieved by utilizing AAS with respect to the omnidirectional case is illustrated in Fig.4.6. In the multihop scenario both the utilization of variable rate and the increase in connectivity have a meaningful impact on the performance. In this numerical example we observe that in the multihop scenario a gain of up to 2, 2.15 and 2.48 is achieved as we approach the single hop scenario with 90^o antenna beamwidths by using variable rate. Fig.4.7 reveals that variable rate provides a very important contribution to the total gain; however, this gain is much higher as we approach the single hop region.

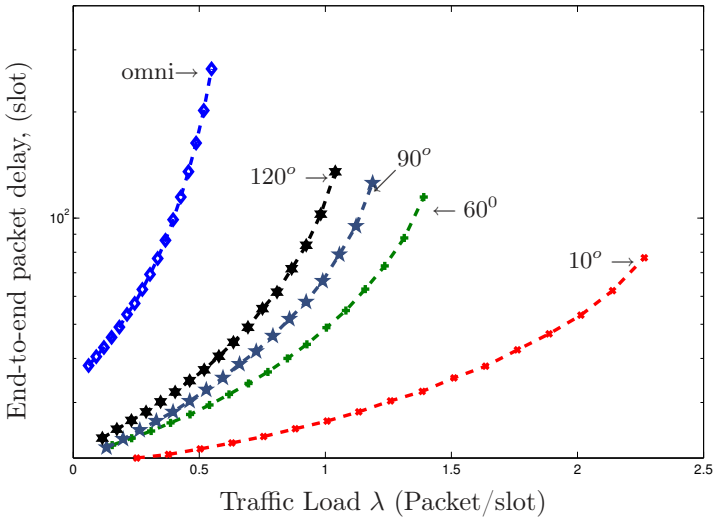

Figure 4.4: Throughput-Delay characteristic (Network A).

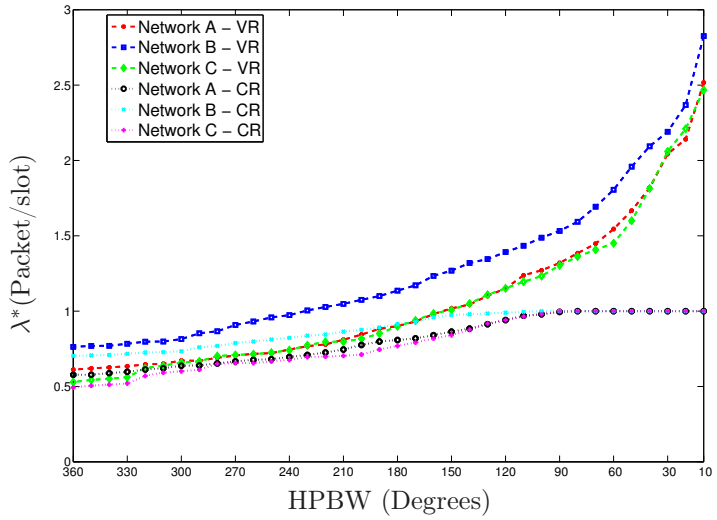

Figure 4.5: End-to-end throughput as a function of the antenna beamwidth when using Constant Rate(CR) and Variable Rate (VR).

4.5 Generalized TDMA versus Spatial TDMA

We would like to conclude our analysis here by going back to our earlier statement that for some small networks utilization of Generalized TDMA could be of interest.

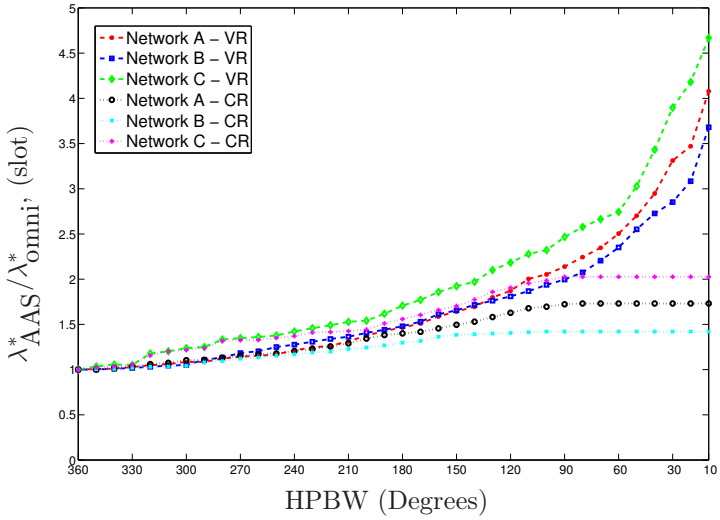

Figure 4.6: Relative Gain with respect to omnidirectional antennas when using Constant Rate(CR) and Variable Rate (VR).

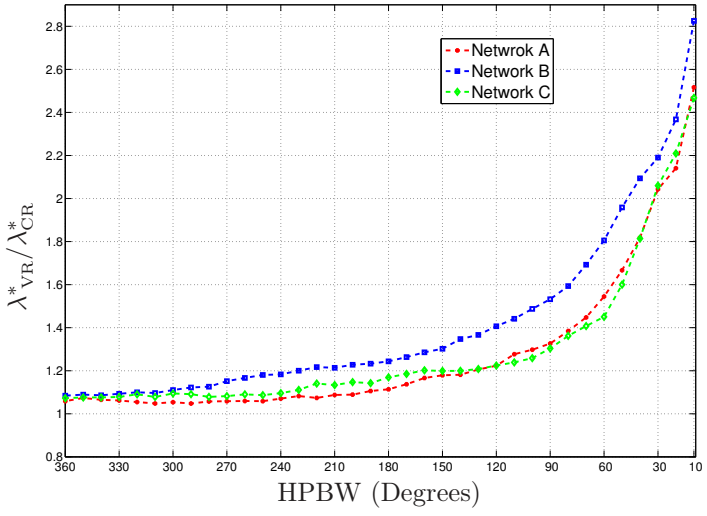

Figure 4.7: End-to-end throughput gain by variable data rate with respect to constant rate.

However the spatial reuse provided by STDMA is not fully exploited when using AAS. In the next chapter we analyze the design of STDMA as a way to better exploit the spatial dimension benefit provided by Advanced antenna systems.

However, at this stage and without going into the details of Spatial TDMA yet, Fig. 4.8 shows that the above statement may be "significantly" true with advanced antenna systems even if we just exploit the spatial reuse capability provided by the AAS. That is, compensating for the system complexity of the STDMA case we assume the system transmits at constant transmission rate R_0. For GTDMA, we assume variable rate with $\mathcal{R}_{set} = \{R_0, 2R_0, 4R_0\}$ is used.

It is interesting to observe that the performance when omnidirectional antennas are used is better for GTDMA since the gain by adaptive bit rate is higher than the gain achieved by only the spatial reuse with omnidirectional antennas. However, this condition changes when using AAS even in this example with rather wide antennas beamwidth of 120^o (3 sectors).

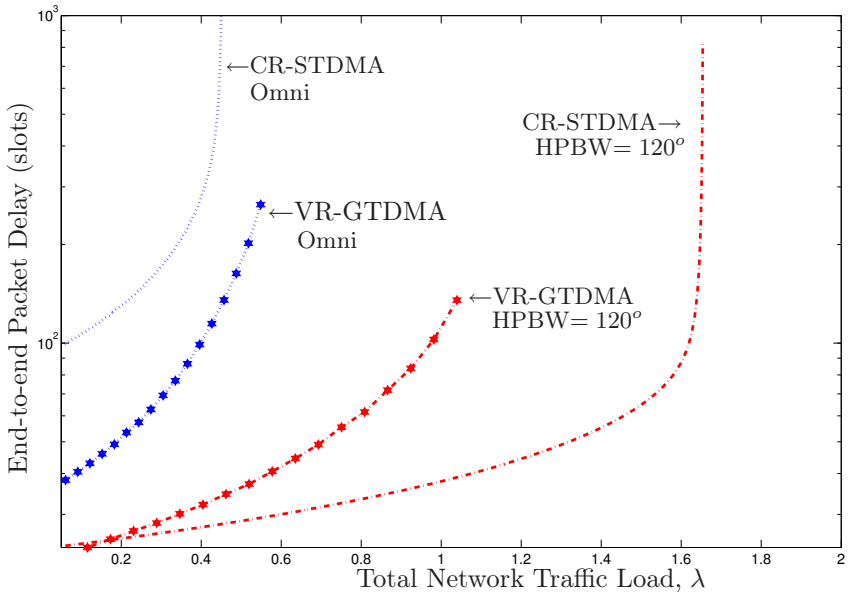

Figure 4.8: Variable rate GTDMA versus Constant transmission Rate STDMA (Network A in Fig.3.2). Constant transmission rate (R_0) is used for STDMA and Variable transmission rate for GTDMA (rate set $\mathcal{R}_{set} = \{R_0, 2R_0, 4R_0\}$).

4.6 Summary

In this chapter we have analyzed the utilization of advanced antenna systems in multihop wireless networks when Generalized TDMA is used as MAC protocol. By applying the flow conservation law the allocation strategy was derived in order to maximize the end-to-end throughput. Next, we have verified the closeness of the derived throughput bound by discrete event (stochastic) simulations. Bursty traffic was considered by Poisson packet arrivals and a modified FIFO priority queue was used to account for variable rate transmissions. Networks composed of nodes using AAS with long enough buffer sizes were used to show that the derived theoretical limit can be closely reached.

The numerical examples show that GTDMA can exploit the benefit of increased connectivity and higher transmission rate but does not exploit the spatial reuse benefit provided by AAS. We have compared the performance of GTDMA with variable transmission rate versus STDMA with constant(fixed) transmission rate. In our experiments we have used 20 nodes networks with average number of hops in the order of two hops. Our numerical examples have shown that when using omnidirectional antennas the gain achieved by variable rate with GTDMA was higher than the gain achieved by spatial reuse by Spatial TDMA. However this was not the case when utilizing AAS even with constant transmission rate and wide antenna beamwidths. We have compared both systems using a moderate antenna beamwidth of 120^o and found that the gain of STDMA with constant rate was large compared to the gain of GTDMA with variable rate.

Chapter 5

Heuristic Approach to Combine Routing and Scheduling in STDMA with AAS

In this chapter the use of beam-steering antennas together with the spatial time division multiple access protocol is analyzed and a novel routing and scheduling strategy to create the link assignment schedule is introduced. The new procedure takes advantage of the spatial filtering properties of the AAS.

5.1 Introduction

Spatial time division multiple access is a MAC protocol where conflicts are avoided by assigning node transmissions into a repetitive pattern of slots of finite length called a *s*chedule.

There are two frequently found slot assignment methods in STDMA called *n*ode assignment (or broadcast scheduling) and *l*ink assignment (or unicast scheduling) [56, 99]. In node assignment a given node i is allowed to transmit on a slot t to any of its neighboring nodes. Other nodes are also allowed to transmit on the same slot if they do not produce mutual conflict. For instance, on the same slot t another node k is allowed to transmit simultaneously to any of its neighboring nodes if the transmission does not cause conflicts with reception of i's transmission to its neighbors and vice versa. Due to this mechanism, node assignment strategies are more suitable for multicast traffic (i.e. from one source to many destinations) management [99].

On the other hand, Link assignment is a link-oriented method where links are assigned to transmit on a given slot within the schedule. For instance, if a given link (i, j) is assigned to transmit on slot k, it means that node i is allowed to transmit only to its neighbor node j on slot k. Other links could be allowed to transmit on the same slot if they don't produce mutual conflicts. Clearly, link assignment

is more suitable for unicast traffic (i.e. from one source to a single destination) management. The performance of STDMA with link assignment scheduling can be significantly improved by utilizing AAS for transmission and reception [60, 75]. To illustrate how link assignment strategy works, refer to Fig.5.1 where a simple 8 nodes network is shown. The (bi-directional) radio links are indicated by lines connecting the nodes. In this network it would, for example, seem feasible to reuse the time slots used for communication on the links $2 \rightarrow 3$ and $4 \rightarrow 6$, whereas $5 \rightarrow 4$ and $2 \rightarrow 1$ would probably not be able to share the same slot.

When assuming no interference caused by transmission of nodes that are more than two hops away, the optimal scheduling can be found by applying graph theory, such as graph coloring. More realistic models consider the aggregate interference of distant transmitters that may cause the SINR to fall below a required threshold for reliable reception. However, finding the "optimum" schedule for interference-based STDMA is in general a computationally hard problem to solve [26, 48]. Exhaustive search has been one method utilized for performance evaluations in some studies [56, 61]. Nonlinear optimization has been another method proposed recently [55, 58]. However, the complexity of the above methods grows exponentially with the number of links. This motivates one to seek good sub-optimal (heuristic) low complexity scheduling algorithms to satisfy end-to-end traffic demands. In MWN, route selection and the external traffic load determine the link traffic demand. Nevertheless, as we explain in the next section, route selection also influences the performance of the STDMA scheduling algorithms.

5.2 Routing & STDMA Scheduling

As presented in section 3.4, an uneven traffic distribution may result in a potential limiting factor of performance in MWN. In general, the uneven traffic distribution could be the result of:

I. Limited network connectivity

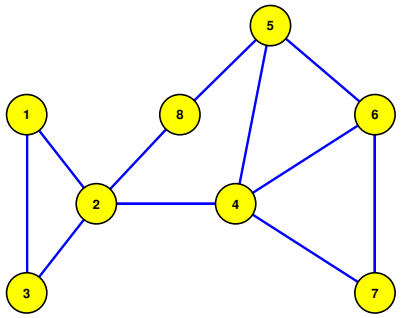

Figure 5.1: Multihop wireless network example with 8 nodes.

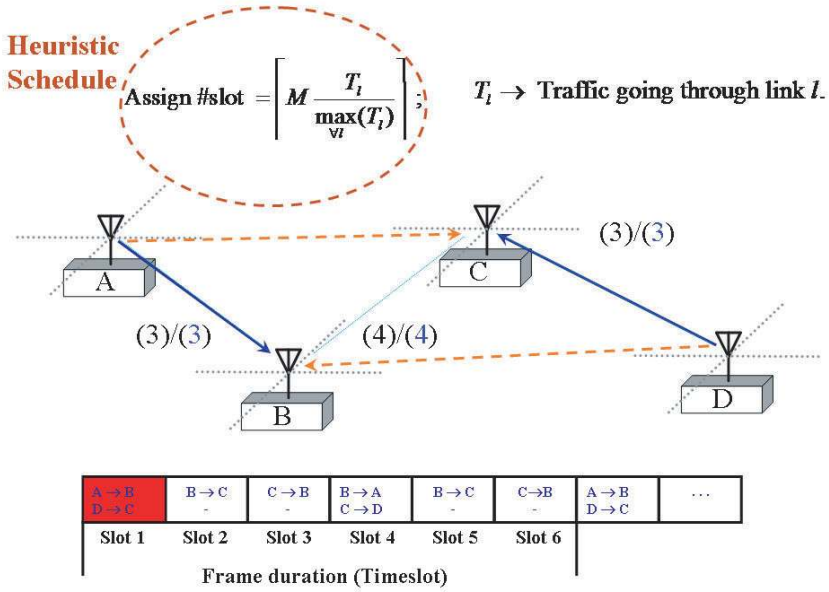

Figure 5.2: The figure illustrates the described simple example for STDMA scheduling with AAS when four nodes comprise a network with low connectivity($\mathcal{C} = 2/N = 0.5$).

Only some joint limiting paths (bottlenecks) are available between a number of (S,D) pairs;

II. Poor route selection when multiple options of paths exist
This may arise, for instance, when more than one path exists between a (S,D) pair and the one with lower capacity (or more congested) is selected.

Fig. 5.2 illustrates an example of limited network connectivity, network $\mathcal{G} = (\mathcal{N}, \mathcal{A})$, with $\mathcal{N} = \{A, B, C, D\}$ and feasible links $\mathcal{A} = \{(A, B), (B, A), (B, C), (C, B), (D, E), (E, D)\}$. Due to the limited connectivity the logical network topology corresponds to a tandem network with network connectivity $\mathcal{C} = 2/N$. Nodes A and D use node B and C as relaying nodes. Hence the links between nodes B and C carry more relative traffic than the links between node AB and CD.

One way to alleviate this problem is to implement schedule algorithms that take traffic distribution into account. These algorithms are commonly referred to as traffic-controlled or traffic sensitive algorithms [45, 50, 99]. For instance in the example shown in Fig. 5.2, the common heuristic scheduling algorithm compensates for the difference in traffic by allocating more slots to links between node B and C. The number of source-to-destination pairs routed through each link is $T_l = \{3, 3, 4, 4, 3, 3\}$. Hence, the algorithm assigns 2 slots to links between node BC

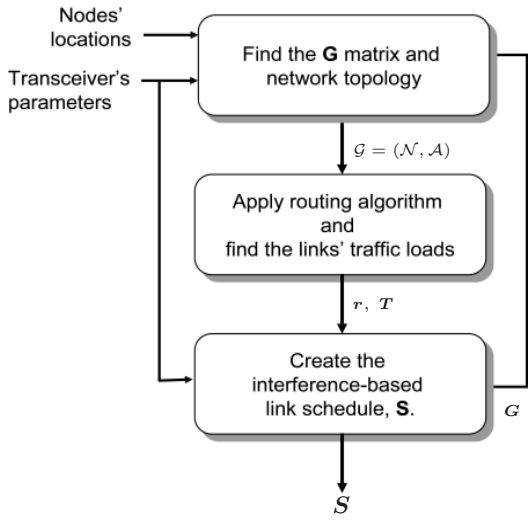

Figure 5.3: Method to construct the traffic-controlled schedule.

and one slot to links between node AB and CD. The nodes are equipped with a four sector switched-beam antenna system such that for instance in slot 1, link (A, B) can be scheduled together with link (D, C) since the received interference is limited by the spatial filtering from beam selection. In slot 2 link (B, C) activation precludes activation of any other link since nodes cannot transmit and receive at the same time nor receive from more than a single node at the same time. A similar situation occurs when link (C, B) is scheduled in slot 3. In slot 4 link (B, A) and (C, D) can be scheduled simultaneously. Then again (B, C) and (C, B) are scheduled to compensate for traffic demands. Note that this is not the only possible ordering and scheduling. Changing the ordering and scheduling in general results in different performances for the throughput-delay characteristics of the network.

The above procedure can be seen as a centralized cross-layer scheduling. The network layer information is accounted for by the relative traffic load and is used to create the link schedule (MAC sublayer). Fig.5.3 illustrates the simulation method utilized in [50, 99] to create the traffic controlled schedule. The procedure is an interference-based method where full knowledge of the radio propagation condition between nodes ($\boldsymbol{G}$ matrix) is assumed. In a real system, this information can be collected when the network is started and could be periodically updated, methods to do this can be found in [26, 38, 100]. With this information as input, the procedure starts by finding the network topology based on the link quality (received power level and sensitivity of the receiver). After that the Minimum Hop Algorithm (MHA) is used to select a particular path from each source node to destination

node. MHA minimizes the number of hops in a multihop "connection" and is independent of the access schedule and the actual traffic flows. For instance Dijkstra algorithm [96, pag.108-112] can be used to find the minimum hop route by setting equal cost for all links.

When setting the routing table, a decision has to be made if several paths with the same minimum number of hops are found. For instance, if we apply Dijkstra algorithm to a ring network with an even number of nodes, the result will be an unbalanced relative traffic load distribution, as illustrated in example 5.2.1.

Example 5.2.1 Consider the ring network made up of the set of nodes labeled $\mathcal{N} = \{1, 2, 3, 4\}$ and the links $\mathcal{A} = \{(1, 2), (2, 3), (3, 4), (4, 1)\}$ as illustrated in Fig.5.2.1. By applying Dijkstra algorithm with equal cost to all links we get the minimum hop routing table $\boldsymbol{r}$ and the relative traffic load matrix $\boldsymbol{T}$ shown in Fig.5.4.

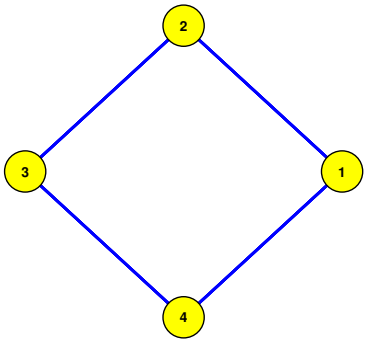

$$\boldsymbol{r} = \begin{bmatrix} 0 & 2 & 2 & 4 \\ 1 & 0 & 3 & 1 \\ 2 & 2 & 0 & 4 \\ 1 & 1 & 3 & 0 \end{bmatrix}$$

$$\boldsymbol{T} = \begin{bmatrix} 0 & 3 & 0 & 2 \\ 3 & 0 & 2 & 0 \\ 0 & 2 & 0 & 1 \\ 2 & 0 & 1 & 0 \end{bmatrix}$$

Figure 5.4: Four nodes ring network.

The entries r_{ij} in the routing table correspond to the label of the forwarding node used by node i to communicate with node j. As the relative traffic load matrix indicates, links with lower node labels get higher relative traffic. In ring networks such behavior appears only for an even number of nodes. ■

For multiple paths fulfilling the minimum distance, when the number of hops is used as decision criteria, a random selection of the path to be utilized seems to be a reasonable choice in comparison to selecting a fixed position (e.g. first or last) found path [1]. This strategy to select the routes is named random MHA in the following evaluations. In [90] MHA has been found to produce shorter packet delay when compared with some other routing algorithms on rough terrains justifying its use.

[1] Decisions of this type may occur for instance in Destination-Sequenced Distance Vector Routing (DSDV). In DSDV when given the choice between two paths with equal destination sequence numbers, the node selects the path with the shortest hop count. However, "if all metrics are equivalent, then the choice between routes is arbitrary" [97, pag. 278].

In Fig.5.3, the resulting routing table is used to compute the relative traffic load matrix $\boldsymbol{T}$ given by (3.20). $\boldsymbol{T}$, and the path gain matrix $\boldsymbol{G}$ are used as input to a traffic-controlled algorithm that aims to assign to each link a number of slots proportional to its relative traffic load. We will refer to this procedure as Minimum Hop Algorithm plus traffic-controlled Scheduling (MHA + TCS).

The schedule $\boldsymbol{S}$ can be expressed in matrix form with columns given by $\{\boldsymbol{s}_k, k = 1, 2, \ldots, K_f\}$; where K_f is the number of slots in the frame. Each column vector $\boldsymbol{s}_k = [s_1 \ \ldots \ s_L]^T$ holds the transmission rate that each link is scheduled to use in slot k and zero if the link is not allowed to transmit. For fixed rate systems, when using an interference-based algorithm to create the schedule, all links $(i, j) \in \boldsymbol{s}_k$ must satisfy equation (3.5).

In general, the aims of the traffic-controlled schedule algorithm are:

- to compensate for the uneven traffic distribution i.e. to satisfy traffic demands,
- maximize the network efficiency by maximizing the reuse of slots and
- minimize the schedule period K_f.

The optimal solution to this problem is NP-complete [48] [99, pag.12] and requires excessive computational effort for even moderately sized networks.

The MHA + TCS procedure's final step corresponds to creating a link schedule that takes into account the relative link traffic demands. Power control and advanced antenna systems are two well known methods commonly used in cellular systems. Further, the MHA + TCS method can straightforwardly be extended to include power control and advanced antennas for substantial improvement of the network efficiency. In particular, the use of advanced antenna systems may result in shorter schedule periods in comparison to omnidirectional antenna systems as indicated by the following proposition.

Proposition 5.1 *Let $\boldsymbol{s}_k$ be the set of links allowed to transmit in slot k using omnidirectional antennas in STDMA multihop wireless networks and let $\Gamma_{ij}^{(omni)}$ be the Signal-to-Interference plus Noise ratio for any link $(i, j) \in \boldsymbol{s}_k$ using constant transmission power. Let $\Gamma_{ij}^{(BS)}$ be the Signal-to-Interference plus Noise ratio for any link $(i, j) \in \boldsymbol{s}_k$ resulting from replacing the omnidirectional antenna system by adaptive beamforming antennas with higher antenna gain and Beam-Steering (BS) as an adaptation method for all nodes in the network. Then,*

$$\Gamma_{ij}^{(BS)} > \Gamma_{ij}^{(omni)} \ ; \ \forall \text{ links } (i, j) \in \boldsymbol{s}_k. \tag{5.1}$$

Proof: Let A_{max} be the maximum gain of the adaptive beamforming antenna, then the antenna radiation pattern is such that

$$A_{ij}(\theta) \leq A_{max} \; \forall \; \theta \; . \tag{5.2}$$

If beam-steering is used, in any link $(i,j) \in \boldsymbol{s}_k$, node i maximizes its antenna gain in the direction of node j and viceversa (the beam is, for example, electronically steered), meaning that

$$A_{ij}(\theta_{ij}) = A_{ji}(\theta_{ji}) = A_{max} \; . \tag{5.3}$$

For all links $(r,k) \in \boldsymbol{s}_k$ such that link $(r,k) \neq (i,j)$ follows from (5.2) and (5.3) that

$$A_{rk}(\theta_{rj}) A_{ji}(\theta_{jr}) \leq A_{max}^2 \; , \tag{5.4}$$

$$\sum_{\substack{\forall \text{ link } (r,k) \in \boldsymbol{s}_k \\ \text{link } (r,k) \neq \text{ link } (i,j)}} P_r G_{rj} A_{rk}(\theta_{rj}) A_{ji}(\theta_{jr}) \leq \sum_{\substack{\forall \text{ link } (r,k) \in \boldsymbol{s}_k \\ \text{link } (r,k) \neq \text{ link } (i,j)}} P_r G_{rj} A_{max}^2 \; , \tag{5.5}$$

Therefore, since the terms in (5.5) are greater than zero,

$$\frac{P_i G_{ij} A_{max}^2}{\displaystyle\sum_{\substack{\forall \text{ link } (r,k) \in \boldsymbol{s}_k \\ \text{link } (r,k) \neq \text{ link } (i,j)}} P_r G_{rj} A_{rk}(\theta_{rj}) A_{jr}(\theta_{jr}) + P_{Noise}} \geq \frac{P_i G_{ij}}{\displaystyle\sum_{\substack{\forall \text{ link } (r,k) \in \boldsymbol{s}_k \\ \text{link } (r,k) \neq \text{ link } (i,j)}} P_r G_{rj} + \frac{P_{Noise}}{A_{max}^2}} \tag{5.6}$$

When omnidirectional antennas are used, the right hand side of equation (5.6) gives a lower bound for SINR because $A_{max} > A_{omni}$.

□

As discussed previously, proposition 4.1 implies that higher reuse may be achieved as the antenna beamwidth is reduced. To create the link-schedule when AAS are used in a fixed rate and a constant transmission power system we propose the algorithm shown in Fig.5.5. This algorithm uses a similar approach to the one proposed for omnidirectional antennas by Grönkvist in [57].

The schedule, $\boldsymbol{S} \in \mathbb{R}^{L \times K_f}$, is created assigning transmission rights to each link on a number of slots proportional to its traffic load. We label the feasible links by $l = 1 \ldots L$. All feasible links are initiated in ListA and remain in ListA until getting their corresponding minimum required slot allocation (stored in the Min_Slot vector). Then they are moved to ListB where they may be allocated some additional slots. In order to search over different activation sets each time

a link is tested for activation, its priority is updated. If the link is allocated in the current slot (slot k), its corresponding priority hold in the vector Pri is set to zero. Otherwise, its priority is incremented proportionally to its relative traffic load. Both lists are ordered according to the link priority at the end of each slot allocation. Besides allocating the link capacity required, the procedure aims to distribute the slot assigned to each link uniformly along the frame to reduce the waiting time in queue.

While creating the schedule, the problem of compensating for uneven traffic distribution by MHA + TCS is done basically by assigning a number of slots proportional to the traffic load of a given link. We can see this algorithm as one solution to an optimization problem where the objective function is to maximize the end-to-end network throughput, λ^*, for the whole network. To explain this, we define n_{ij} to be the number of slots within a period of the schedule, K_f, allocated

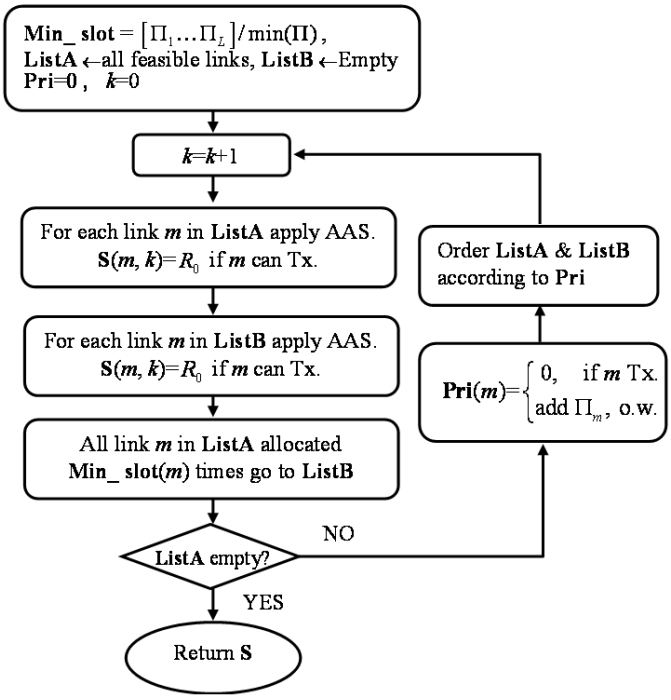

Figure 5.5: Flow chart of a heuristic traffic-controlled algorithm with advanced antenna systems.

to link (i, j); then the relative link capacity C_{ij} is given by:

$$C_{ij} = \frac{n_{ij}}{K_f} \ , \tag{5.7}$$

which constitute the elements of the network *c*apacity matrix $\boldsymbol{C}$.

The values for C_{ij} and the relative traffic load are all we need for an estimation of the maximum end-to-end network throughput λ^*. Assuming infinite buffer length, if the average traffic load routed through link (i, j) is $\lambda_{i,j}$, for stable condition $\lambda_{i,j}$ must be lower than C_{ij}. Consequently, the maximum end-to-end network throughput over any link that produces a finite packet delay, D_{ij}, is given by [99]:

$$\lambda < \lambda^* = N(N-1) \min_{\forall \text{ link } (i,j)} \left\{ \frac{n_{ij}}{K_f T_{ij}} \right\} \ . \tag{5.8}$$

Equation (5.8) reveals that a link schedule that utilizes the shortest frame length while at the same time assigning a number of slots proportional to the relative traffic load for all links maximizes λ^*. Therefore, as previously stated, the MHA + TCS aims to maximize the end-to-end throughput once the route selection has been done. However, the frame length K_f is also a function of n_{ij} which in turn is a function of the spatial reusability of slots and therefore influenced by the multiple access interference, network topology and routing. In addition to interference, the schedule's period is also influenced by the fact that a node cannot receive from more than a single source, as illustrated by the following example.

Example 5.2.2 Let us consider the case illustrated in Fig.5.6 where all nodes select a route to transmit to node E using narrow beam-steering antennas such that the multiple access interference is effectively eliminated. If the minimum hop algorithm is applied for route selection, two possible relative traffic distributions may result as indicated by the number over each directed link on the graph. In this example, link (D,E) carries 3 times more traffic than links (A,D), (B,D), and (C,E) if Route selection 1 is the result of the MHA. If we use a traffic-controlled schedule, link (A,D) must be guaranteed 3 slots. The resulting schedule has frame length $K_f = 5$ slots with a total number of slot assignments of 7 in the frame, corresponding to 7/5 total link capacity. If route selection 2 is used as an input to the traffic controlled algorithm then there will be a total link capacity of $8/4 = 2$ which is more efficient. The resulting maximum throughput is 1/5 for route selection 1 and 1/4 for route selection 2, which corresponds to 25% higher end-to-end throughput. ■

As the example shows, it is possible to implement a better combined routing & scheduling approach than the MHA + TCS to improve the system performance in terms of the end-to-end throughput. In order to do that we introduce the following approach.

Reuse Adaptive Minimum Hop Algorithm (RA-MHA)

In MHA + TCS routing information is used by the MAC protocol through the relative traffic load. Two-way information could be used as a way to integrate the

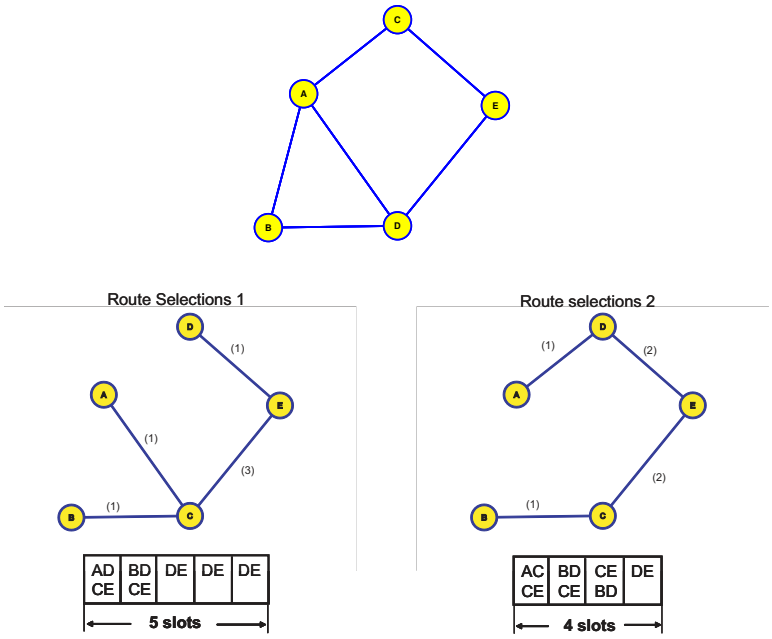

Figure 5.6: Example of the impact of route selection when effective reduction of MAI is achieved by using narrow beamwidth antennas.

routing and schedule better, that is from routing to the traffic schedule algorithm and from the scheduling to a routing that takes into account the resulting link capacity. Fig.5.7 illustrates the procedure that we refer as Reuse Adaptive Minimum Hop Algorithm (RA-MHA).

Similar to the previous method, the algorithm starts by computing the $\boldsymbol{G}$ matrix based on node locations and the terrain database. The second step aims to spread the traffic with the objective of spreading the multiple access interference. This is achieved by employing the routing decision for RA-MHA (Appendix A), which takes into account the set of minimum hop paths and capacity assigned to each link for route selection. In this step, it is assumed that all links have the same capacity ($C_{ij} = 1$) and the generated routing table is labeled $\boldsymbol{r}_1$ for later decision. The relative traffic load (T_{ij}) produced by $\boldsymbol{r}_1$ for every link can be computed and is used in the next step to find the schedule as an output by applying a Traffic Controlled Schedule (TCS) algorithm.

From the resulting schedule the number of slots assigned to each link and the period of the schedule can be found to compute the resulting capacity of each link; i.e. $C_{ij} = n_{ij}/K_f$. The relative traffic load matrix $\boldsymbol{T}$ and capacity matrix $\boldsymbol{C}$ are used in the next step to find the maximum throughput achieved with the routing $\boldsymbol{r}_1$ using (5.8).

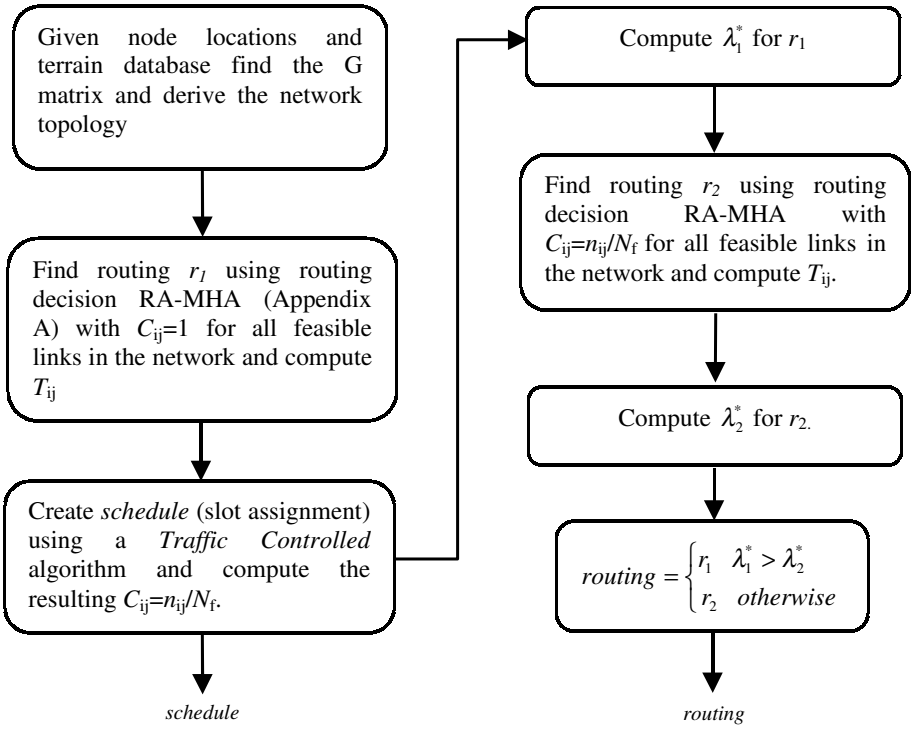

Figure 5.7: Procedure to create the link schedule for STDMA called Reuse Adaptive Minimum Hop Algorithm RA-MHA.

The next step aims to improve the route selection by considering the actual resulting capacity matrix $\boldsymbol{C}$. The capacity assigned to each link by the schedule is used to find a new routing table $\boldsymbol{r}_2$ with the routing decision for RA-MHA. Next, the maximum throughput achieved by routing $\boldsymbol{r}_2$ and the schedule is computed. Finally, the routing to be used is the one that produces the highest throughput. The difference between $\boldsymbol{r}_2$ and $\boldsymbol{r}_1$ is that $\boldsymbol{r}_2$ utilizes the real network capacity obtained by the traffic-controlled algorithm to try to maximize the throughput.

The main idea of the routing decision for RA-MHA is described here and a detailed step by step algorithm can be found in appendix A. The required inputs are the network topology and link capacity C_{ij}. The algorithm could be summarized by,

I. Collect the set of paths with the shortest distance between all (S, D) pairs in the network. MHA can be used to find the set of paths.

II. Put (S, D) pairs in ascending order according to the number of possible paths. If two (S, D) pairs have an equal number of possible paths, give priority to

the one with the higher number of hops.

III. From the set of paths for each (S, D) pair, select the one that produces $\max\{\min\{C_{ij}/T_{ij}\}\}$ for all links within the path and update the traffic load for all links within the selected path with $T_{ij} = T_{ij} + 1$.

IV. Repeat III until all (S, D) pairs have been considered.

Note that in step II, priority is given to the path with longer distance since its selection will affect a higher number of links. Every time a route is selected the relative traffic load is updated, adding one to all links within the selected path to influence the next routing decision. Note that the increment by 1 in T_{ij} is the result of the assumption of even traffic load among nodes, however it could be modified to include differences in traffic between different (S, D) pairs. Note also that the resulting routing table used by each node is a matrix (rather than a vector as in MHA), with row and column indexes corresponding to sources and destinations respectively, and the value held is the index of the relaying node to be used to deliver the packet.

In order to evaluate the performance of RA-MHA we utilize an analytical model approximation for the throughput-delay characteristic of STDMA.

5.3 Analytical Model for STDMA

As described in section 3.5, a randomly selected packet transmitted from node S to node D experiences a random delay D_{SD} that is the sum of the delays on every link utilized to route the packet. Averaging over all the equal likely (S, D) pairs in the network, the expected *e*nd-to-end delay is given by

$$E[D] = \sum_{\forall \text{ link } (i,j)} \frac{T_{ij}}{N(N-1)} E[D_{ij}] \,, \tag{5.9}$$

Although an exact analysis for $E[D_{ij}]$ (the expected packet delay over link (i, j)) appears to be difficult [34, 63] an approximate model can be employed to obtain a numerical estimation. For this purpose the following assumptions are needed:

I. each node uses an infinite buffer length for every feasible outgoing link,

II. packet arrival time to be transmitted over each link is poisson distributed with arrival rate λ_{ij}, and

III. the slots assigned to link (i, j), n_{ij}, are uniformly distributed within the schedule.

Assumption II implies that packet arrival to each link is independent from the delay and queue process over the previous relaying link. This is known as Kleinrock's principle of independence [101]. If the above assumptions are used, the expected packet delay through link (i, j), $E[D_{ij}]$ could be modeled as the resulting packet delay in a TDMA system with a frame length K_f/n_{ij}, with a packet transmission time of 1 slot (M/D/1 queueing model) [[29], page 13]. Hence, the equation (3.21) can be approximated by (5.10).

$$E[D] \approx \sum_{\forall \text{ link } (i,j)} \frac{\lambda_{ij}}{\lambda} \left[\frac{1}{2(C_{ij} - \lambda_{ij})} + 1 \right] \quad \text{Slot.} \tag{5.10}$$

5.4 Numerical Results

Sample networks A, B and C in Fig.3.3 have been used to evaluate the performance result of MHA + TCS and RA-MHA. Network A is a sparse network with relatively weak links but reasonably connected with an average 7.5 neighbors per node and an average number of hops between any (S, D) pair of 1.8 hops. On the other hand network B is more dense getting a better connected network than A, with an average 10.2 neighbors per node and an average number of 1.5 hops. Network C is much less connected than A with only 6.9 neighbors on average per node needing on the average 2.1 hops to send a packet between a (S, D) pair. Each node transmits with constant power that produces a maximum radio range of 40 km with propagation constant $\alpha = 3$.

First we verify that equation (5.10) does not give favorable results for either MHA + TCS or RA-MHA. In Fig.5.8 we have evaluated the approximation by utilizing computer simulations for network A when beam-steering antenna systems of 60^o beamwidth are used. In the simulation, external packets arriving at each node were generated according to a Poisson process with equally likely destination among nodes. Each node had a 100 packet buffer length First-In-First-Out (FIFO) for each outgoing link where transit and local packets were placed for transmission after its reception. As shown in the figure, the model produces a relatively small underestimation for low traffic for both methods. For moderate and relatively high traffic, a more accurate result is achieved. In [70] we have evaluated the approximation as given by (5.10) for various topologies, traffic loads and network sizes showing that it provides a reasonable estimation for other network topologies as well.

Fig. 5.9 shows the cumulative distribution function of the maximum throughput for networks RA-MHA and random MHA + TCS with 100 independent trials. Furthermore, Fig.5.10 shows the end-to-end packet delay versus the external total traffic load, λ (a single snapshot in random MHA was used in this case). Similar results were found for networks B and C and can be found in [102]. Note that the maximum throughput using RA-MHA (indicated with *) occurs with probability one, therefore the CDF is a unitary step function $u(\lambda - \lambda^*)$.

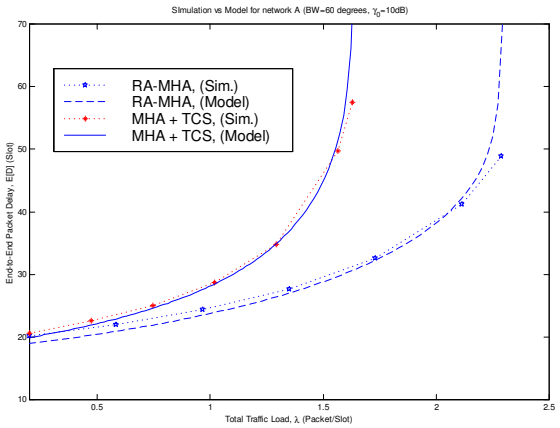

Figure 5.8: Approximation (5.10) versus simulation for a randomly network with 20 nodes.

As expected, when narrow antenna beamwidth is used the new method (RA-MHA) may produce significantly higher throughput than random MHA + TCS. For instance, the throughput improvement applying RA-MHA with 60^o antennas was 32%, 6% and 18% higher throughput for network A, B and C respectively, when compared to the mean value achieved with random MHA + TCS. The lowest improvement in network B is produced because nodes are very close to each other as revealed by its topology. Note that in networks A the same throughput is achieved with 60^o and 10^o antennas in Fig.5.10. This indicates that interference is effectively reduces by the beam-steering antenna system already with 60^o.

The results in Fig.5.10 demonstrate that the use of RA-MHA may also result in lower delays for almost all traffic conditions with respect to MHA + TCS. An interesting result is that higher maximum throughput is achieved with 120^o antenna beamwidth with RA-MHA than with 60^o and 10^o with MHA + TCS. As before, note that little improvement is achieved in network A when 10^o antennas are used with respect to 60^o antennas.

Fig.5.11 and 5.12 summarize the maximum throughput improvement obtained by RA-MHA compared with the mean value achieved with MHA + TCS. In scenarios where nodes are close to each other, as in sample network B, higher improvement is obtained with very narrow antenna beamwidth. The gain with omnidirectional antennas is very small, suggesting that the traffic-controlled schedule algorithm effectively manage the uneven traffic distribution created by the routing because interference dominates. Furthermore, the results demonstrate that AAS can produce a tremendous capacity improvement with respect to omnidirectional antennas with relatively simple antennas arrays (big improvement with only 120^o antenna beamwidth was achieved).

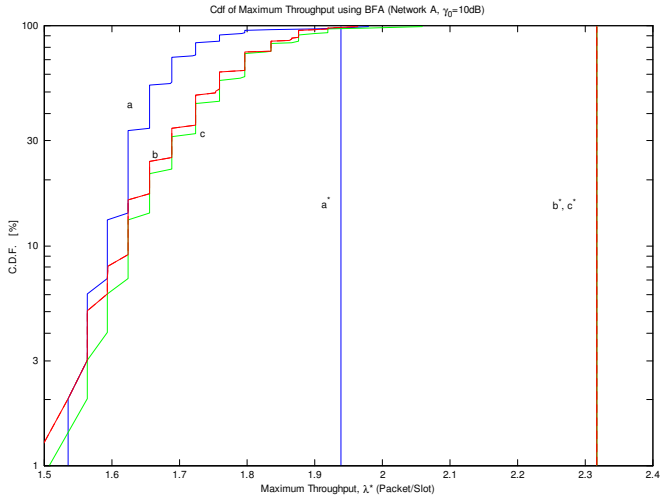

Figure 5.9: Cumulative distribution function of maximum throughput using beam-steering antenna systems (Network A). On the graph, letters a, b and c correspond to MHA + TCS with 120^o, 60^o and 10^o respectively. The use of RA-MHA is indicated with a*, b* and c*.

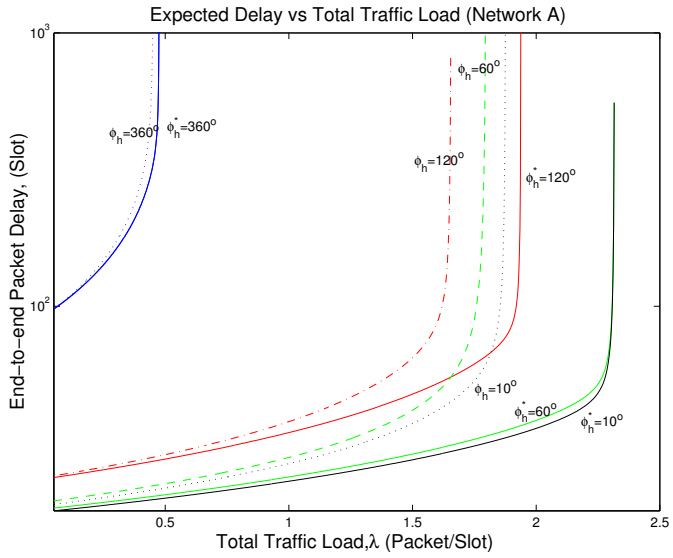

Figure 5.10: Packet Delay vs. traffic load (Network A).
MHA + TCS : $\phi_h = 360^o$, $\phi_h = 120^o$, $\phi_h = 60^o$, and $\phi_h = 10^o$ beamwidth.
RA-MHA: $\phi_h^* = 360^o$, $\phi_h^* = 120^o$, $\phi_h^* = 60^o$ and $\phi_h^* = 10^o$ beamwidth.

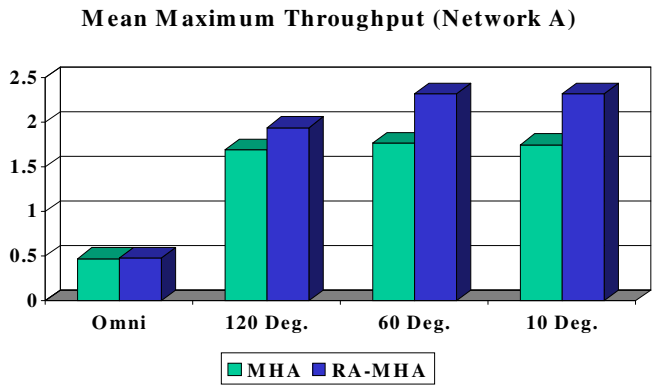

Figure 5.11: Maximum throughput for different antenna beamwidths (Network A).

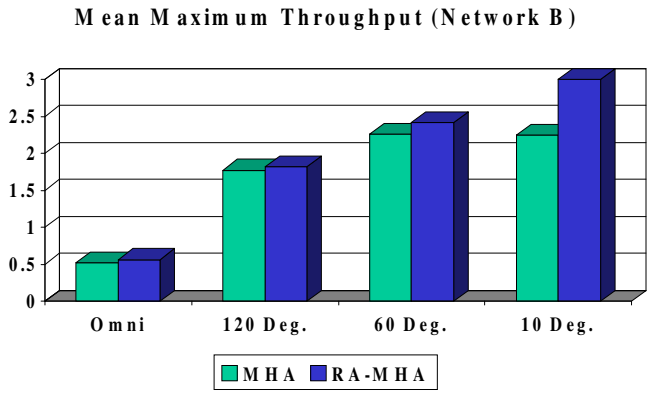

Figure 5.12: Maximum throughput for different antenna beamwidths (Network B).

5.5 Summary

In this chapter we have analyzed the utilization of Advanced Antenna Systems (AAS) with the conflict-free MAC protocol called Spatial Time Division Multiple Access (STDMA). Networks where nodes were equipped with beam-steering antennas and transmit with fixed rate and constant power were considered. Link assignment scheduling was performed by extending existing heuristic algorithms to utilize AAS. It has been demonstrated that if in a given slot the transmitting node and the receiving node adapt their antennas to maximize the received power (referred as beam-steering), the resulting SINR is reduced compared to the omnidirectional case as the antenna beamwidth reduces, potentially increasing the slot reuse. The results demonstrate that utilization of AAS produces a tremendous capacity improvement with respect to omnidirectional antennas with relatively simple antenna arrays (big improvement with only 120^o antenna beamwidth was found).

Routing was found to be a very important factor limiting the potential network throughput. When interference reduction measures such as narrow antenna beamwidth are used, the fact that a node cannot receive and transmit at the same time (half-duplex transceiver) becomes an important limiting factor. To improve the network performance a novel procedure to create the link schedule that combines routing & scheduling, called Reused Adaptive Minimum Hop Algorithm, was introduced and its performance was evaluated. Both lower end-to-end packet delay and higher throughput were demonstrated through application of the new approach.

The proposed algorithm utilizes the minimum number of hops, link traffic load and allocated link capacity. Other metrics have been investigated later by other researchers in this area, for instance utilization of the link quality through the link transmission rate in [62] and by the SINR in [103]. A comparison between the performance using other metrics, including the link transmission rate, to the metrics used by RA-MHA can be found in [104]. In addition, by the time of writing this thesis, some wireless equipment already incorporates this type of enhanced routing for wireless multihop networks. For instance the IEEE 802.11a/b/g based (mesh)equipment in [105] indicates the utilization of the number of hops together with the signal strength for cost metric routing.

Chapter 6

Fixed-Rate STDMA Systems with Advanced Antennas and Power Control

In the previous chapter the system was assumed to use constant transmission power and fixed transmission data rate. The advantage of such a system is simplicity compared to systems where adjustment of transmission power is possible (power control). However, there are two main reasons that may motivate the use of power control schemes in fixed data rate STDMA systems. First, the transmission power affects the link quality and interference environment, therefore by adjusting the transmission power higher spatial reuse might be possible. Secondly, even if a higher number of simultaneous transmission is not possible (e.g. because of blocking), valuable terminals' energy could be wasted by transmitting with constant power since some links might get an SINR in excess of that required for reliable communication.

In this chapter we study the utilization of power control and advanced antenna for fixed-rate systems in STDMA.

6.1 Introduction

In the previous chapter we introduced a heuristic scheduling algorithm for constant transmission power with advanced antenna systems (see Fig.5.5). In this chapter we extend the proposed link scheduling algorithm to combine AAS and SINR balancing power control. Furthermore, we present a methodology to benchmark the performance of the heuristic schemes to the performance bound provided by optimal schedule found by nonlinear optimization. Nonlinear optimization methods applied to the radio resource allocation problem for WMN and STDMA have been formulated recently. For instance in [94] the utilization of flat-top sector antennas and power control for one-hop transmission requests was studied. Björklund et al.

in [55] have proposed the use of nonlinear optimization method by a column generation approach to create the STDMA schedule. Johansson and Xiao in [58] has presented a column generation approach to find the "optimal" end-to-end communication rates, (multiple-path) routing, power allocation and transmission schedule with variable slot lengths. However, as expounded by the authors, the approach has exponential complexity in the number of links limiting the network size that can be studied. Nevertheless, in this chapter we extend their proposed method to also address AAS. We use the results from the optimal schedule to compare the performance achieved by our proposed heuristic schemes in networks with nodes equipped with beam-steering circular arrays.

6.2 General System Considerations

The main focus in the following analysis is on the methodology of analysis and performance evaluation of link scheduling in fixed-rate systems with AAS with and without power control. Therefore, in order to compare systems under commonly known conditions we use one-way routing information exchanged to determine the link traffic demand and create the link scheduling (section 5.2). The Dijkstra algorithm [96] is used to find the minimum hop route from a source node to a destination node.

Antenna Systems

We study the case when the network is deployed with all nodes equipped with AAS and also the reference case when the nodes utilize omnidirectional antennas. Beam-steering circular arrays have been selected as the AAS (see section 3.1). Fig.6.1 shows examples of the antenna radiation patterns utilized by a node (node 2) to transmit to another node (node 1 (left)/node 3 (right)) utilizing a circular array antenna with 60^o half-power beamwidth (HPBW).

It is assumed that the time domain is divided into slots, each long enough to transmit one data packet using a bit rate R_0 bps. In a given slot, a set of links are scheduled for transmission if the SINR given by (3.5) is greater than or equal to γ_0.

For mathematical convenience, we use the labels $l = 1 \dots L$ ($L \leq N(N-1)$) for the set of feasible links in the network. In the following, we use the variables l and m to indicate link labels. Hence the expression for the SINR in (3.5) can be rewritten by:

$$\Gamma_l = \frac{G_{ll} F_{ll} P_l}{P_{Noise} + \sum\limits_{\forall m \neq l} G_{ml} F_{ml} P_m x_m} > \gamma_0, \tag{6.1}$$

where G_{ml} corresponds to the path gain between the transmitting node on link m and the receiving node on link l, P_m is the power used by the transmitting node on link m, and the antenna factor is mapped into the link representation by $F_{ml} = A_{rk}(\theta_{rj}) A_{ji}(\theta_{jr})$.

Network Topologies

Connectivity is commonly used as an important network parameter to characterize the network topology [57]. Recall that the network connectivity is given by (3.8). However, two networks could have the same *connectivity* but still be very different in both physical and logical topology. In order to observe the performance for those cases, the networks used in this study are generated by randomly located nodes and their radio ranges are progressively increased until reaching a target *connectivity*.

In our evaluation, we use 300 sample network topologies deployed over a 20×20 km^2 area with $\mathcal{C} \in [2/N, 1]$. The antenna system is changed maintaining the network topology by finding the required maximum transmission power,

$$P_{\max} = \frac{P_{Noise}\gamma_o}{\min\limits_{\forall \text{ feasible } \text{link}(i,j)} [G_{ij}A_{ij}(\theta_{ij})A_{ji}(\theta_{ji})]} \tag{6.2}$$

where P_{Noise} is the noise power and γ_o is the SNR for a link to be reliable in the absence of multiple access interference.

Fig.6.2 shows a sample network used in our performance evaluation illustrating the antenna pattern and the transmission power level used for one slot transmisision activated a fraction α_1 of the time length of the *schedule*.

Performance Measure

As presented in section 3.5 the common performance measures utilized in WMN are the *End-to-end network throughput* and the average *End-to-end packet delay*.

In this chapter we are particularly interested in the maximum end-to-end network throughput, λ^*, defined as the upper bound limit to the maximum total external traffic load that produces finite average end-to-end packet delay for all source-to-destination pairs in the network. This leads us to a meeting point for

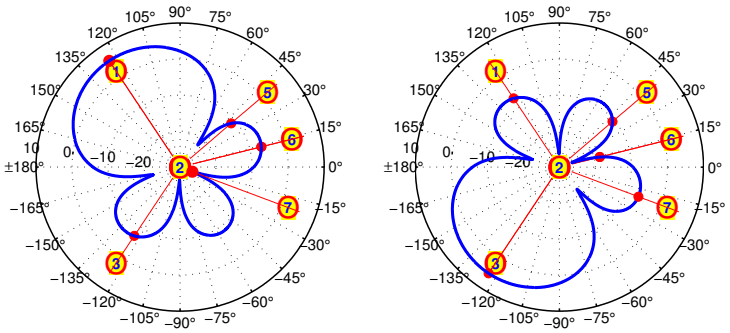

Figure 6.1: Circular Array Antenna azimuthal radiation pattern utilized by node 2 to transmit to node 1 (left) and node 3 (right). The interference reduction toward other node directions is also illustrated.

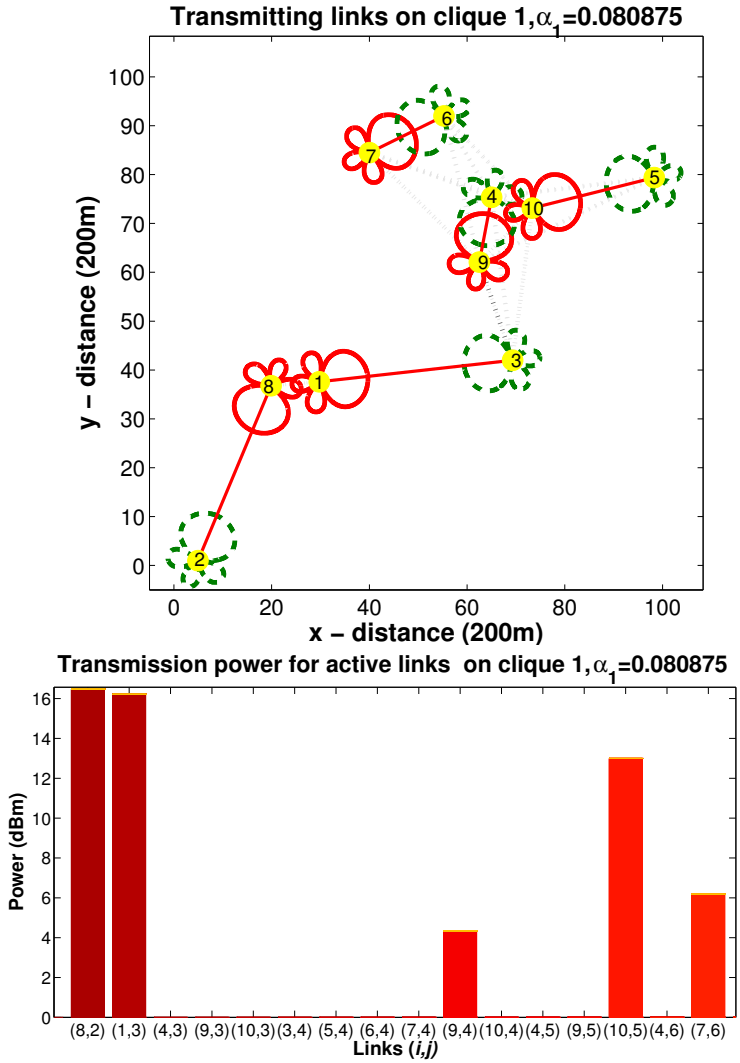

Figure 6.2: A sample network ($\mathcal{C} = 0.42$) and a set of simultaneously transmitting links (a *clique*) in the STDMA *schedule* when using Beam-Steering with 60^o Circular array beamwidth. The transmitting antenna radiation pattern is illustrated by a solid line and the receiving antenna pattern by dashed lines. The allocated transmission power for 10 dB SINR is also shown.

fairness, throughput and delay. Fairness is a key issue in allocating the network resources. For instance, maximizing the overall network throughput can lead to an extremely unfair allocation of resources to users [106] and results in an unbounded average end-to-end packet delay (e.g. allocation of zero capacity to some links).

This motivates one to study and design the system to maximize the end-to-end network throughput to all source to destination pairs.

6.3 STDMA Scheduling for Fixed Rate Systems

We represent by $\boldsymbol{S} \in \Re^{L\times K}$ the compatible link activation sets utilized for the STDMA link schedule. The column vectors of $\boldsymbol{S}$, $\boldsymbol{s}_k = [s_1 \ \dots \ s_L]^T$, hold the transmission bit rate for links that can transmit simultaneously and zero for those that are not allowed to transmit. The columns of $\boldsymbol{S}$ can be linearly combined to create the STDMA *schedule* by defining the vector of weights $\boldsymbol{\alpha} = [\alpha_1 \dots \alpha_K]^T$ corresponding to the fraction of the time that each column vector of $\boldsymbol{S}$ is activated within a STDMA frame. Hence, the allocated link capacity, $\boldsymbol{c} = [c_1 \dots c_L]^T$ is given by

$$\boldsymbol{c} = \boldsymbol{S}\boldsymbol{\alpha} \ ; \qquad \sum_{k=1}^{K} \alpha_k = 1. \tag{6.3}$$

For instance, in a WMN with L feasible links, if spacial reuse is not possible, $\boldsymbol{S}$ is a diagonal matrix as follows:

$$\boldsymbol{S} = R_0 \boldsymbol{I}_L = \begin{bmatrix} R_0 & \cdots & 0 \\ \vdots & \ddots & \vdots \\ 0 & \cdots & R_0 \end{bmatrix}.$$

Assuming infinite buffer capacity for each link, according to the flow conservation law and stability condition, (6.4) must hold.

$$\boldsymbol{\Pi} = \boldsymbol{R}\boldsymbol{\Lambda} \prec \boldsymbol{c} \ ; \quad \boldsymbol{\Lambda} \succeq \boldsymbol{0} \, , \tag{6.4}$$

where, as defined in section 3.4, $\boldsymbol{\Lambda} = [\ \lambda_1 \ \dots \ \lambda_{N(N-1)}\ ]^T$ is the external traffic load, $\boldsymbol{R}$ is the *link-route incident matrix*, and $\boldsymbol{\Pi} = [\ \Pi_1 \ \dots \ \Pi_L\ ]^T$ is the link traffic.

In general, the capacity allocation to each link can be done to maximize an objective function (see for instance [106] and [107]) and can be formulated as an optimization problem by:

$$\begin{aligned} &\text{maximize} \quad u(\boldsymbol{\Lambda}) \\ &\text{subject to} \quad \boldsymbol{R}\boldsymbol{\Lambda} \preceq \boldsymbol{S}\boldsymbol{\alpha} \quad ; \sum_{k=1}^{K} \alpha_k = 1 \\ &\boldsymbol{\Lambda} \succeq \boldsymbol{0} \quad ; \boldsymbol{\alpha} \succeq \boldsymbol{0} \end{aligned} \tag{6.5}$$

The optimum allocation for that problem is in general computationally hard to solve since it depends on the selection of links scheduled for transmission in each slot. The number of combinations to find the column vectors in $\boldsymbol{S}$ grows exponentially with the number of links. However, for relatively small networks, some methods exist to find the solution.

Nonlinear optimization approach for scheduling

We use the formulation by Johansson and Xiao in [58] for the allocation problem as expressed by (6.5) and apply the column generation method (in the following referred as the convex optimization method) to find the column vectors of $\boldsymbol{S}$ that maximize the minimum source-to-destination rates (max-min fair rate scheduling). A source-to-destination rate allocation is said to be max-min fair if it is not possible to increase the rate from a source to a destination without reducing the rate of another source-to-destination of an already smaller rate [106,108]. The set of source-to-destination rates, λ_p, can be found by solving (6.6) (referred as the *restricted master problem* in [58]).

$$\begin{array}{l} \text{maximize} \quad \lambda_{\min} \\ \text{subject to} \quad \lambda_{\min} \leq \lambda_p \ , \ p = 1 \ldots N(N-1) \\ \boldsymbol{R\Lambda} \preceq \boldsymbol{S\alpha} \quad ; \ \sum_{k=1}^{K} \alpha_k = 1 \\ \boldsymbol{\Lambda} \succeq \boldsymbol{0} \quad ; \boldsymbol{\alpha} \succeq \boldsymbol{0} \end{array} \tag{6.6}$$

where $\lambda_{\min}$ is the maximum-minimum rate from a source-to-destination. Hence, the upper bound for the end-to-end network throughput that produces a finite average network end-to-end delay is given by:

$$\lambda^* = N(N-1)\lambda_{\min}/R_0 \text{ (packet/slot)}. \tag{6.7}$$

To find the columns of $\boldsymbol{S}$ the method starts by taking an initial valid set. Solving (6.6) with this initial set may result in a suboptimal solution that provides a starting *lower bound* for $\boldsymbol{\Lambda}$. An *upper bound* can be found by the dual formulation of the problem from which the dual upper bound on constraints for (6.6) are found (Lagrange multiplier) and used to find a column vector, $\boldsymbol{s}_{k+1}$, to be added to $\boldsymbol{S}$. In our case, when AAS are utilized, if $\boldsymbol{\mathcal{L}}$ is the Lagrange multiplier vector, the new column vector to be added is found by solving the following mixed integer problem:

I) Constant Transmission Power

$$\begin{array}{l} \text{maximize} \quad \boldsymbol{\mathcal{L}}^T \boldsymbol{x} \\ \text{subject to} \\ \left(P_{Noise} + \sum_{m \neq l} G_{ml} F_{ml} P_{\max} \right) x_l + \sum_{m \neq l} G_{ml} F_{ml} P_{\max} x_m \\ \qquad \leq \sum_{m \neq l} G_{ml} F_{ml} P_{\max} + \gamma_o G_{ll} F_{ll} P_{\max} \ , \\ \sum_{l=1}^{L} |a_{il}| \, x_l \leq 1 \ , \\ x_l \in \{0,1\} \, , l = 1 \ldots L \ , \ i = 1 \ldots N; \end{array} \tag{6.8}$$

II) SINR Balancing Power Control

$$\begin{aligned}
&\text{maximize} \quad \boldsymbol{\mathcal{L}}^T \boldsymbol{x} - \epsilon^+ \boldsymbol{P} \\
&\text{subject to} \\
&\gamma_o \sum_{m \neq l} G_{ml} F_{ml} P_m - G_{ll} P_l + \\
&\gamma_o \left(P_{Noise} + \sum_{m \neq l} G_{ml} F_{ml} P_{\max} \right) x_l \leq \gamma_o P_{\max} \sum_{m \neq l} G_{ml} F_{ml} \ , \\
&\sum_{l=1}^{L} |a_{il}| \, x_l \leq 1 \ , \\
&0 \leq P_l \leq P_{\max}, \ x_l \in \{0,1\} \, , \forall l \ , \ i = 1 \ldots N;
\end{aligned} \tag{6.9}$$

where, as in [109], ϵ^+ is a sufficiently small positive constant selected to be $\epsilon^+ = \mathcal{L}^+_{\min}/(2LP_{\max})$ and $\mathcal{L}^+_{\min}$ is the smallest strictly positive component of $\boldsymbol{\mathcal{L}}$.

The second constrain in (6.8) and (6.9) corresponds to the half-duplex operation.

Heuristic approach for scheduling

In the previous chapter we already introduced a heuristic scheduling algorithm for constant transmission power (Fig.5.5). Here we extend the proposed link scheduling algorithm to combine AAS and SINR balancing power control. We use constant length slots, hence the actual schedule, $\boldsymbol{S}$, is created assigning transmission rights to each link on a number of slots proportional to its traffic load.

All feasible links are initiated in ListA and remain in ListA until getting their corresponding minimum required slot allocation (stored in the Min_Slot vector). Then they are moved to ListB where they may be allocated some additional slots. For the k-th slot, the links in listA are sequentially tested to determine if they can be assigned to transmit simultaneously with the links already scheduled to transmit in the current slot (by this procedure the k-th column vector of *boldsymbolS* is created). Simultaneous transmission is tested by applying AAS and SINR power control. Next, the same procedure is applied to the links in ListB. In order to search over different activation sets each time a link is tested for activation its priority is updated. If the link is allocated in the current slot (slot k), its corresponding priority hold in the vector Pri is set to zero. Otherwise, its priority is incremented proportionally to its relative traffic load. Both lists are ordered according to the link priority at the end of each slot allocation. Besides allocating the link capacity required, the procedure aims to distribute the slot assigned to each link uniformly along the frame to reduce the waiting time in queue. In addition, we target to do a max-min fair allocation by setting the source-to-destination traffic loads to be equal.

The set of maximum source-to-destination rates, λ_p, allocated by the heuristic algorithm can be found by solving (6.6). In this case the frame is composed of K_f timeslots corresponding to the number of column vectors of $\boldsymbol{S}$ (the actual schedule).

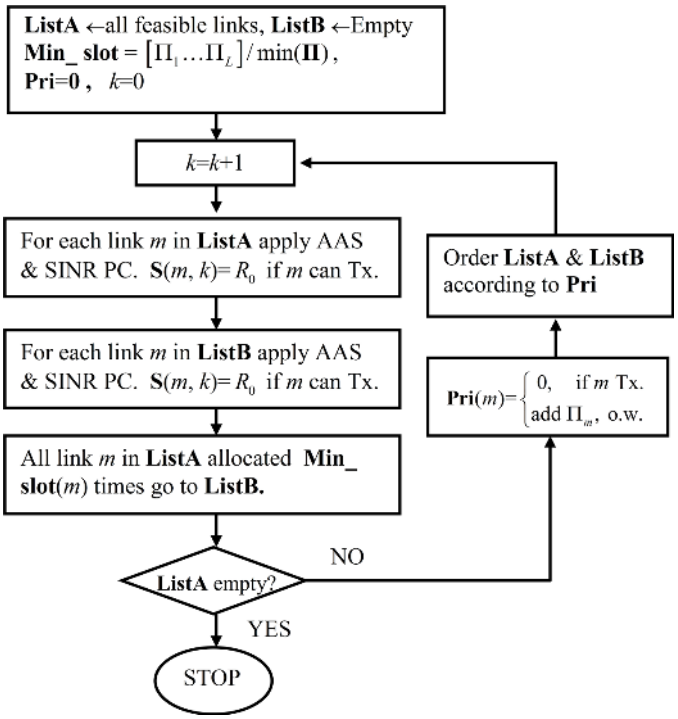

Figure 6.3: Algorithm for STDMA with AAS and SINR balancing power control.

The corresponding activation time is $\alpha_k = 1/K_f, \;\; k = 1 \ldots K_f$. However, the bound for the end-to-end throughput can be derived from the flow conservation law [57] and is given by

$$\lambda^* = N(N-1)\lambda_{\min}/R_0 = N(N-1) \min_{\forall l=1\ldots L} \left(\frac{n_l}{\Pi_l K_f} \right) \tag{6.10}$$

where n_l is the number of slots assigned to link l.

6.4 Numerical Results

The performance has been evaluated over 300 sample networks composed of 10 nodes as described in section 6.2 with parameters $R_o = 1$ Mbps,$\gamma_0 = 10$dB, $P_{Noise} = 1.27 \times 10^{-13}$, and distance dependent radio propagation model with $\alpha = 3$.

Fig.6.4 shows the allocated maximum source-to-destination traffic load (Packet/timeslot) for two of our sample networks when utilizing 60^o antenna beamwidth. Note that our heuristic approach effectively exhibits the max-min fair allocation targeted by its design. For the lower connected network ($\mathcal{C} = 0.3778$), the heuristic method

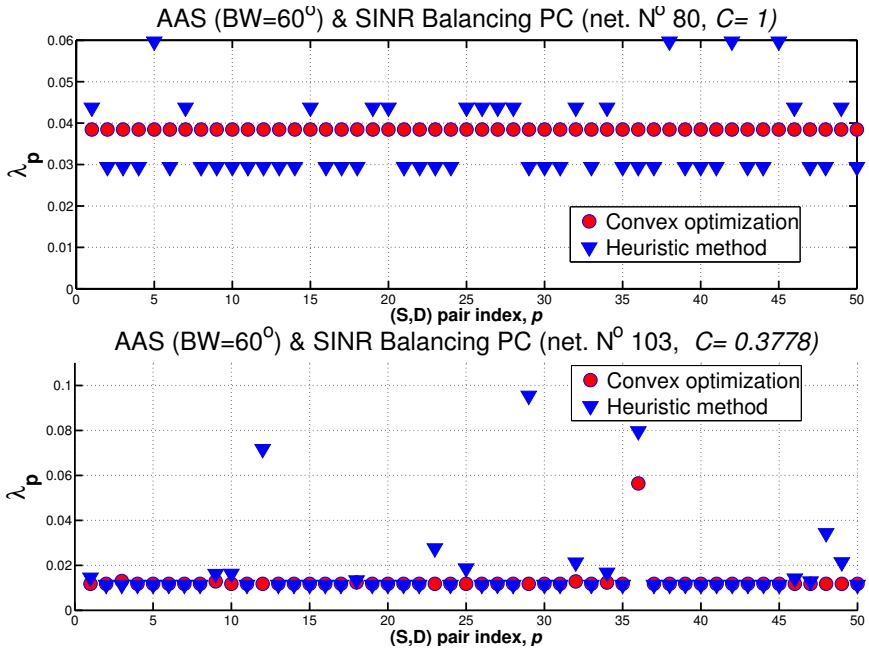

Figure 6.4: Maximum source-to-destination throughput, λ_p (Packet/timeslot), for two sample networks with different connectivity utilizing 60^o AAS (50 (S,D) pairs of $N(N-1)$ are shown).

performs very similarly to the convex optimization method allocating similar traffic load capacity to most of the source-to-destination pairs. For $\mathcal{C} = 1$ the convex optimization method results in equal traffic load allocation. At this point the gain with respect to the heuristic method becomes larger. Similar performance was observed for different antenna beamwidths and for constant transmission power (see Fig.6.5).

Fig.6.5 (a) shows the average maximum *End-to-End network throughput* as a function of the network connectivity and the antenna system utilized for constant transmission power and Fig.6.5 (b) shows the results when SINR power control is used.

For the omnidirectional case both methods perform similarly for all connectivities for both constant transmission power and SINR balancing power control. When AAS are used a significant performance improvement is achieved by both methods even with a moderate 60^o beamwidth. The heuristic approach achieved very good performance, close to the convex optimization method, from low to relatively high connectivity (up to $\mathcal{C} = 0.85$). As the antenna beamwidth reduces and the connectivity increases the performance gain achieved by the convex optimization method increases compared to the heuristic. The difference becomes significant as the connectivity approaches one. As the antenna beamwidth gets narrower the

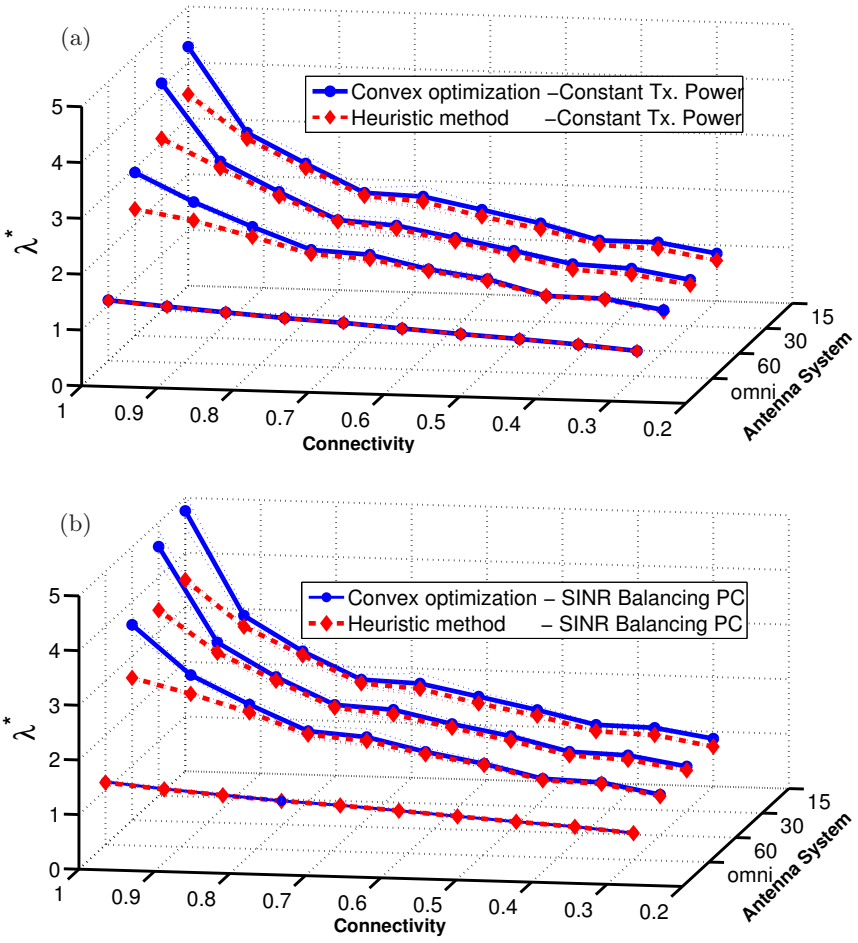

Figure 6.5: Average *End-to-End network throughput* (in Packet/timeslot) as a function of the network connectivity and the Antenna System with: (a) Constant Transmission Power and (b) SINR balancing power control.

convex optimization method achieves on average up to 4.3 and 4.8 packets per slot for constant transmission power and SINR balancing power control, respectively. This is very close to the theoretical limit set by the number of nodes in the network since at most $N/2$ activations can be allocated per timeslot due to half-duplex operation. At this point the heuristic approach was able to allocate on average up to 3.5 packets per timeslot. This is because for the high connectivity, there are $L = N(N-1) = 90$ links to schedule and the heuristic, by its design, does a limited search (at most 90 iterations on the first list) which is a limited search and

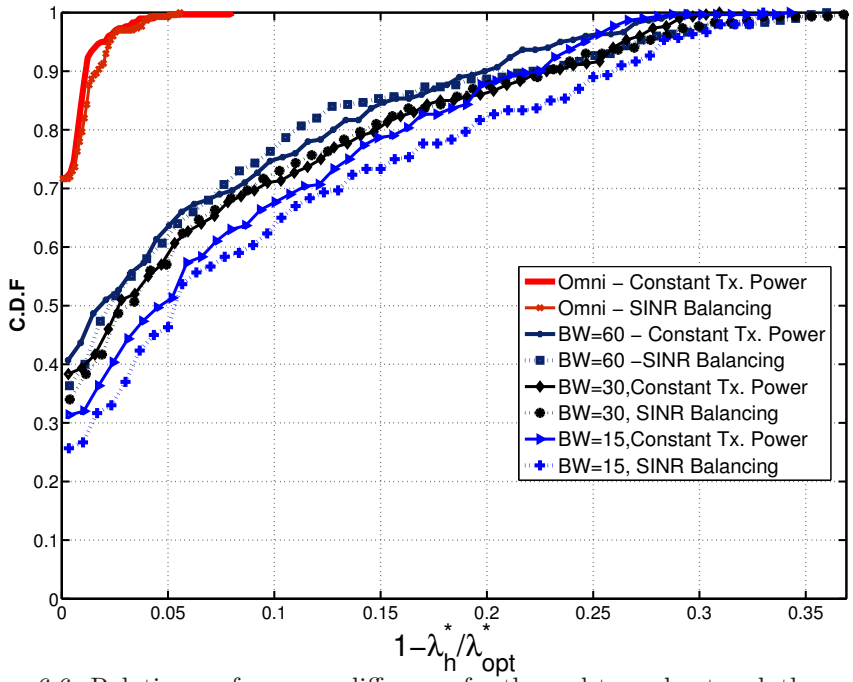

Figure 6.6: Relative performance difference for the end-to-end network throughput achieved by the heuristic method with respect to the optimum schedule.

besides that all links are seen as equal since only the relative traffic load is used as weight. Those effects are not significant for the omnidirectional antenna case since interference dominates in the single hop scenario. On the other hand, as the network connectivity increases, the convex optimization method needed much more time and iterations to converge but the interference reduction provided by the AAS increase the number of possible compatible link transmission sets (there are $2^{90} - 1$ possible combinations excluding the all zero test).

It is interesting to observe the overall performance for both methods. Fig. 6.6 shows the cumulative distribution function (CDF) for the relative performance difference between the heuristic and the convex optimization method for all sample networks independently of their connectivity. For the omnidirectional case, the relative difference is less than 2% for 90% of the networks under study and almost equal performance for 72% of the networks.

When using AAS the relative difference is less than 10% for around 75%, 70% and 65% of the networks for half-power beamwidth of 60^o, 30^o and 15^o, respectively. Also in this case, almost the same performance occurs for 25% to 40% of the networks.

6.5 Concluding Remarks

In this chapter we have studied interference-based link scheduling for fixed-rate systems in STDMA multihop wireless networks utilizing AAS with and without power control. Two heuristic allocation schemes based on the one proposed in [57] have been extended to utilize AAS and also for SINR balancing power control. We have presented a methodology to compare the performance of these schemes, in terms of the end-to-end network throughput, to the performance bound provided by optimal schedule. To find the optimal schedule the nonlinear optimization method proposed in [58], extended to include the use of AAS, was used. The evaluation was done in networks where nodes were equipped with beam-steering circular array antennas.

As expected, a significant performance gain is achieved by using AAS for both methods compared to systems with omnidirectional antennas (up to 5 times in our experiments). Our heuristic allocation schemes achieved very close performance to the performance of the (variable slot-length) optimal schedule found by nonlinear optimization when using omnidirectional antennas (less than 2% difference for 90% of the networks studied). When AAS were used, the relative difference was found to be less than 10% for low-to-moderate network connectivity (up to $\mathcal{C} = 0.85$).

When the network connectivity increases to the single hop scenario ($\mathcal{C} = 1$), the difference in performance increases in favor of the nonlinear optimization method. This is because the relative traffic load, used as a weighting function by our heuristic allocation schemes, is no longer a dominant parameter, leaving space for further improvement.

Chapter 7

Power and Rate Control in STDMA with AAS

In this chapter we investigate the combined effects of adaptive rate selection, advanced antenna systems, power control and link scheduling in multihop wireless networks. Advanced antenna systems and/or power control can be utilized to some extent to control the link quality and interference environment created by multiple access to the channel. In addition, link scheduling and adaptive bit rate can be utilized to better exploit the improved link quality and multiple access interference that the above techniques provide. To assess the optimum performance of the various techniques in multihop wireless networks we utilize nonlinear optimization.

7.1 Introduction

Most modern wireless communications systems are today capable not only of sending information at high transmission rates, but also of adapting the rate to the instantaneous radio channel conditions. This is possible by utilizing, say, multilevel modulation schemes together with error control coding with variable coding rates. As an example, the Direct Sequence Spread Spectrum (DSSS) PHY specification for the IEEE 802.11 standard [24] utilizes two baseband modulation schemes for two discrete bit rate adaptation levels on the 2.4GHz frequency band. The system can automatically select the appropriate modulation scheme (data rate) to match the prevailing channel conditions. For poor channel conditions differential binary phase shift keying (DBPSK) is used to provide data rate of 1 Mbit/s and under good channel conditions differential quadrature phase shift keying (DQPSK) is used to provide 2 Mbit/s. As the technology has evolved, new devices are capable of selecting from more discrete step transmission rates. For instance, IEEE802.11b compliant devices can select from the set of rates $\mathcal{R}_{set} = \{1, 2, 5.5, 11\}$ Mbps and IEEE802.11g has the available set $\mathcal{R}_{set} = \{1, 2, 5.5, 11\} \cup \{6, 9, 12, 18, 24, 36, 48, 54\}$ Mbps.

The availability of multiple discrete transmission rates in multihop wireless networks raises the problem of selecting them in a reliable and spectrally efficient way while at the same time satisfying end-to-end communication traffic demands. In wireless networks the transmission rates used are closely related to the Signal-to-Interference plus Noise ratios (SINRs) [110], and the SINRs can be controlled by utilization of advanced antenna systems and/or power control.

We analyze the use of advanced antenna systems utilizing variable transmission bit rate with and without power control in STDMA multihop networks. The optimal link schedule for the end-to-end network throughput is found by the nonlinear optimization method. We evaluate the performance of the various variable rate schemes to the case when omnidirectional antennas are used and also to the case of fixed transmission rate systems with and without power control.

7.2 General System Considerations

As in the previous chapter, we study the case when the network is deployed with all nodes equipped with AAS and also the reference case when the nodes utilize omnidirectional antennas. Beam-steering circular arrays have been selected as the AAS (see section 3.1). In order to compare the systems under commonly assumed conditions we use the traditional method where only one-way routing information is used to create the link scheduling (section 5.2). Proactive routing is utilized applying the Dijkstra algorithm [96] to find the minimum hop route from the source node to the destination node.

We assume that the physical layer of each node that comprises the network has a set of r discrete transmission rates, $\mathcal{R}_{set} = \{R_0, R_1, \ldots, R_{r-1}\}$; $R_0 < R_1 < \ldots < R_{r-1}$. Selection of the transmission bit rate is done depending on link SINR level; that is transmissions from node i to node j (on link labeled l) utilize bit rate $R_l(\Gamma_l)$ such that:

$$R_l(\Gamma_l) = \begin{cases} R_0\ , & \gamma_0 \le \Gamma_l < \gamma_1 \\ R_1\ , & \gamma_1 \le \Gamma_l < \gamma_2 \\ \vdots & \vdots \\ R_{r-1}\ , & \Gamma_l \ge \gamma_{r-1} \end{cases} \tag{7.1}$$

where as before, Γ_l is the SINR at node j and, in a given slot, is given by:

$$\Gamma_l = \frac{G_{ll} F_{ll} P_l}{P_{Noise} + \sum\limits_{\forall m \neq l} G_{ml} F_{ml} P_m x_m}\ , \tag{7.2}$$

where P_{Noise} is the noise power, G_{ml} corresponds to the path gain between the transmitting node on link m and the receiving node on link l, P_m is the power used by the transmitting node on link m, and the antenna factor is mapped into the link representation by $F_{ml} = A_{rk}(\theta_{rj}) A_{ji}(\theta_{jr})$ and $x_m \in \{0, 1\}$

Furthermore, it is assumed that the time domain is divided into slots, each long enough to transmit one data packet using a bit rate R_0 bps.

In our evaluation, we use sample networks deployed over a 20×20 km^2 area with $\mathcal{C} \in [2/N, 1]$ to recreate the long-range rural environment. For performance comparisons the antenna system is changed maintaining the network topology by finding the required maximum transmission power,

$$P_{\max} = \frac{P_{Noise}\gamma_o}{\min_{\forall \text{ feasible } \text{ link}(i,j)} [G_{ij}A_{ij}(\theta_{ij})A_{ji}(\theta_{ji})]} \tag{7.3}$$

where P_{Noise} is the noise power and γ_o is the SNR for a link to be reliable in the absence of multiple access interference.

To represent the logical network topology in compact form we utilize the *node-arc incidence matrix*, $\boldsymbol{A}$, whose entries are given by:

$$a_{il} = \begin{cases} +1 & \text{if node } i \text{ is the transmitter on link } l \\ -1 & \text{if node } i \text{ is the receiver on link } l \\ 0 & \textit{otherwise} \end{cases} \tag{7.4}$$

Fig.7.1 shows a sample network used in our performance evaluation and illustrate the antenna patterns, transmission power level and bit rate used by a set of simultaneously transmitting links for one slot transmission activated a fraction α_1 of the time length of the *schedule*.

7.3 STDMA Scheduling for Variable Rate Systems

To analyze the system we follow a similar approach to the one used in [58]. We define the rate compatible index vector for link l as $\boldsymbol{x}_l = [x_l^{(0)} \dots x_l^{(r-1)}]$ holding one for the index of the transmitting bit rate R_k that satisfies the required SINR $\gamma_k \leq \Gamma_l < \gamma_{k+1}$ and zero otherwise. For example if $\boldsymbol{x}_l = [0\ 0\ 1\ 0\ \dots\ 0]$ means that the transmission bit rate utilized is R_2. In a given clique, the transmission rate assigned to link l is given by:

$$s_l = \sum_{k=0}^{r-1} R_k x_l^{(k)}, \forall l \tag{7.5}$$

In addition, since only one rate can be utilized by a link when transmitting, the above equation must be subject to the constraint:

$$\sum_{k=0}^{r-1} x_l^{(k)} \leq 1\ ,\ x_l^{(k)} \in \{0, 1\} \tag{7.6}$$

Similar to the case for fixed-rate systems (chapter 6), we represent by $\boldsymbol{S} \in \Re^{L \times K}$ the compatible link activation sets utilized for the STDMA link schedule. The

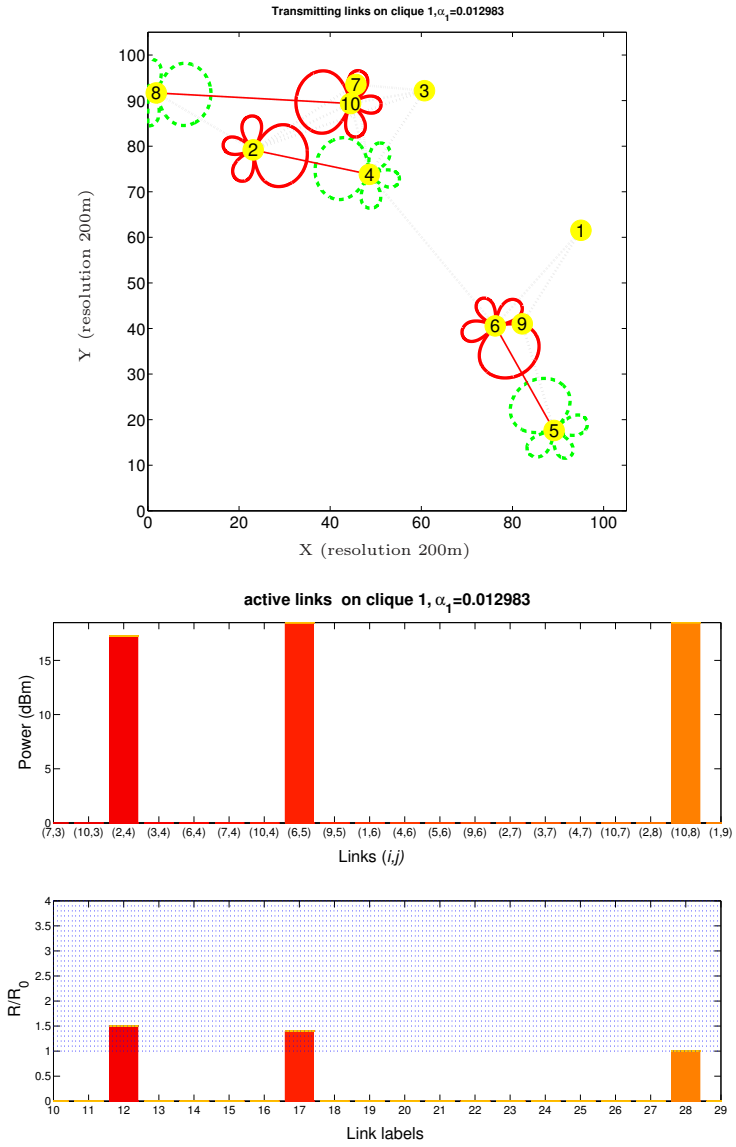

Figure 7.1: Sample network A ($\mathcal{C} = 0.4$) and a set of simultaneously transmitting links (a *clique*) in the STDMA *schedule* utilizing beam-steering circular arrays with 60^o HPBW. The transmitting antenna radiation patterns are indicated by solid lines and the receiving antennas by dashed lines. For clique 1, the transmission powers and normalized transmission bit rates are also shown.

column vectors of $\boldsymbol{S}$ correspond to the possible cliques for the multihop network, $\boldsymbol{s}_k = [s_1 \dots s_L]^T$. The columns of $\boldsymbol{S}$ can be linearly combined to create the STDMA schedule by defining the vector of weights $\boldsymbol{\alpha} = [\alpha_1 \dots \alpha_K]^T$ corresponding to the fraction of time that each column vector of $\boldsymbol{S}$ is activated within a STDMA frame. For a given $\boldsymbol{\alpha}$ the allocated link capacity, $\boldsymbol{c} = [c_1 \dots c_L]^T$ is given by:

$$\boldsymbol{c} = \boldsymbol{S}\boldsymbol{\alpha} \; ; \qquad \sum_{k=1}^{K} \alpha_k = 1. \tag{7.7}$$

Similar to what is done for fixed-rate systems, the capacity allocation to each link can be formulated as an optimization problem to maximize a utility function $u(\cdot)$ as follows:

$$\begin{aligned} &\text{maximize} \quad u(\boldsymbol{\Lambda}) \\ &\text{subject to} \quad \boldsymbol{R}\boldsymbol{\Lambda} \preceq \boldsymbol{S}\boldsymbol{\alpha} \quad ; \sum_{k=1}^{K} \alpha_k = 1 \\ &\boldsymbol{\Lambda} \succeq \boldsymbol{0} \quad ; \boldsymbol{\alpha} \succeq \boldsymbol{0} \end{aligned} \tag{7.8}$$

Note that the computational complexity for the optimum allocation is even harder than for fixed-rate systems. That is, the number of combinations to find all possible column vectors in $\boldsymbol{S}$ grows exponentially with the number of links and number of discrete rates to test for compatibility (equations 7.1, 7.5 and 7.6).

However, as for the fixed rate case, for relatively small networks we can utilize the nonlinear column generation method proposed by Johansson and Xiao in [58] to find the column vectors of $\boldsymbol{S}$ that maximize the utility function $u(\cdot)$. As before, we apply the method to maximize the minimum source-to-destination rates (max-min fair rate scheduling) which can be related to the end-to-end network throughput. The set of source-to-destination rates, λ_p, can be found by solving equation (7.9).

$$\begin{aligned} &\text{maximize} \quad \lambda_{\min} \\ &\text{subject to} \quad \lambda_{\min} \leq \lambda_p \;\; , \;\; p = 1 \dots N(N-1) \\ &\boldsymbol{R}\boldsymbol{\Lambda} \preceq \boldsymbol{S}\boldsymbol{\alpha} \quad ; \quad \sum_{k=1}^{K} \alpha_k = 1 \\ &\boldsymbol{\Lambda} \succeq \boldsymbol{0} \quad ; \boldsymbol{\alpha} \succeq \boldsymbol{0} \end{aligned} \tag{7.9}$$

where $\lambda_{\min}$ is the maximum-minimum rate from source-to-destination. Hence, the upper bound for the end-to-end throughput that produces a finite average network end-to-end delay is given by equation (7.10) [68].

$$\lambda^* = N(N-1)\lambda_{\min}/R_0 \text{ (packet/slot)}. \tag{7.10}$$

As explained in chapter 6, to find the columns of $\boldsymbol{S}$ the method starts by taking an initial valid set. Solving (7.9) with the initial set may result in a suboptimal solution that provides a starting *lower bound* for $\boldsymbol{\Lambda}$. An *upper bound* can be found by the dual formulation of the problem from which the dual upper bound on constraints

for (7.9) are found (Lagrange multiplier) and used to find a column vector, $\boldsymbol{s}_{k+1}$, to be added to $\boldsymbol{S}$. The upper bound on constraints are flow-based, then if the allocated capacity is lower than the flow the corresponding Lagrange multiplier will be more positive meaning more capacity needs to be allocated for the corresponding link [106].

The application of the method to AAS with Constant Rate (CR) and Power Control (PC) has already been presented in chapter 6 and here we extend it to the cases of AAS with variable rates and Power Control.

In the following, if $\boldsymbol{\mathcal{L}}$ is the Lagrange multiplier vector, the new column vector to be added to $\boldsymbol{S}$ can be found by solving the subproblem:

Variable Transmission Rate and constant transmission power (VR)

When allocated for transmission, a node utilizes the constant transmission power P_{max} and one out of r discrete transmission bit rates can be selected from $\mathcal{R}_{set}$. For this case we suggest finding the next column vector, $\boldsymbol{s}_k = [s_1 \ \ldots \ s_L]^T$, by solving the following sub-problem:

$$\begin{aligned}
&\text{maximize } \sum_{l=1}^{\mathrm{L}} \mathfrak{L}_l s_l = \sum_{l=1}^{\mathrm{L}} \mathfrak{L}_l \sum_{k=0}^{r-1} R_k x_l^{(k)} \\
&\text{subject to} \\
&\left(P_{Noise} + \sum_{m \neq l} G_{ml} F_{ml} P_{\max} \right) x_l^{(k)} + \sum_{k=0}^{r-1} \sum_{m \neq l} G_{ml} F_{ml} P_{\max} x_j^{(k)} \\
&\quad \leq \gamma_k^{-1} G_{ll} F_{ll} P_{\max} + \sum_{m \neq l} G_{ml} F_{ml} P_{\max}, \forall l, \ \forall k; \\
&\sum_{k=0}^{r-1} \sum_{l=1}^{L} |a_{il}| x_l^{(k)} \leq 1, , \ i = 1 \ldots N \ ; \\
&\sum_{k=0}^{r-1} x_l^{(k)} \leq 1 \ , \ x_l^{(k)} \in \{0, 1\} \ , \ \forall l \ .
\end{aligned} \tag{7.11}$$

The demonstration that the set of constraints in (7.11) corresponds to variable rate STDMA systems with constant transmission power is as follows:

Proof: In a given slot, from the link SINR (7.2) and transmission rate condition (7.1), link l can transmit at a rate R_k if

$$\begin{aligned}
&G_{ll} F_{ll} P_{\max} x_l^{(k)} + M_l (1 - x_l^{(k)}) \\
&\geq \gamma_k \left(P_{Noise} + \sum_{k=0}^{r-1} \sum_{m \neq l} G_{ml} F_{ml} P_{\max} x_j^{(k)} \right)
\end{aligned} \tag{7.12}$$

Where M_l is an auxiliary variable introduced to set as a valid value the case when $x_l^{(k)} = 0$, hence

$$M_l \geq \gamma_k \left(P_{Noise} + \sum_{k=0}^{r-1} \sum_{m \neq l} G_{ml} F_{ml} P_{\max} x_m^{(k)} \right) \tag{7.13}$$

By considering (7.6), a valid value for M_l is

$$M_l = \gamma_k \left(P_{Noise} + \sum_{m \neq l} G_{ml} F_{ml} P_{\max} \right) + G_{ll} F_{ll} P_{\max} \tag{7.14}$$

Replacing (7.14) into (7.12) and after simplifying terms, we have to satisfy the following constrains:

$$\begin{aligned} \left(P_{Noise} + \sum_{m \neq l} G_{ml} F_{ml} P_{\max} \right) x_l^{(k)} + \sum_{k=0}^{r-1} \sum_{m \neq l} G_{ml} F_{ml} P_{\max} x_j^{(k)} \\ \leq \gamma_k^{-1} G_{ll} F_{ll} P_{\max} + \sum_{m \neq l} G_{ml} F_{ml} P_{\max}, \ \forall l, \forall k \end{aligned} \tag{7.15}$$

Besides constraints (7.6) and (7.15) we have to add the constraint for half-duplex operation of a node:

$$\sum_{k=0}^{r-1} \sum_{l=1}^{L} |a_{il}| x_l^{(k)} \leq 1, \ i = 1 \ldots N \tag{7.16}$$

where a_{il} is an entry of the *Node-arc incident matrix* defined as

$$a_{il} = \begin{cases} +1 \text{ if node } i \text{ is the transmitter on link } l \\ -1 \text{ if node } i \text{ is the receiver on link } l \\ 0 \text{ otherwise} \end{cases} \tag{7.17}$$

□

Variable Transmission Rate and Power Control(VR+PC)

For this system the physical layer capability of a node allows control of the transmission power and rate selection. It is assumed that $P_l \in [0, P_{max}]$ and one out of r discrete transmission bit rates can be selected from R_{set}. Following a similar procedure to the one used in [58] it can be shown that the next column vector to be added, $\boldsymbol{s}_k = [s_1 \ \ldots \ s_L]^T$, can be found by solving:

$$
\begin{aligned}
&\text{maximize } \sum_{l=1}^{\mathrm{L}} \mathfrak{L}_l s_l = \sum_{l=1}^{\mathrm{L}} \mathfrak{L}_l \sum_{k=0}^{r-1} R_k x_l^{(k)} \\
&\text{subject to} \\
&\gamma_k \left(\sum_{m \neq l} G_{ml} F_{ml} P_m \right) + \gamma_k \left(P_{Noise} + P_{\max} \sum_{m \neq l} G_{ml} F_{ml} \right) x_l^{(k)} \\
&\quad - G_{ll} F_{ll} P_l \leq \gamma_k P_{\max} \sum_{m \neq l} G_{ml} F_{ml}, \forall l, \forall k \; ; \qquad (7.18) \\
&\sum_{k=0}^{r-1} \sum_{l=1}^{L} |a_{il}| x_l^{(k)} \leq 1, , \; i = 1 \ldots N \; ; \\
&\sum_{k=0}^{r-1} x_l^{(k)} \leq 1 \; , \; \forall l \; ; \\
&0 \leq P_l \leq P_{max} \; , \forall l \; ; \quad x_l^{(k)} \in \{0, 1\} \, .
\end{aligned}
$$

Following a similar procedure to the one used in [58] the formulation for the set of constraints in (7.18) is as follows:

Proof: In a given clique, the transmission rate allocated for a link l corresponding to the l-th entry of the column vector $\boldsymbol{s}_k \in \boldsymbol{S}$ is given by:

$$s_l = \sum_{k=0}^{r-1} R_k x_l^{(k)}, \forall l \qquad (7.19)$$

In a given clique, the power allocation vector for link transmissions correspond to $P = [P_1 \, P_2 \, \ldots P_L]$ and a particular link l can transmit at a rate R_k if the power allocation vector is such that:

$$G_{ll} F_{ll} P_l \geq \gamma_k \left(P_{Noise} + \sum_{m \neq l} G_{ml} F_{ml} P_m \right) \qquad (7.20)$$

We can rewrite the above expression introducing a sufficiently large auxiliary constant M_l such that the above condition becomes true when the corresponding bit rate is not selected, that is when $x_l^{(k)} = 0$. Then

$$G_{ll} F_{ll} P_l + M_l (1 - x_l^{(k)}) \geq \gamma_k \left(P_{Noise} + \sum_{m \neq l} G_{ml} F_{ml} P_m \right) \qquad (7.21)$$

Therefore, for $x_l^{(k)} = 0$:

$$M_l \geq \gamma_k \left(P_{Noise} + \sum_{m \neq l} G_{ml} F_{ml} P_m \right) - G_{ll} F_{ll} P_l .$$

The above is then satisfied by selecting:

$$M_l = \gamma_k \left(P_{Noise} + \sum_{m \neq l} G_{ml} F_{ml} P_{\max} \right)$$

Replacing this value into (7.21) and after some manipulation we obtain the following set of constraints:

$$\begin{aligned} &\gamma_k \left(\sum_{m \neq l} G_{ml} F_{ml} P_m \right) + \gamma_k \left(P_{Noise} + P_{\max} \sum_{m \neq l} G_{ml} F_{ml} \right) x_l^{(k)} \\ &\quad - G_{ll} F_{ll} P_l \leq \gamma_k P_{\max} \sum_{m \neq l} G_{ml} F_{ml}, \forall l, \forall k \; ; \end{aligned} \tag{7.22}$$

As before, besides constraints (7.6) and (7.22) we have to add the constraint for the half-duplex operation of a node (7.16).

□

7.4 Numerical Results

The performance has been evaluated using three sample networks consisting of 10 nodes equipped with beam-steering circular array antenna systems. We consider a scenario where the radio parameters are: $R_o = 1$ Mbps, $\gamma_0 = 10$dB, $P_{Noise} = 1.27 \times 10^{-13}$ W, and a distance dependent radio propagation model with $\alpha = 3$ is used. Network A has connectivity 0.4 (36 feasible links out of a total of 90 potential links), network B has connectivity 0.4444 (40 feasible links) and Network C has connectivity of 0.8222 (74 feasible links). The data rate can be controlled in 30 equal bit rate steps from R_0 to $4R_0$. The maximum rate, $4R_0$, was selected ensuring that if any feasible link transmits alone with maximum power, the achievable transmission rate will stay below this value. To determine the SINR limits in (7.1) we use the Shannon capacity limit. In Fig.7.1 we have illustrated the available rate set using the above settings.

Fig.7.2 shows the end-to-end network throughput, λ^* in packet/slot, for networks A, B and C with nodes using 60^o HPBW circular array antenna systems and the radio Resource Management (RRM) schemes: Constant bit rate (CR), SINR balancing power control (PC), Variable Rate Control (VR) and Variable Rate and Power Control (VR+PC). The results for omnidirectional antenna systems and constant bit rate (omni CR) are also included as reference. Furthermore, Fig.7.3 shows

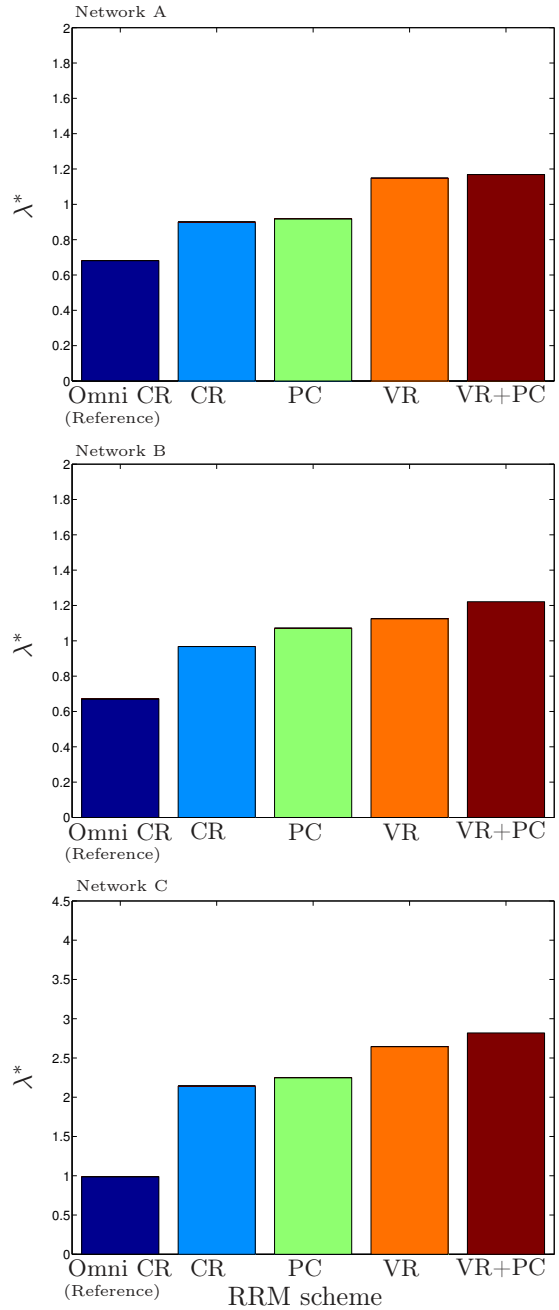

Figure 7.2: End-to-end network throughput, λ^* (packet/slot), for Networks A, B and C with HPBW=60^0 AAS and RRM schemes: (CR) Constant bit rate, (PC) SINR balancing power control, (VR) Variable Rate Control and (VR+PC) Variable Rate and Power Control. Omnidirectional antenna systems with constant bit rate (omni CR) is used as reference.

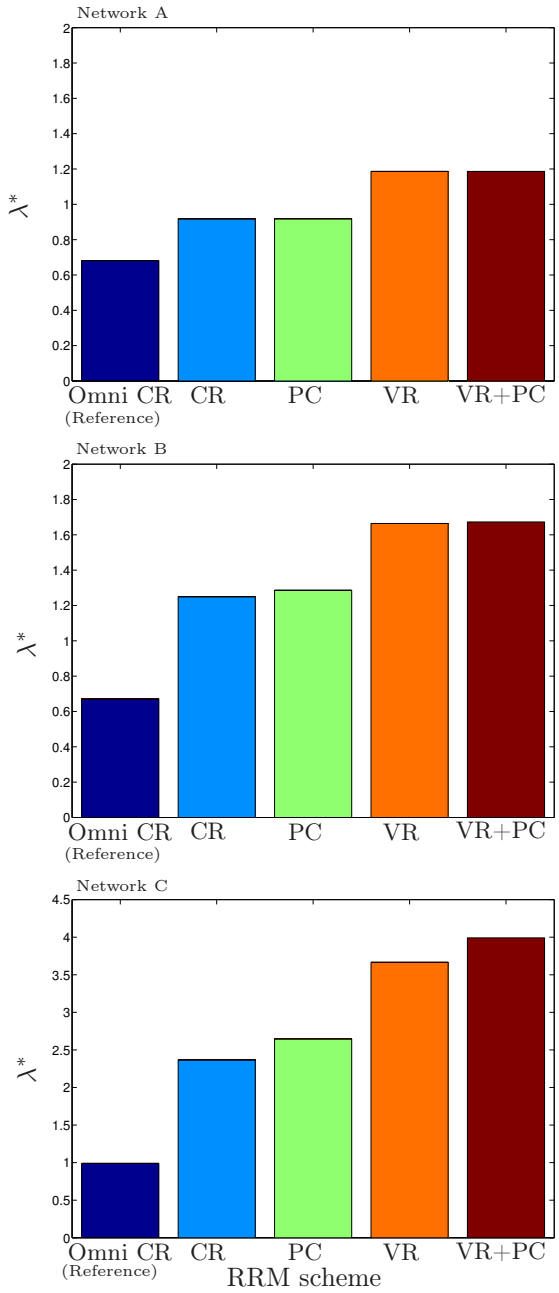

Figure 7.3: End-to-end network throughput, λ^* (packet/slot), for Networks A, B and C with HPBW=15^0. AAS and RRM schemes: (CR) Constant bit rate, (PC) SINR balancing power control, (VR) Variable Rate Control and (VR+PC) Variable Rate and Power Control. Omnidirectional antenna systems with constant bit rate (omni CR) is used as reference.

the performance when 15^o HPBW Circular array antenna systems were used.

For all RRM schemes, the results show that utilization of AAS provides a significant gain with respect to systems utilizing omnidirectional antennas and constant rate (Omni CR). The level of improvement increases as the connectivity increases and also as the HPBW reduces as seen by comparing the results in Fig.7.2 with the results in Fig.7.3.

We also can observe that variable rate schemes (VR and VR+PC) produce an important improvement in the performance compared to the one achieved by fixed rate schemes (CR and PC). When utilizing 60^o HPBW, the maximum gain with respect to CR was 1.27, 1.26, 1.32 for network A, B and C respectively. When reducing the HPBW to 15^o the maximum gain with respect to CR increases to 1.29, 1.34, 1.69 for network A, B and C, respectively.

By comparing the results of CR against PC and VR against VR+PC we can notice that utilization of power control adds only a limited additional gain. As shown in Fig.7.2, even for the moderate beamwidth of 60^0 antennas, CR has similar performance to PC and VR performs similarly to VR+PC. As the antenna beamwidth is reduced this latter effect is even more pronounced. This can be observed from Fig.7.3 where almost equal performance was found for VR as for VR+PC (the highest gain was only 1.08 and corresponds to the case of Network C; for Network A and B the performance was almost the same).

7.5 Concluding Remarks

In this chapter we have studied the combined effect of utilizing advanced antenna systems, power control, rate control and interference-based link scheduling in multihop wireless networks. Both advanced antenna systems and power control are interference reduction techniques that are commonly used to improve the link quality and interference environment created by multiple access to the wireless channel. To better exploit the improvement that those techniques provides, link scheduling and adaptive bit rate (rate control) can be utilized.

We have assessed the performance of several RRM schemes by finding the optimal scheduling using nonlinear optimization applying the column generation method proposed in [58]. We have studied the case when nodes are equipped with beam-steering circular array and also the reference case when the nodes utilize omnidirectional antennas. In our evaluations for variable rate systems, the data rates utilized by nodes were selected from a discrete set depending on the related

Signal-to-Interference plus Noise ratios (SINRs).

The results show that variable rate systems provide a significant gain with respect to constant rate systems. The use of power control together with advanced antenna systems typically produces an additional gain but in our experiments this gain was not significant (less than 8% improvement was observed). This effect became even more pronounced when more narrow-beam antenna systems were used. In the context of omnidirectional antennas a similar result was found in [61].

These results suggest that advanced antenna systems, variable transmission rate and link scheduling with constant transmission power can be the selected RRM scheme when the main objective is to maximize the end-to-end network throughput.

Finally, our ability to study larger network sizes was limited by the computational complexity of finding the optimal solution intrinsic to the interference-based scheduling problem. This encourage the search for low-complexity scheduling algorithms.

Chapter 8

A Reuse-Greedy Algorithm for STDMA with AAS and Rate Control

As presented in the previous chapter, the introduction of multiple discrete transmission rates and their selection adapted to the wireless channel condition is a promising way to improve the performance of STDMA multihop wireless networks even when using constant transmission power. In this chapter we present a novel, low complexity algorithm for rate selection and scheduling in a Spatial Time Division Multiple Access (STDMA).

8.1 Introduction

In multihop wireless networks, the capability of nodes for multiple discrete rate selection raises the problem of how to select them in a reliable and spectrally efficient way adapted to the wireless channel condition while at the same time satisfying end-to-end communication traffic demands. Spatial Time Division Multiple Access (STDMA) [34] has been proposed as an efficient solution. When assuming no interference caused by transmission of nodes that are more than two hops away, the optimal scheduling can be found by applying, for instance graph, coloring methods. More realistic models consider the aggregate interference of distant transmitters that may cause the SINR to fall below a required threshold for reliable reception [56, 57]. However, as discussed in previous chapters of this thesis, the optimal solution to interference-based scheduling is computationally hard to solve even for fixed-rate systems [48]. Exhaustive search has been one method utilized for performance evaluations in many studies [56, 61]. Another method is the column generation method [55,58] utilized in previous chapters of this thesis. However, the complexity of the above-mentioned methods grows exponentially in the number of links.

This motivates the proposal and study of sub-optimal (heuristic) low-complexity scheduling algorithms. Heuristic interference-based scheduling for multihop wireless networks has been studied extensively in the context of fixed-transmission rate

systems, for instance [45, 56, 57, 60, 68, 111]. There have also been some studies on heuristic link-scheduling utilizing variable rate with omnidirectional antennas, for instance [112]. However, few studies can be found on the context of variable transmission rates and advanced antenna systems.

The results obtained in the the previous chapter by using nonlinear optimization show that combined scheduling, AAS and variable transmission rate significantly improve the network throughput compared to fixed-rate schemes. Also shown is that adding a power control mechanism only produces limited additional gain. In the context of omnidirectional antennas a similar result was found in [61].

In this chapter we propose a novel, low complexity algorithm for rate selection and interference-based link scheduling in STDMA networks with advanced antenna systems. We compare the performance of this algorithm to the performance of the optimal link-schedule found by the nonlinear optimization method studied in the previous chapters.

8.2 System Model and STDMA Scheduling

As in the previous chapter, it is assumed that the $l$ink transmission schedule is created by dividing the time domain into slots, each long enough to transmit one data packet using a bit rate R_0 bps. We assume that the physical layer of all nodes allows rate selection from the discrete set $\mathcal{R}_{set} = \{R_0, R_1, \ldots, R_{r-1}\}$; $R_0 < R_1 < \ldots < R_{r-1}$. Selection of the transmission bit rate is done depending on link SINR level; that is, transmissions from node i to node j (on link labeled l) utilize bit rate $R_l(\Gamma_l)$ such that:

$$R_l(\Gamma_l) = \begin{cases} R_0 \ , & \gamma_0 \leq \Gamma_l < \gamma_1 \\ R_1 \ , & \gamma_1 \leq \Gamma_l < \gamma_2 \\ & \vdots \\ R_{r-1} \ , & \Gamma_l \geq \gamma_{r-1} \end{cases} \tag{8.1}$$

where Γ_l is the SINR at node j and, in a given slot, is given by:

$$\Gamma_l = \frac{G_{ll} F_{ll} P_l}{P_{Noise} + \sum\limits_{\forall m \neq l} G_{ml} F_{ml} P_m x_m} \ , \tag{8.2}$$

where we have used the label m for link (r, k) and define $P_l = P_i$, $G_{ml} = G_{rj}$, the antenna factor is defined as $F_{ml} = A_{rk}(\theta_{rj}) A_{ji}(\theta_{jr})$ and x_m is a binary variable set to 1 if link m is scheduled to transmit.

Using (8.1) and (8.2) we can find sets of *cliques* containing links having the property that all links in the same clique can transmit simultaneously selecting one of the available data rates.

As done in the previous chapter, we define the rate compatible index vector for link l as $\boldsymbol{x}_l = [x_l^{(0)} \ldots x_l^{(r-1)}]$ holding one for the index of the transmitting bit rate

R_q that satisfies the required SINR $\gamma_q \leq \Gamma_l < \gamma_{q+1}$ and zero otherwise. For example if $\boldsymbol{x}_l = [0\ 0\ 1\ 0\ \ldots\ 0]$ it means that the transmission bit rate utilized by link l is R_2. Hence, for a possible clique the transmission rate assigned to a link l is given by:

$$s_l = \sum_{q=0}^{r-1} R_q x_l^{(q)}, \forall l \tag{8.3}$$

Since only one rate can be utilized by a link when transmitting, the above equation must be subject to the constraint:

$$\sum_{q=0}^{r-1} x_l^{(q)} \leq 1 \ ; \ x_l^{(q)} \in \{0, 1\} \tag{8.4}$$

We can represent the actual link schedule by the matrix $\boldsymbol{S} \in \Re^{L \times K_f}$ where K_f corresponds to the frame length of the STDMA schedule. The k-th column vector of $\boldsymbol{S}$, $\boldsymbol{s}_k = [s_{1k} \ldots s_{Lk}]^T$ corresponds to the clique utilized in slot k. Hence, by defining the vector of weight $\boldsymbol{\alpha} = [1/K_f \ldots 1/K_f]^T$ that corresponds to the fraction of time that each column vector of $\boldsymbol{S}$ is active during the STDMA frame, the allocated link capacity, $\boldsymbol{c} = [c_1 \ldots c_L]^T$ is given by

$$\boldsymbol{c} = \boldsymbol{S}\boldsymbol{\alpha} \ ; \qquad \sum_{k=1}^{K_f} \alpha_k = 1. \tag{8.5}$$

The capacity allocation is done through a scheduling algorithm. The scheduling algorithm allocates slots and transmission rates depending on the amount of traffic passing though each link.

Reuse Greedy and Rate Selection Algorithm for Link Scheduling (Greedy RS)

We propose the Greedy RS algorithm illustrated in Fig.8.1. This algorithm aims to exploit the reuse enhancement capability provided by AAS. The algorithm is said to be *reuse greedy* since it aims at maximizing the number of simultaneous (parallel) transmissions in each slot k. It uses the relative traffic load carried by a link, represented by the vector $\boldsymbol{\Pi}/\min(\boldsymbol{\Pi}), \min(\boldsymbol{\Pi} > 0$, as a weighting function for the slot assignment.

The schedule, $\mathbf{S}$, is created assigning transmission rights to each link on a number of slots proportional to its traffic load (Min_Slot vector). M_f is a proportionality factor and its value influences the frame length (see section 6.4). At the beginning of each slot allocation the list of links (ListOfLinks vector) is sorted according to its current Min_Slot value hence links with higher values will be considered first. Then links are sequentially tested for simultaneous transmissions using AAS and the lowest available transmission rate (R_0) for greedy reuse. When such a

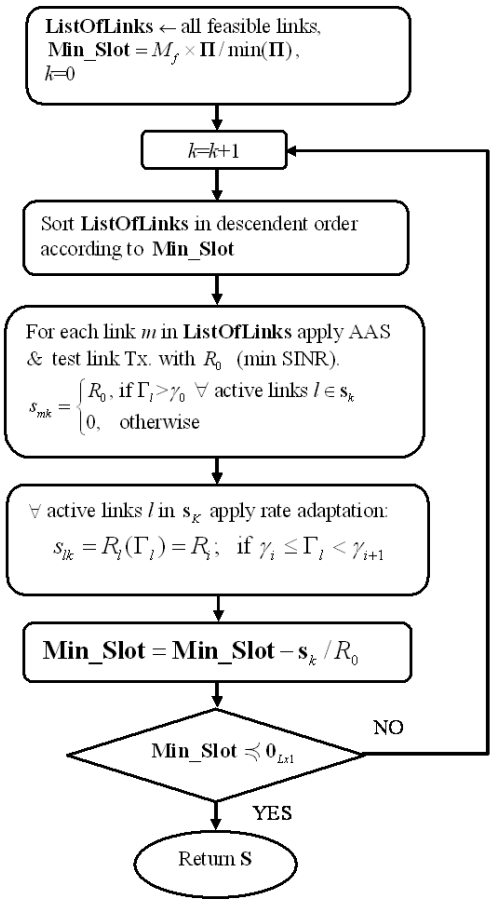

Figure 8.1: Greedy RS Algorithm for Link Scheduling with AAS.

set of links is found, we increase their transmission rates accordingly to fully utilize the achieved SINR. Then, the corresponding number of required slots is updated. The algorithm stops when all elements in Min_Slot are non-positive. In addition, we target a max-min fair allocation by setting the end-to-end traffic demand to be equal for all source-destination pairs.

The set of max-min source-to-destination rates, λ_p, allocated by the heuristic algorithm can be found by solving (8.6) [68].

$$\begin{array}{lll} \text{maximize} & \lambda_{\min} & \\ \text{subject to} & \lambda_{\min} \le \lambda_p \ , & p = 1 \ldots N(N-1) \\ \boldsymbol{R\Lambda} \preceq \boldsymbol{S\alpha} & ; \quad \boldsymbol{\Lambda} \succeq \mathbf{0} & ; \end{array} \tag{8.6}$$

Hence, the upper bound for the end-to-end network throughput that produces a finite average network end-to-end delay is given by [68]:

$$\lambda^* = N(N-1)\lambda_{\min}/R_0 \text{ (packet/timeslot)}. \tag{8.7}$$

8.3 Numerical Results

To analyze the results of the proposed algorithm we consider a scenario where the radio parameters are: $R_o = 1$ Mbps,$\gamma_0 = 10$dB, $P_{Noise} = 1.27 \times 10^{-13}$W and a distance dependent radio propagation model with $\alpha = 3$ is used. The data rate can be controlled in 30 equal bit rates steps from R_0 to $4R_0$. The maximum rate, $4R_0$, was selected ensuring that if any feasible link transmits alone with maximum power, the achievable transmission rate will stay below this value. To determine the SINR limits in (8.1) we use the Shannon capacity limit. A sample network deployed in a 20×20 km^2 area utilized in our performance evaluations is shown in Fig.8.2. The figure also shows an example of the antenna patterns utilized by the links allocated for transmission in slot 1 and the corresponding bit rates resulting from applying the Greedy RS algorithm.

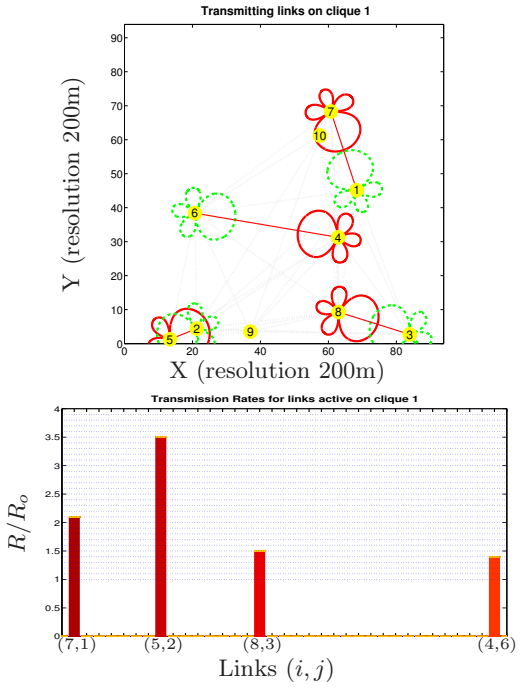

Figure 8.2: Illustration of one-slot allocation done by Greedy RS.

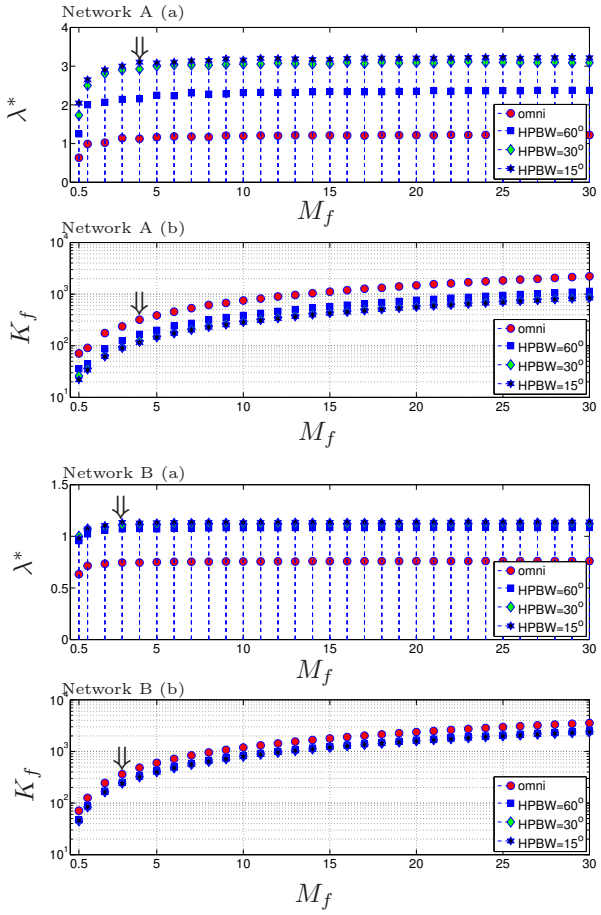

Figure 8.3: End-to-end throughput, (a), and frame length, (b), as function of M_f.

Selection of the Parameter M_f

M_f is an important parameter that influences the performance of the Greedy Algorithm in terms of throughput and frame length. By increasing the value of M_f the algorithm transfers more capacity to links with relatively higher traffic but that also implies longer computational time and longer frame lengths. We investigated how the selection of the parameter M_f influences the frame length and throughput. Fig.8.3 shows the end-to-end throughput (λ^*) and the frame length (K_f) as a function of M_f for two sample networks. Network A has connectivity of 0.8222 (74 feasible links) and network B has connectivity 0.4 (36 feasible links).

The figure shows the performance when utilizing omnidirectional antennas and

Table 8.1: Frame lengths as a function of M_f.

Network A

M_f	omni	HPBW 60	HPBW 30	HPBW 15
4	320	167	123	116
10	753	389	295	285

Network B

M_f	omni	HPBW 60	HPBW 30	HPBW 15
4	483	335	322	319
10	1190	831	803	795

AAS with Half-Power Beamwidth (HPBW) of 60^o, 30^o and 15^o. We observe from the throughput performance in network A (a) that it is convenient to select $M_f \geq 4$. After that point the throughput increases almost linearly with a very small slope. Similarly, from network B (a) a convenient value is $M_f \geq 3$.

The results for the frame length, K_f, in Fig.8.3 (labeled network A (b) and network B (b)) show that a selection of $M_f \in [4, 10]$ produces reasonable frame lengths and end-to-end throughput. In table 8.1 we summarize the resulting frame length for this selection.

Slot distribution Analysis

The Greedy RS algorithm allocates link capacity to maximize the end-to-end throughput, λ^*. However, the slot distribution is an important factor that influences the throughput-delay characteristic of STDMA as discussed in chapters 4 and chapter 5.

Fig.8.4 shows the slot distribution for network A when beam-steering circular array antennas were used with $HPBW = 15^o$.

As a consequence of the difference in traffic demands, we observe that links with higher traffic demands are mostly spread over the whole frame(e.g. links 20 and 14). However, links with lower traffic demands get concentrated over a part of the frame. In order to improve on the queue waiting time for relatively low external traffic we suggest applying a pseudo-random permutation of the schedule to distribute link access to the channel uniformly within the frame. Fig.8.5 shows the resulting schedule by using this procedure. The pseudo-random permutation used is a lagged Fibonacci generator combined with a shift register random integer generator as implemented in MATLAB ® (function randperm) [70].

Performance Comparison to the "optimal" Scheduling

We assess the performance of the proposed algorithm by comparing it to the performance achieved by the (variable slot-length) optimal scheduling scheme. For the

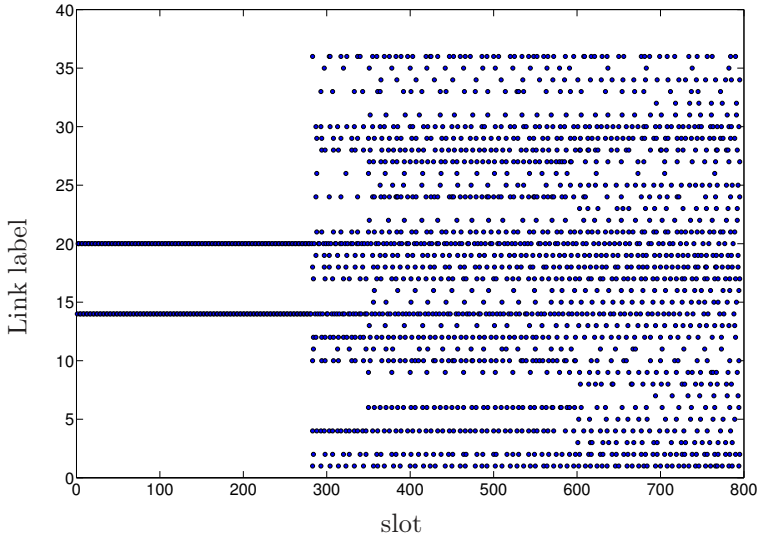

Figure 8.4: Slot assigned to links for network A (AAS HPBW=15^o, $Mf = 10$).

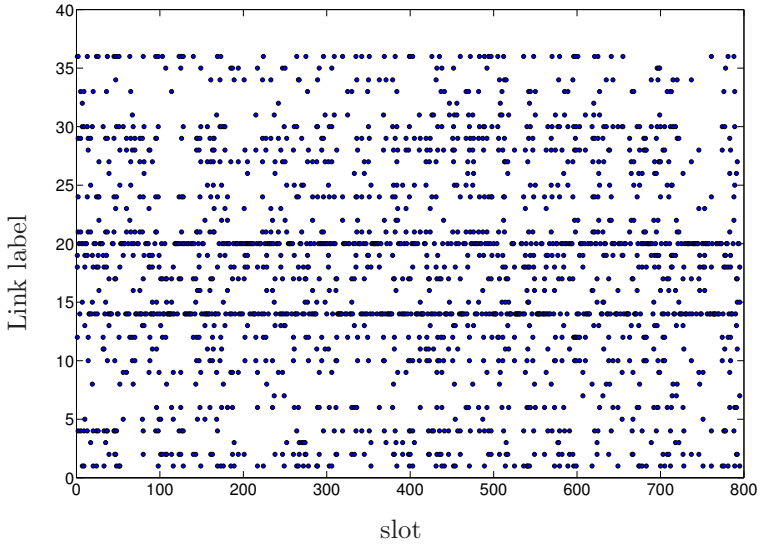

Figure 8.5: Slot assigned to links after *schedule scrambling* for network 1 (AAS HPBW=15^o, $Mf = 10$).

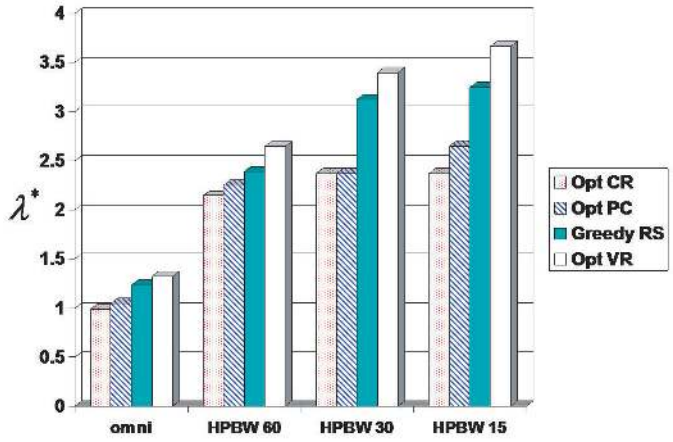

Figure 8.6: End-to-end throughput of Greedy RS, Optimum Fixed Rate scheduling (Opt CR), Optimum Power Control Scheduling (Opt PC) and Optimum Variable Rate scheduling (Opt VR) for the sample network illustrated in Fig.8.2.

Table 8.2: Gain of Greedy RS with respect to the optimum schemes.

	omni	HPBW60	HPBW30	HPBW15
Opt CR	1,25	1.12	1.32	1.37
Opt PC	1.18	1.1	1.32	1.22
Opt VR	0.93	0.91	0.92	0.89

latter purpose, the nonlinear column generation optimization method discussed in the previous chapter has been used.

We compare the performance of Greedy RS to the performance of (hypothetical) optimal scheduling. Fig.8.6 shows the end-to-end throughput of Greedy RS, Optimum Fixed Rate scheduling (Opt CR), Optimum Power Control Scheduling (Opt PC) and Optimum Variable Rate Scheduling (Opt VR) for network A. We have used $M_f = 100$ for a reasonable performance comparison versus the variable slot length assumption in the optimal scheduling schemes.

These results show that Greedy RS significantly exceeds the performance of the optimal fixed rate schemes (CR and PC). The resulting gain with respect to the optimum CR, optimum PC and Optimum VR are summarized in table 8.2 for the different antenna settings utilized. We can notice that the relative performance difference obtained by the Greedy RS algorithm with respect to the optimum Variable Rate scheme (Opt VR) was found to be within ten percent for all antenna systems.

8.4 Concluding Remarks

In this chapter we have proposed a novel, low complexity algorithm for link transmission scheduling in Spatial Time Division Multiple Access with Advanced Antenna Systems and bit rate selection (rate control).

The purpose of the algorithm is to exploit the reuse enhancement capability provided by AAS. We say that the algorithm is reuse-greedy because it aims to maximize the number of simultaneous (parallel) transmissions in each slot according to link priorities (weights based on link-traffic demands).

The throughput performance of the proposed algorithm has been evaluated in networks where nodes were equipped with beam-steering circular array antenna systems. The results were compared to the performance of the optimal (variable slot-length) scheduling for fixed-rate schemes and for variable rate schemes found by nonlinear optimization methods. The results show that the proposed algorithm, although being of low complexity, exhibits a throughput that exceeds the performance of optimal scheduling for fixed-rate schemes. Further, our evaluation shows that the algorithm achieves a performance that is within about 10% the performance of the one obtained by the optimization method.

Chapter 9

Utilizing AAS with Random MAC Protocols

In previous chapters Spatial Time Division Multiple Access has been studied and found to be efficient and fair; the draw-back is that it may not offer a fast response to bursty traffic demands. On the other hand, random access protocols are distributed, simpler to implement and have shown that they provide low delays under relative low traffic conditions. Among these protocols, the Carrier Sense Multiple Access/ Collision Avoidance (CSMA/CA) with handshaking promises efficiency and the possibility of being integrated with the utilization of AAS. The setup procedure utilized in this protocol makes it possible to use AAS at both the transmitter and the receiver. It is expected that the application of AAS in CSMA/CA with handshaking can provide significant improvement with respect to the omnidirectional case; however, as presented in this chapter, the system design needs careful consideration. Since cost is of paramount importance, the study has been limited to utilization of switched-beam antenna systems with one half-duplex transceiver at each node. We assume that the beam selection of the antenna system is controlled by the MAC-sublayer. Several beam selection policies are proposed and their performance evaluated.

9.1 Introduction

Utilization of handshaking procedure to avoid the hidden terminal problem was first proposed by Phil Karn in [32]. Several variants of this protocol have been proposed including the IEEE 802.11 standard [9–12, 33].

In our framework, a CSMA/CA with handshake node uses a simple half-duplex transceiver controlled at the link layer to receive or to transmit. At the MAC sub-layer, transition from transmission to reception is based on the CSMA/CA protocol, which is designed to reduce the probability of collisions by handshaking between the transmitting node and the receiving node. This is done by transferring

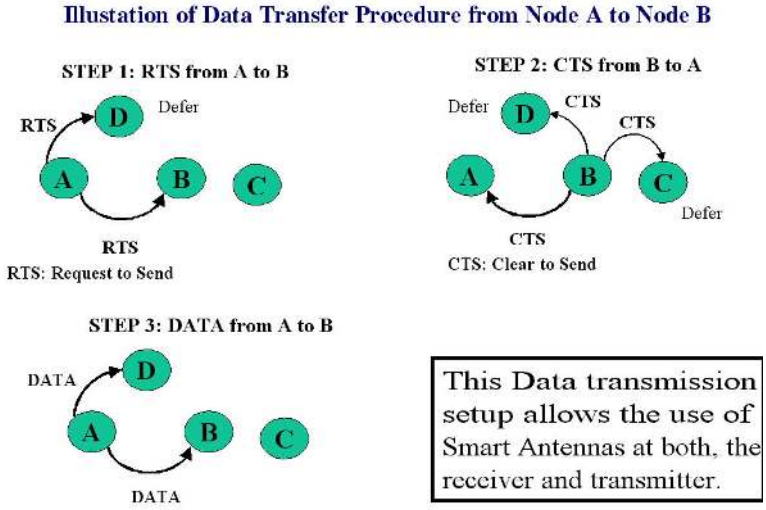

Figure 9.1: Data transfer procedure from Node A to Node B using Carrier Sense Multiple Access Collision Avoidance with RTS and CTS.

a data packet in three major steps as illustrated in Fig.9.1 plus the packet reception acknowledgment. Firstly, a node that has data to transmit sends a short Request to Send (RTS) packet. All nodes hearing the RTS, excepting the target receiver node, defer their transmissions. Secondly, the target node transmits a short Clear to Send (CTS) and all nodes hearing the CTS, excepting the originating node, defer their transmission until after the end of the data packet. Finally, the originating node transmits the data, now having a fair degree of confidence that the channel will be free of interference. In addition to these three steps a node inhibits its transmission if it senses another transmitter on the channel, i.e. Carrier Sense (CS). Link layer acknowledgement could follow the data packet immediately after its reception, as in IEEE 802.11 standard [24]. The type of CSMA/CA implemented to evaluate and generate the results in this chapter is very similar to FAMA described in [11] where higher layer acknowledgement solutions are assumed to be used. Details about the simulation of this protocol can be found in appendix C.

Two well known problems found in CSMA/CA with handshaking are the *hidden* terminal and *exposed* terminal problem. Fig. 9.2 illustrates a packet transmission from Node A to Node B using omnidirectional antennas. The maximum range of Carrier Sensing d_{CS} is greater than the range of error-free reception d_{RTS} of an RTS (or Data) in absence of MAI. Note that Node C cannot sense the RTS yet may be close enough to Node B to interfere with RTS's reception. Node C is said to be the *hidden* terminal. Carrier Sensing is important in reducing the *hidden* terminal problem [31]. Alternatively Node D can sense the RTS and DATA but

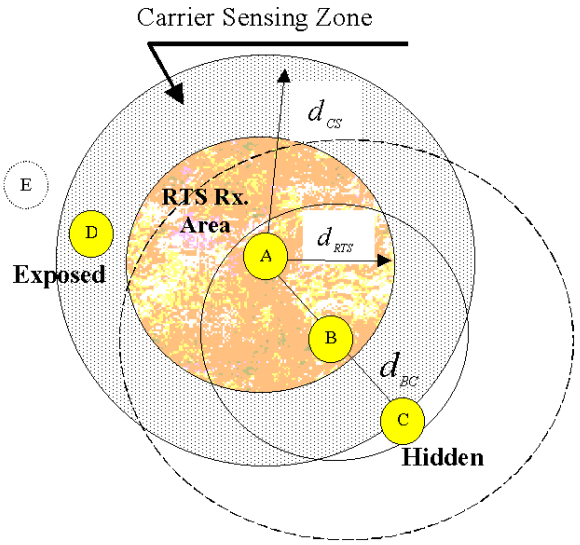

Figure 9.2: Carrier Sensing and RTS reception zones. If A transmits a RTS, B may decode it correctly, D may detect the channel busy but not C

may be able to transmit without interfering with the DATA packet's reception. If this is so, then Node D is said to be *exposed*. The range of the RTS and CTS is set by the modulation and coding while the range of carrier sensing is determined by the carrier sensing time constant and threshold.

Carrier detection can be performed at the physical layer through a power detector to produce a local estimation of the MAI. Let x_i be the i-th input sample to the power detector and $\overline{x}$ the average output power over an M samples window; the output power estimation level is then given by

$$\overline{x} = \frac{1}{M} \sum_{i=0}^{M-1} x_i^2 \tag{9.1}$$

Let I_{CD} be a binary variable with a 1 used to indicate carrier sense and 0 otherwise. Then the value I_{CD} passed to the MAC-sublayer is given by

$$I_{CD} = \begin{cases} 1 & \text{if } \overline{x} > P_{Th} \\ 0 & \text{otherwise} \end{cases} , \tag{9.2}$$

P_{Th} is the carrier detection power level threshold. Since x_i is the sum of signal plus noise on the channel, setting the carrier sensing threshold too low may cause a node to falsely detect the channel busy due to background noise only. On the other hand, setting P_{Th} too high will result in a bad MAI estimation. The selected value

for P_{Th} can be expressed as a function of the noise power and is given by (9.3).

$$P_{Th} = \gamma_{cs} P_{Noise} \ , \tag{9.3}$$

γ_{cs} is the signal to noise ratio for carrier sensing, $1 < \gamma_{cs} \leq \gamma_0$.

The minimum value for P_{Th} must be chosen to minimize false carrier detection. In absence of any node transmission (noise limited system), the white Gaussian noise dominates and the output of the power detector $\overline{x}$ is distributed as chi-square with M degrees of freedom with mean P_{Noise} and variance $\sigma^2 = 2P_{Noise}^2/M$ [113]. If we do a fairly large number of samples a good estimation of the noise power (low variance) could be achieved. However, the use of large M also produces an undesirable *carrier detection delay* while receiving that could result in reduction in performance [30]; therefore short M is also desirable. In this work it is considered that a minimum carrier detection threshold of 3dB above the noise floor can be used. The receiver needs a minimum time to sense the carrier included within our simulations through the *microslots* period. By setting the microslot period to much less than the length of an RTS the probability of collision is reduced.

It has been previously stated that carrier sensing could be removed to rely only on the RTS/CTS handshaking in protocols likes MACA [32]. The *hidden* terminal and *exposed* terminal problems are difficult to analyze thoroughly, however RTS collisions are considered to be critical [114]. How carrier sensing could help with RTS collisions is better understood through an example.

Example 9.1.1 We want to illustrate the relation between carrier sensing threshold and the probability of RTS collision between two given nodes when using omnidirectional antennas.

Lets assume for simplicity a distance dependent radio propagation model. Then, in absence of multiple access interference, the range for error-free reception of the RTS, d_{RTS} is given by (see Fig.9.2),

$$d_{RTS} = \sqrt[\alpha]{\frac{P_A}{\gamma_0 P_{Noise}}} \ . \tag{9.4}$$

The RTS reception area can be computed by $A_{RTS} = \pi d_{RTS}^2$.

In similar way, the carrier detection distance can be computed

$$d_{CS} = \sqrt[\alpha]{\frac{P_A}{\gamma_{cs} P_{Noise}}} = \sqrt[\alpha]{\frac{P_A}{P_{Th}}} \ . \tag{9.5}$$

Assume that a hidden Node C lies just out of carrier-sensing range, as shown in Fig. 9.3 ($d_{AC} = d_{cs}$). The received SIR Γ_{AB} (ignoring background noise) is

$$\Gamma_{AB} = \frac{P_{AB}}{P_{CB}} = \left(\frac{d_{BC}}{d_{AB}}\right)^{\alpha} \geq \gamma_0 \ , \tag{9.6}$$

where $d_{BC}^2 = d_{AB}^2 + d_{CS}^2 - 2 d_{AB} d_{CS} \cos\theta$. Hence, the distance for which A's RTS survives is $d_{AB} = d_{cap}$. Then

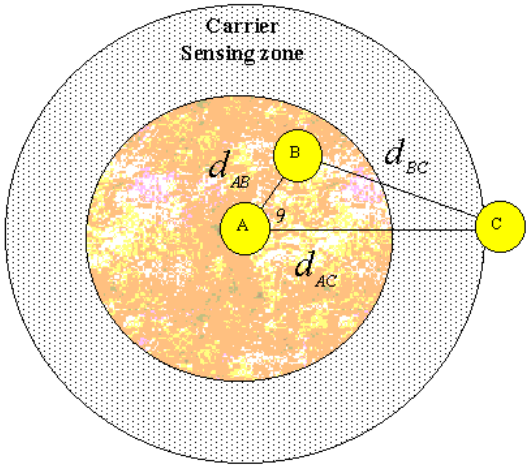

Figure 9.3: Carrier Sensing and RTS reception zones. If A transmit a RTS, B may decode it correctly, D may detect the channel busy but no C

$$\left(\frac{d_{cs}}{d_{cap}}\right)^2 - 2\left(\frac{d_{cs}}{d_{cap}}\right)\cos\theta + 1 \geq \gamma_0^{2/\alpha} \ . \tag{9.7}$$

Hence, the capture range can be approximated by

$$d_{cap} \approx \min\left(d_{RTS}, \frac{d_{cs}}{\cos\theta + \sqrt{(\gamma_0^{2/\alpha} - 1) + \cos^2\theta}}\right) \ . \tag{9.8}$$

Some examples of the resulting relative capture area using (9.8) are drawn in Fig.9.4 using the parameters of table I with carrier-sensing thresholds of 3dB, 6dB, 9dB and 10dB (No CD zone) above the noise floor. It can be seen from the figure that the correct detection area of the RTS is shrunk to 75.6%, 57.9%, 40.8%, 34.9% for 3dB, 6dB, 9dB, and 10dB carrier-sensing threshold respectively. If nodes are uniformly distributed over this area, this corresponds to the probability of successful reception of the RTS.

Collision with a short RTS packet is less costly in performance than data packet collisions. This could be true if the data packet size is much bigger than the RTS and CTS packet. To verify the impact on the *end-to-end packet delay* of RTS collisions we have done discrete step simulations with the simulation parameters summarized in table 9.1. We have selected RTS and CTS packet size of 25 bytes each, which are small when compared with the Data packet size of 500 bytes. The impact of different carrier-sense thresholds with omnidirectional antennas in network A and B are shown in Fig. 9.5. Using the minimum carrier-sense threshold of 3dB yields better performance at relatively high traffic load. However the per-

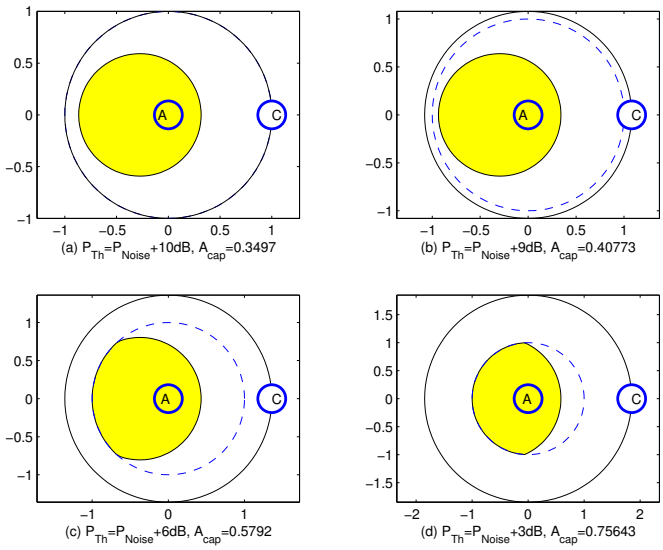

Figure 9.4: Reception area of A's RTS when a hidden terminal C is located at the carrier detection boundary for different values of CS threshold. RTS reception in absence of MAI is indicated by a dotted line.

formance improvement by selecting a low carrier detection threshold is only 7% for network A and 6% for network B.

Depending on the antenna adaptation use during RTS/CTS and Data transmission, Carrier-sensing impact may not be that important when narrow beam antennas are utilized. In addition, while the use of directional patterns for RTS and CTS transmission could help overcome the *exposed* terminal problem by spatial filtering of the interference, may increase the *hidden* terminal problem; thus a careful system design is needed.

In the following, it is assumed that each node is equipped with a switched-beam antenna system. The MAC sublayer must select the type of antenna (if using omnidirectional or directional) to transmit or to receive triggered by a given event (e.g. reception of an RTS), creating the need to utilize what we will call a *Beam Selection Policy*.

9.2 Beam Selection Policies

For each transmission from i to j over link (i, j), node i and node j must select the appropriate antenna sector. Five cases have been studied:

I. **Omnidirectional Antennas**: All nodes within the network use omnidirectional antennas for communications the whole time. This is the reference

Table 9.1: Simulation Parameters used for Performance Evaluation

Parameter	Value
Packet Size (PS)	500 Bytes
RTS size	25 Bytes (5% PS)
CTS size	25 Bytes
Data Rate	100 Kbps
Buffer Length (FIFO)	100 packets
Clock Step (microslot)	5 Bytes (1% PS)
Number of Nodes (N)	20
Packet Transmitted per Node	2000
External Packet Arrival	Poisson Distributed
Packet Destination	Uniform Distributed
Routing Method	Minimum Hop Algorithm (MHA)
Maximum Radio Range	40 km
Minimum SINR	$\gamma_0 = 10dB$
Receiver Noise Figure	15 dB
Equivalent Receiver	
Noise Bandwidth (B)	100 kHz
Carrier Sensing Threshold	+3 dB minimum
above the Noise Floor	+10dB maximum

case.

II. **Beam Selection Policy I (Omni-RTS)**: During the transmission of an RTS both nodes use omnidirectional antennas while during CTS and DATA transmissions both nodes use directional beams. See Fig.9.6.a.

III. **Beam Selection Policy II (Di-RTS)**: This policy is the same as policy I except that the RTS is transmitted using a directional beam. See Fig.9.6.b.

IV. **Beam Selection Policy III (Di-RTS/Omni-CTS)**: This policy is the same as policy II except that the CTS is transmitted using a omni-directional beam. See Fig.9.6.c

V. **Beam Selection Policy IV (Omni-RTS/ Omni-Rx.CTS/Di-CTS)**: During the transmission of an RTS both nodes use omnidirectional antennas while during reception of the CTS the originating node uses omnidirectional antenna and the receiving node transmits the CTS directionally. See Fig.9.6.d

In all cases a receiving node (the one to which the data is intended) uses an omnidirectional reception of the CTS since it doesn't know which node will transmit to it. To keep the same radio range we utilized a simple power control strategy where

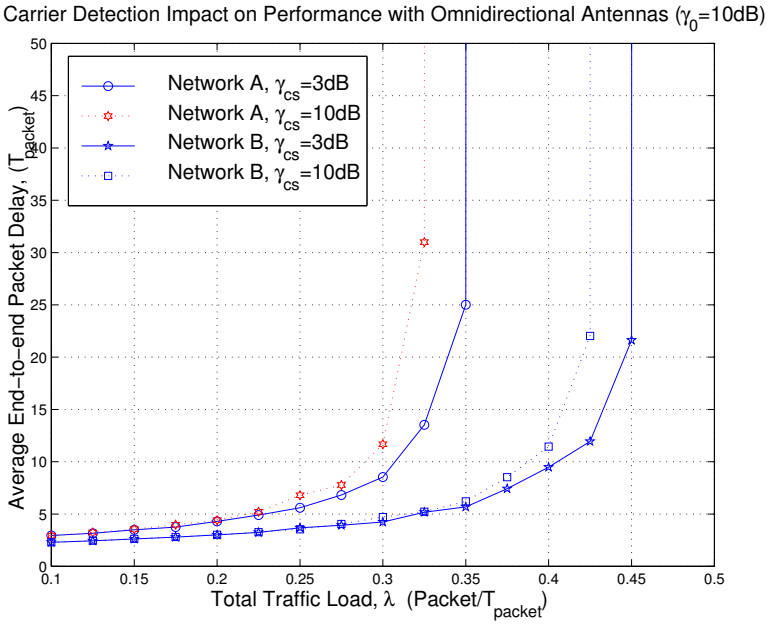

Figure 9.5: Fig.7. Performance of Network A and B with omnidirectional antennas and carrier detection threshold of 3dB and 10 dB above the Noise Floor. T_{packet} is the data packet transmission time.

the transmission power of node i to transmit to node j is given by

$$P_i = \frac{P_{omni}}{A_i(\theta_{ij})} \ , \tag{9.9}$$

where P_{omni} is the transmission power when transmitting with omnidirectional antenna.

Due to the complexity of the wireless Multiple Access Interference and the MAC protocol functionality, it is not clear which policy performs the best. For instance, Policy I could help prevent collisions of CTS at the originating node and may help prevent RTS collision at the receiving node. However, Omnidirectional transmission of RTS packets may cause unwanted interference. The use of directional transmission of CTS relies on the spatial filtering capability of the selected beam to transmit the data. On the other hand, Policy II is a more aggressive beam selection policy that relies completely on the interference rejection capability provided by the directional radiation pattern of the antenna. A more conservative strategy is given by policy III where transmission of an omnidirectional CTS may prevent transmissions that may or may not affect the receiving node. This may result in an unnecessary

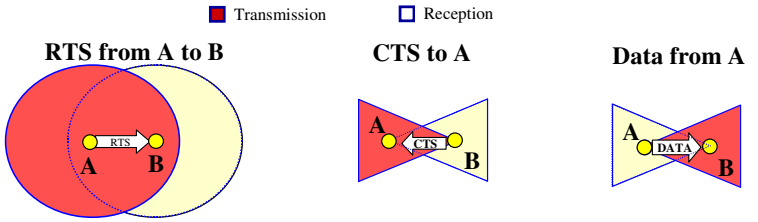

(a) Beam Selection Policy I (Omni-RTS)

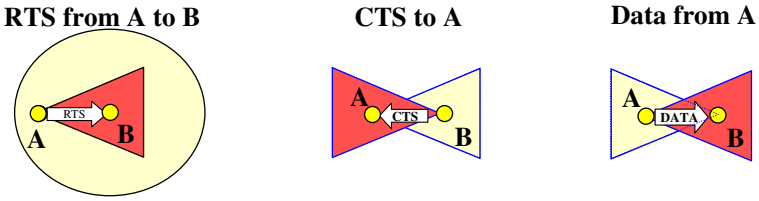

(b) Beam Selection Policy II (Di-RTS)

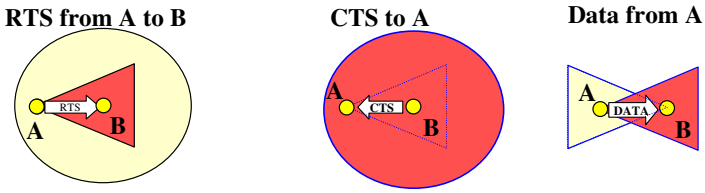

(c) Beam Selection Policy III (Di-RTS/Omni-CTS)

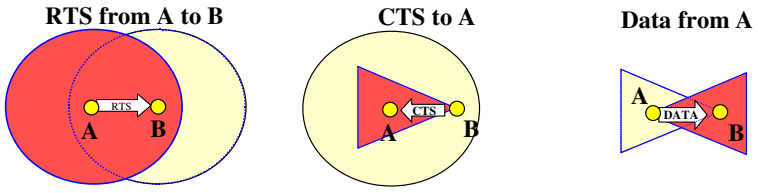

(d) Beam Selection Policy IV (Omni-RTS/Omni-Rx.CTS/Di-CTS)

Figure 9.6: Beam Selection Polices used by node A to communicate with node B. Circles indicate the use of omnidirectional antennas and triangles directional antennas.

channel reservation that does not take advantage of spatial interference reduction of smart antennas.

Policies I,II and III are very convenient if a node has total location information about its neighboring nodes. This could be the case for static or nomadic networks with very slow mobility. For a mobile scenario, Policy IV is a possible and interesting solution. In a mobile scenario the originating node may not know exactly where its neighbors are located, therefore it starts sending an omnidirectional RTS. After receiving the RTS the receiving node gets the location information of the originating node and therefore can transmit a directional CTS which is received by the originating node using an omnidirectional antenna pattern. After that, the data transmission could be done using directional patterns by both nodes.

Note that other selection policies are possible but were considered to result in lower performance improvement. For instance, it is possible to use both Omni-RTS and Omni-CTS but we can expect no significant benefit of reserving the channel this way.

9.3 Numerical Results

The performance using the above selection policies was evaluated using sample networks A and B in Fig.3.3. A carrier-sensing threshold of 3dB above the noise floor was used since it performed best in the omni-directional case.

Policy I (Omni-RTS)

The results for sample network A and B are shown in Fig.9.7 and 9.8, respectively. It can be noted that in both networks for very low traffic load no significant impact on packet delay is observed using this policy. This is an expected result since for low traffic the probability that two nodes attempt simultaneous transmission is rather small. For medium and high traffic, lower packet delay is always achieved by using narrower antenna beamwidth.

The use of of narrower antenna beamwidth always results in higher throughput. Fig.9.9 summarizes the end-to-end maximum throughput achieved using this policy.

Note that higher throughput is achieved for network B since it is better connected than network A (the average number of neighbors in network A is 7.5 while in network B it is 10.5). On the other hand the relative improvement with respect to the omnidirectional(see table 9.2) case is higher for network A since the network is more spread out allowing better filtering of interference with 90^o, 60^o and 30^o antenna beamwidths that with network B. The used of narrower antenna beamwidth result in an increasing SIR, achieving substantially lower delay and higher throughput.

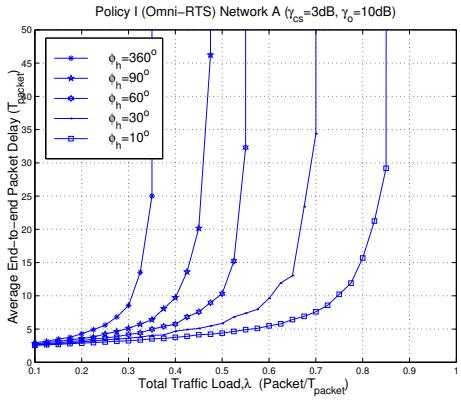

Figure 9.7: Performance of Policy I (Omni-RTS) for network A.

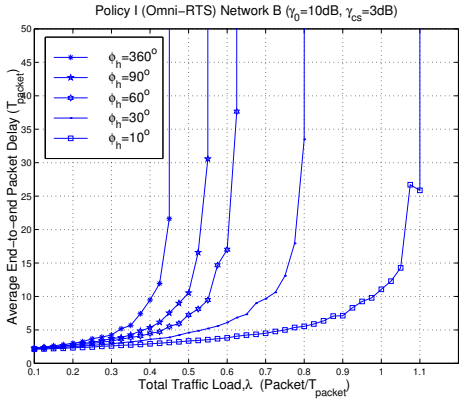

Figure 9.8: Performance of Policy I (Omni-RTS) for network B.

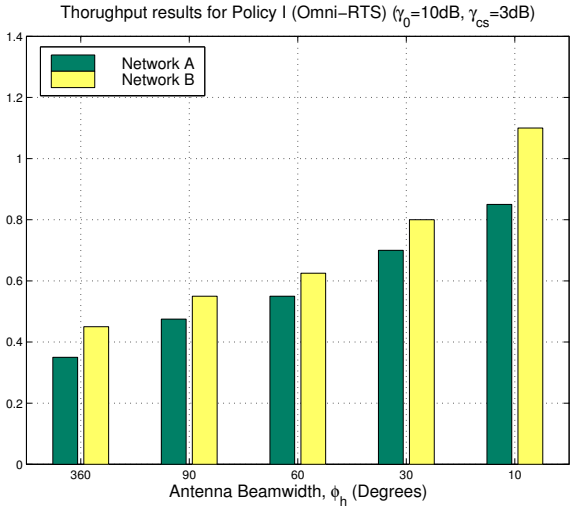

Figure 9.9: Maximum throughput using Policy I (Omni-RTS) for networks A and B.

Policy II (Di-RTS)

One possible problem with Policy I could be the potential data packet collision with omnidirectional RTS transmissions. If a node is unable to hear a CTS after hearing an RTS and neither detect the presence of a carrier on the channel, it assumes that it can transmit since its estimation of the MAI indicates that it is out of the antenna

front-end of the receiving node. This estimation could be completely wrong since the transmitting node uses a directional transmission of data. This create the risk that those nodes that were considered exposed in the omnidirectional case, starts transmitting an omnidirectional RTS that may produce significant interference at the receiving node while receiving the data packet, resulting in degradation of the required SIR.

Policy II tries to improve on this problem by implementing a more aggressive transmission strategy, transmitting with directional antennas during the whole procedure. This also produces the additional benefit of hardware complexity reduction since the need for power control is eliminated.

The performance using beam selection policy II is shown in Fig. 9.10 and Fig. 9.11 for networks A and B, respectively.

Similar to policy I, lower delay for medium and high traffic is obtained by this strategy. As expected, higher throughput is always obtained as the antenna beamwidth is reduced.

The end-to-end throughput improvement for policy I and II is summarized in Fig.9.12. It is clear that policy II(Di-RTS) performs better than Policy I (Omni-RTS) in all cases. This confirms our previous analysis that omnidirectional transmission of RTS packets reduces the performance because they may collide with data packets.

The performance improvement in end-to-end throughput using policy I respect to policy II is shown in Fig. 9.15. A throughput improvement of 21%, 32%, 21% and 19% for network A, and 9%, 12%, 19% and 18% for network B was obtained. Note that the improvement for network A increases up to 60^0 antenna beamwith and then decreases with 30^0 and 10^0 beamwidth. Similarly, the improvement also increases until 30^0 antenna beamwidth and decreases for 10^0 beamwidth for network

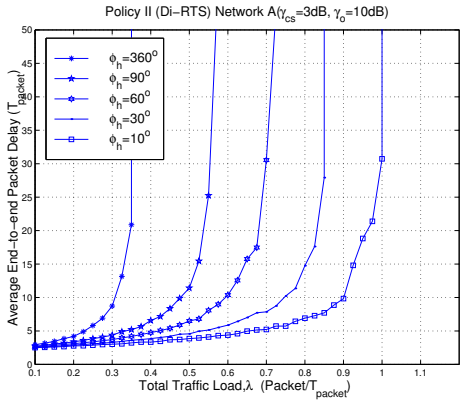

Figure 9.10: Performance of Policy II (Di-RTS) for network A.

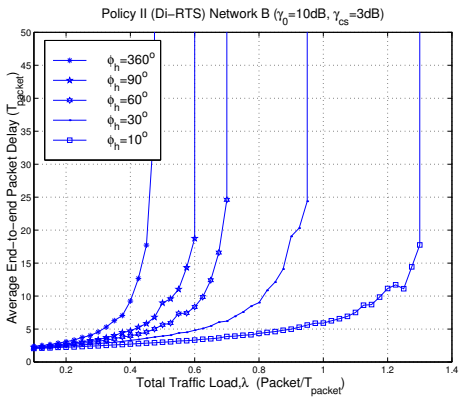

Figure 9.11: Performance of Policy II (Di-RTS) for network B.

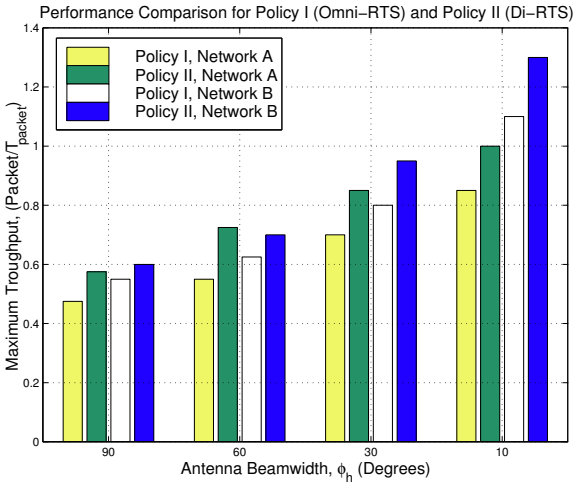

Figure 9.12: End-to-end throughput comparison for Policy I and Policy II for networks A and B.

B. This is because the omnidirectional impact of RTS transmission reduces as the antenna beamwidth reduces, which also confirming our previous statement.

Policy III (D-RTS/Omni-CTS)

A potential problem with policy II is that it does not prevent transmission toward a receiving node even if this transmission may produce significant interference. One possibility to overcome this problem is through the use of Policy III (D-RTS/Omni-CTS)where transmission of an omnidirectional CTS is utilized. This results in a more conservative strategy since it prevents transmission even when that may not result in destructive interference.

The results with this strategy evaluated on our two sample networks Fig.9.13 and 9.14, show the performance on networks A and B, respectively. As can see the use of this strategy results in poorer capacity improvement. Similar results to the Policy I and II for low traffic is obtained. However a significant lower throughput was found. This is an expected result since this strategy does not fully exploit the interference reduction achieved with directional antenna patterns. The use of omnidirectional CTS prevents transmissions that simply might interfere with outgoing data transmission. This seems to be the dominant effect. This can be confirmed by the result of network A where nodes are more spread out, limiting the number of nodes that are deferred by hearing a CTS.

The reason this protocol does not produce significant improvement is because it does not consider the direction of the intended data packet receiver to prevent

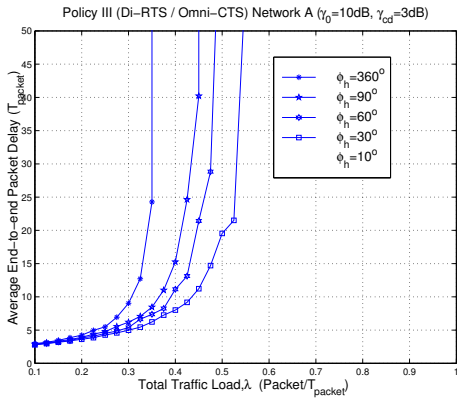

Figure 9.13: Performance of Policy III (Di-RTS/Omni-CTS) for network A.

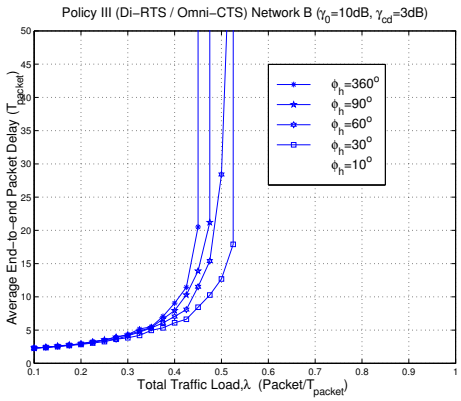

Figure 9.14: Performance of Policy III (Di-RTS/Omni-CTS) for network B.

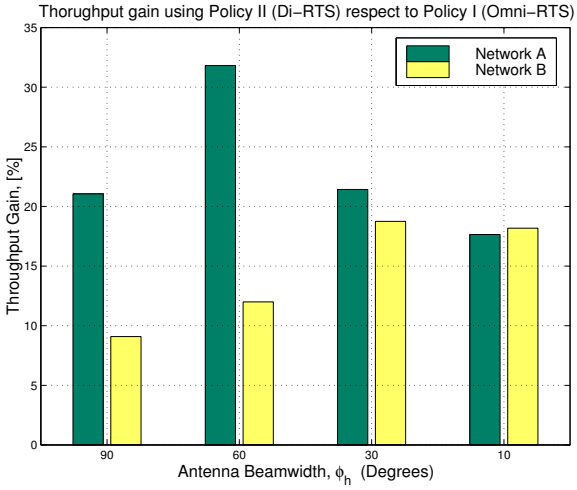

Figure 9.15: Throughput improvement using policy II with respect to Policy I.

transmission in that direction only. A smarter way to improve on this problem potentially producing better results could be find in [39] where they consider that multiple beams could be combined. Even with a single beam selection, the use of location information to prevent transmission in the direction of the receiver, may result in better performance. Due to the complexity of changing our simulator to include this functionality, this research will be considered in further works.

Policy IV (Omni-Tx.RTS/Omni-Rx.CTS/Di-CTS)

As mentioned in section 9.2, this policy is suitable for mobile networks where exact knowledge of the location of a given node does not exist. Since the procedure starts transmitting with an omnidirectional RTS and waits with an omnidirectional antenna pattern, lower performance could be expected with this policy than with Policy I and II for static networks.

Fig.9.16 and 9.17 show the results obtained by implementing this policy in networks A and B, respectively. As expected, similar behavior to policies I and II for low and relatively high traffic is achieved. However the throughput improvement is reduced by both RTS and data collision as well as CTS collisions under high traffic conditions.

The interesting thing with this result is that a big improvement in the overall performance is achieved by using this strategy which may justify its use in mobile scenarios. The end-to-end throughput improvement obtained with respect to the omnidirectional case was approximatly 29%, 50%, 86%, and 121% for network A and 22%, 39%,72% and 128% for network B using 90^0, 60^0, 30^0, and 10^0 antenna beamwidth respectively.

9.4 Beam Selection Policies in Rough Terrain

In this section impact of terrain roughness on the performance of the different policies is analyzed. Two different rural scenarios are evaluated using the terrain model described in Appendix B with roughness parameter $\sigma = 10m$ and $\sigma = 40m$ and smoothness parameter $\rho = 5km$ over a squared area of 50km x 50km. The

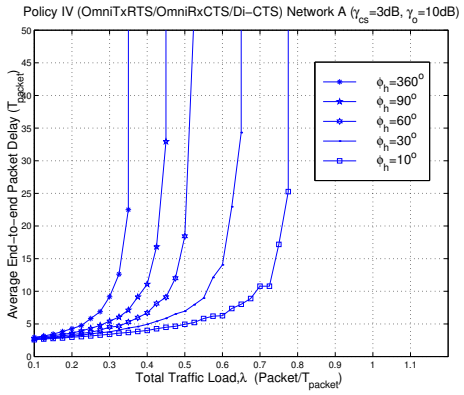

Figure 9.16: Performance of Policy IV (Omni-Tx.RTS/Omni-Rx.CTS/Di-CTS) for network A.

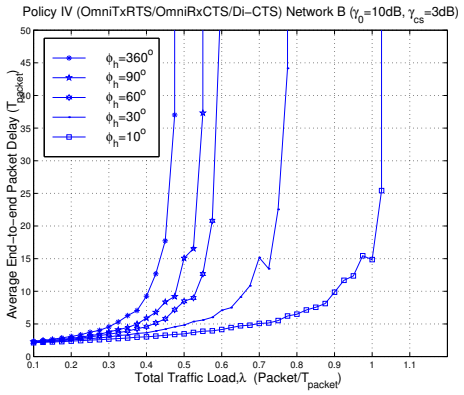

Figure 9.17: Performance of Policy IV (Omni-Tx.RTS/Omni-Rx.CTS/Di-CTS) for network B.

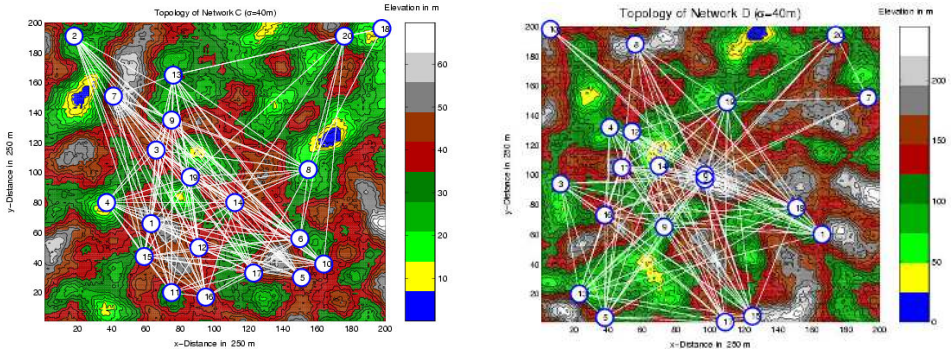

Figure 9.18: Topology of network C with terrain standard deviation $\sigma = 10m$ and network D over rough terrain with standard deviation $\sigma = 40m$.

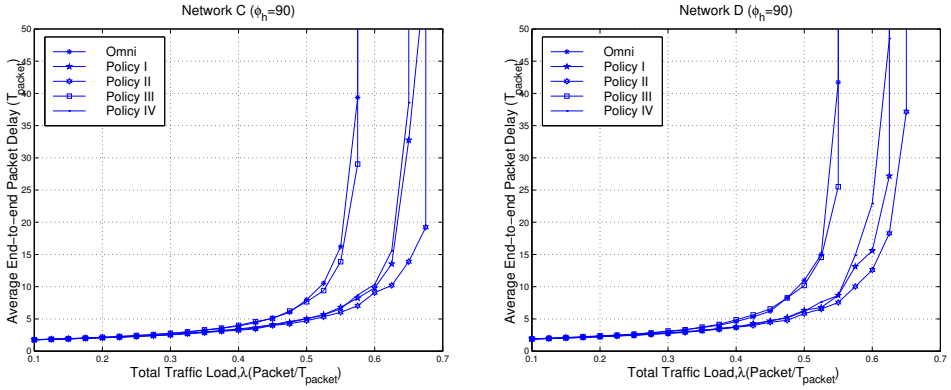

Figure 9.19: Performance on networks C and D with $\phi_h = 90^o$ antenna beamwidth.

network was deployed using 20 nodes randomly dispersed over the terrain until a connected network was found using the same criteria described in chapter 3 but with constant transmission power $P_i = 2$dB. Fig. 9.18 shows two networks topologies, network C and D, over the rough terrain used in the numerical examples below. The average number of neighbors was 13.9 for network C and 12.6 for network D.

Fig. 9.19, 9.20 and 9.21 show the performance results using 90^o, 60^o and 30^o antenna beamwidths, respectively, and using the 4 different policies and omnidirectional antennas. In general we can say that beam selection policy II produces the highest throughput in both networks, yielding the same previous conclusion independent of the terrain roughness.

An interesting result is that Policy IV performs very similarly to Policy I. The probable reason for this is that the shielding provided by mountains reduces the received interference while waiting for the CTS with omnidirectional antenna pat-

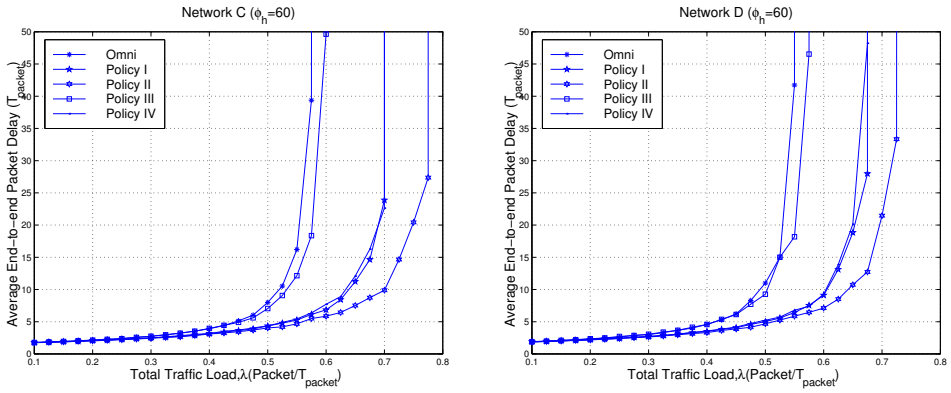

Figure 9.20: Performance on networks C and D with $\phi_h = 60^o$ antenna beamwidth.

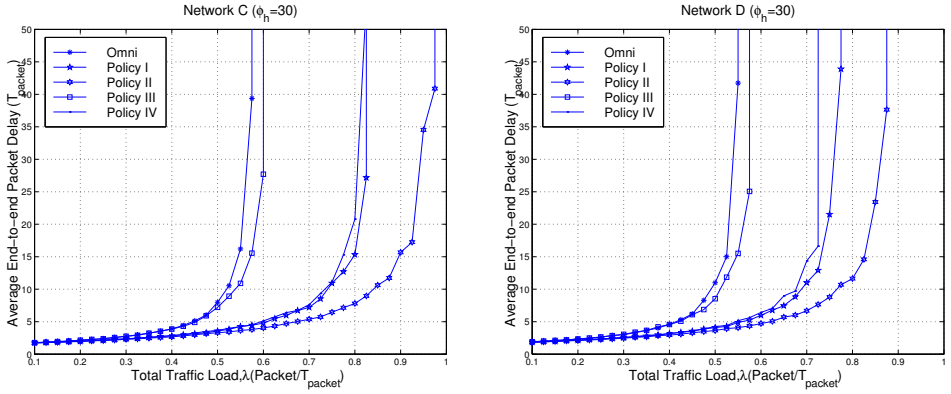

Figure 9.21: Performance on networks C and D with $\phi_h = 30^o$ antenna beamwidth.

tern.

Finally, Policy III produces the poorest results which are almost the same as using omnidirectional antennas. This is mainly because the channel is reserved over 13.9 and 12.6 neighbors (on average) preventing almost any other transmission on the network.

9.5 Concluding Remarks

In this chapter we have proposed and evaluated the performance of Carrier Sense Multiple Access/ Collision avoidance with RTS/CTS control handshaking using omnidirectional and smart antennas. Since cost is of paramount importance in civilian applications we address the problem of implementing switched-beam technologies as the smart antenna method to increase the end-to-end throughput.

Four different Beam selection policies were proposed and their performance evaluated by discrete step simulation. Policy I, II and III are well applied to static or nomadic networks while policy IV could be implemented for mobile networks where neither the transmitter nor the receiver knows in advance the exact location of its neighbors.

Table 9.2 summarizes the throughput improvement with respect to the omnidirectional case for all the beam selection policies when applied to the two sample networks A and B used to evaluate the performance. From this table it is found that the most aggressive strategy, Policy II (Di-RTS), which utilizes directional antenna patterns all the time performs the best. Up to 185% improvement in throughput with respect to the omnidirectional case was achieved by using this beam selection policy. An additional advantage with this policy is that it can be implemented without power control to keep the same radio range of RTS and Data transmissions, which results in lower hardware cost.

Table 9.2: Throughput Improvement with Respect to the Omnidirectional Case

Network A

Antenna Beamwidth (ϕ_h)	90^o	60^o	30^o	10^o
Beam Selection Policy I (Omni-RTS)	36 %	57%	100%	143%
Beam Selection Policy II (Directional-RTS)	64%	107%	143%	186%
Beam Selection Policy III (Di-RTS/Omni-CTS)	28%	43%	-	57%
Beam Selection Policy IV	29%	50%	86%	121%

Network B

Antenna Beamwidth (ϕ_h)	90^o	60^o	30^o	10^o
Beam Selection Policy I (Omni-RTS)	22%	39%	78%	144%
Beam Selection Policy II (Directional-RTS)	26%	47%	100%	173.7%
Beam Selection Policy III (Di-RTS/Omni-CTS)	5%	17%	-	17%
Beam Selection Policy IV	22%	39%	72%	127.8%

The throughput improvement of beam selection policy IV may justify its implementation in mobile networks. Up to 128% throughput improvement was obtained in our evaluation for network B.

Policy III (Di-RTS/Omni-CTS) could be considered the more conservative strategy evaluated, producing the poorest result. A possible way to improve the results of this policy is using the location information to prevent transmission only in the direction of the intended receiver. The incorporation of such changes together with neighbor-discovering procedures with AAS [100] could be an interesting subject for further work.

Chapter 10

On the application of MWN technology in Nicaragua - a simple example of Deployment

In this chapter we present a methodology for capacity evaluation of user-deployed multihop wireless networks in rural areas. The capacity is described by the maximum end-to-end transmission rate (throughput) provided to each node that comprises the network under heavy traffic load demand. A user-deployed scenario for Internet access is studied utilizing 13 sites in rural communities of Nicaragua (telecenter candidate sites). To reduce the Internet service cost, shared common access points are used in mesh configuration under asymmetric traffic demands. The results provide useful figure-of-merits and show that MWN is a feasible alternative to provide rural communication to those communities.

10.1 Introduction

The rural communities of interest in this example have been provided by the regulatory body of Nicaragua, TELCOR, through the Project Coordination Unit (UCP). The UCP is a special unit that coordinates, proposes and evaluates projects carried out through the National Fund for Telecommunication Investment (FITEL, by its acronym in Spanish) oriented to provide access to telecommunication services in low-income and rural areas of the country (see chapter 2).

The rural communities are located in the north central highlands region of the country, in the departments of Estelí, Madriz and Nueva Segovia. Fig. 10.1 shows the geographical locations of the communities utilizing a digital map of the terrain. The geographical coordinates of the communities can be found in appendix D.

TELCOR's final objective is to install telecenters for Internet Access in those communities. The general research question of interest to be answered is: • What is the capacity that a user-deployed MWN can provide subject to low-cost deployment

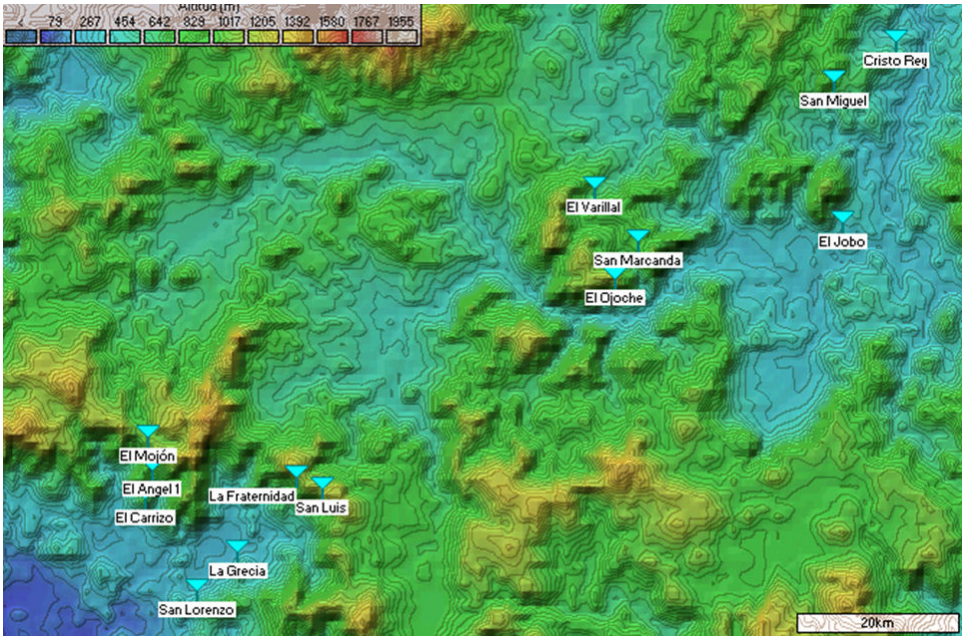

Figure 10.1: Rural communities of Nicaragua for case study ($120km \times 80km$). Source: Map was derived using the freeware software "Radio Mobile" [115].)

constraint for internet access for the 13 community sites (telecenters)?

For low-cost user-deployed scenario we consider the following:

- Share internet access: for low-cost internet service (network service recurrent cost) nodes share access provider.
- Economy of scale: we assume the utilization of radio equipment parameters on the 2.4GHz frequency band. In Nicaragua, that frequency band is part of the allocated unlicensed radio spectrum subject to rules in AA001-2006 [116]. These rules are similar to the FCC part 15 in the USA.

10.2 Method of Analysis

To share common Internet access points in a mesh configuration we assume asymmetric traffic demand from each node to a gateway node connected to the internet and viceversa.

The user-deployed scenario is analyzed estimating the radio propagation environment of located nodes. The path-losses in the network are derived utilizing

the digital map GTOPO30 (W100N40) [117] with the Longley-Rice model [118] as implemented by the Radio Mobile freeware program by VE2DBE [115].

The (upper-bound) capacity resulting from a user-deployed approach is evaluated by finding the interference-based link transmission schedule applying nonlinear optimization posed and solved as described in the following sections.

Analysis and User-deployed Methodology:

We can summarize the general methodology applied in the following sections by the following steps:

I) **Network Deployment:**

i. Determine the radio network parameters that will be used.

ii. Define the Internet gateway to be used (e.g. closest available land-based infrastructure).

iii. Determine the link-budget between stations including the gateway.

iv. Determine the current network topology.

v. If there are nodes that cannot reach the gateway, add digital-repeater nodes (digipeaters) to extend the connectivity by multihopping and go to step I–iii

II) **Capacity analysis:**

i. Define the external traffic load demand from each node to the Internet gateway and viceversa.

ii. Determine the routing matrix.

iii. From steps II–i and II–ii estimate the link-traffic load.

iv. Compute the equivalent link-path routing matrix R_{mesh}.

v. Determine the network capacity by interference-based scheduling (STDMA)

Recreation of the user-deployment is related to step I–i to I–v where users try to connect their communities to the Internet gateway. At the early stage, the WMN start comprised only by the nodes located in the communities. Then, progressively from the gateway towards the communities, the users add digital-repeaters to connect the network.

To determine the network topology we assume that the hardware utilized has the physical layer parameters shown in table 10.1. Those parameters are based on utilizing equipment with similar physical layer to IEEE 802.11g operating on the 2.4GHz frequency band [119] but under FCC part 15 rules. Note that the receiver sensitivity utilized is conservative as compared for instance with the specifications for the equipment in [105].

Table 10.1: Physical layer parameters

Frequency [GHz]	2.4	2.4	2.4	2.4	2.4	2.4	2.4	2.4	2.4	2.4
Data rate (R_set)[Mbps] *	1	2	6	9	12	18	24	36	48	54
Modulation	'CCK'	'CCK'	'BPSK'	'BPSK'	'QPSK'	'QPSK'	'16QAM'	'16QAM'	'64QAM'	'64QAM'
Code rate	1	1	1/2	3/4	1/2	3/4	1/2	3/4	2/3	3/4
Peak output power** [dBm]	30	30	30	30	30	30	30	30	30	30
Transmitter antenna gain [dBi]	6	6	6	6	6	6	6	6	6	6
EIRP [dBm]	36	36	36	36	36	36	36	36	36	36
Receiver antenna gain [dBi]	0	0	0	0	0	0	0	0	0	0
Bandwidth [MHz]	22	22	22	22	22	22	22	22	22	22
Thermal Noise [dBm/Hz]	-174	-174	-174	-174	-174	-174	-174	-174	-174	-174
Receiver Noise Figure [dB]	10	10	10	10	10	10	10	10	10	10
Noise Power [dBm]	-90.6	-90.6	-90.6	-90.6	-90.6	-90.6	-90.6	-90.6	-90.6	-90.6
Interference Margin [dB]	2	2	2	2	2	2	2	2	2	2
Minimum Es/N0 [dB]	0.6	3.6	4	5	7	9	12	16	20	21
Sensitivity (minimum Rx. Power) [dBm]***	-88	-85	-84.6	-83.6	-81.6	-79.6	-76.6	-72.6	-68.6	-67.6
Maximum allowed path loss[dB]	124	121	120.6	119.6	117.6	115.6	112.6	108.6	104.6	103.6

*Rates 5.5 and 11 are omitted assuming that all nodes use parameters similar to the one utilize at the physical layer of equipment based on IEEE802.11g.
** According to FCC part 15.247 (b)(1) and (b)(3)(i): the power must be reduced by 1dB for every 3dB that the directional gain of the antenna exceeds 6dBi. For omnidirectional antennas FCC part 15.247(b)(3) and (b)(3)(iii) apply, i.e. the maximum EIRP must be 36dBm (4W).
*** By increasing the interference margin the minimum required receive power is increased and the network topology could be modified.

To find the path losses, we assume utilization of the first channel on IEEE802.11g that operates on the frequency range: 2401 MHz- 2423MHz. The radio propagation path losses are found using the "Radio Mobile" freeware software and assuming that nodes utilize 20 meter antenna height.

Asymmetric Traffic Model

We assume asymmetric traffic demand from each node to the gateway node connected to the internet. Under this assumption the average traffic from node i to the internet gateway, node g, is defined as λ_i^g and from the gateway to node i as λ_g^i. Hence, the total network traffic load is given by:

$$\lambda = \sum_{\forall i \neq g} \lambda_i^g + \sum_{\forall i \neq g} \lambda_g^i$$

We assume that the average traffic from nodes to the Internet is 10% of the traffic from the internet to the nodes. We think this is a reasonable assumption if for instance the gateway is connected via an ADSL (Asymmetric Digital Subscriber Line) service and we would like to share this connection providing similar service to

all telecenters connected to the same gateway. In ADSL over Plain Old Telephone Service (POTS), ITU G.992.1 Annex A standard, the downstream rate is 12Mbps and the upstream rate is 1.3Mbps (which is 10.8% of the downstream rate). With this assumption the total traffic load can be rewritten by:

$$\begin{aligned}\lambda &= \sum_{\forall i \neq g} \lambda_i^g + \sum_{\forall i \neq g} \lambda_g^i \\ &= (N-1)(\lambda^{(UL)} + \lambda^{(DL)}) = 1.1(N-1)\lambda^{(DL)}\end{aligned} \tag{10.1}$$

where $\lambda^{(UL)}$ is the uplink traffic (from node to the gateway), $\lambda^{(DL)}$ is the downlink traffic (from the Internet to node) and $(N-1)$ the number of nodes (telecenters) interconnected to the Internet gateway. Hence, we can also rewrite the downlink allocation per node as:

$$\lambda_g^i = \lambda^{(DL)} = \frac{\lambda}{1.1(N-1)}, \forall i$$

In the following, to better explain the application of the method we utilize a simple network example.

Example 10.2.1 Capacity Evaluation with 4-nodes network

To illustrate the methodology we utilize the 4-nodes ring network shown in Fig.10.2. The distance between nodes is set to 15km. For this illustrative example we use a distance dependent radio propagation model to find the path gain matrix with $\alpha = 3$. Hence, the $\boldsymbol{G}$ matrix is given by:

$$\boldsymbol{G} = \begin{bmatrix} \infty & -129.8 & -134.3 & -129.8 \\ -129.8 & \infty & -129.8 & -134.3 \\ -134.3 & -129.8 & \infty & -129.8 \\ -129.8 & -134.3 & -129.8 & \infty \end{bmatrix} \text{ [dB]}$$

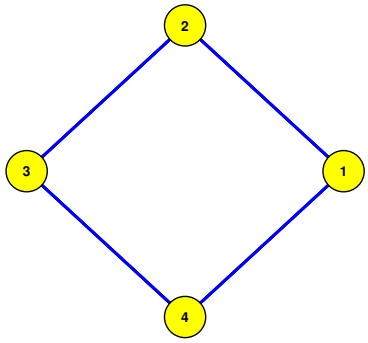

$$\boldsymbol{r} = \begin{bmatrix} 0 & 2 & 2 & 4 \\ 1 & 0 & 3 & 1 \\ 2 & 2 & 0 & 4 \\ 1 & 1 & 3 & 0 \end{bmatrix}$$

Figure 10.2: Four nodes ring network

If nodes are assumed to utilize 6dBi omnidirectional antennas and the physical layer parameters in table 10.1, the received power, P_r, result to be:

$$\boldsymbol{P}_r = \boldsymbol{P}_t + G_r + G_t + \boldsymbol{G} = \begin{bmatrix} \infty & -87.8 & -92.3 & -87.8 \\ -87.8 & \infty & -87.8 & -92.3 \\ -92.3 & -87.8 & \infty & -87.8 \\ -87.8 & -92.3 & -87.8 & \infty \end{bmatrix} \text{[dBm]}$$

where P_t is the transmitted power, G_t and G_r are the antennas´gains for transmission and receptions, respectively and G denotes the path gain matrix. Since the received sensitivity is -88dBm, the feasible links are those for which $P_r \geq -88$dBm (sensitivity at rate $R_0 = 1$Mbps). The resulting network topology and routing table $\boldsymbol{r}$ using Dijkstra algorithm with equal cost for all links (minimum hop routing) are shown in Fig.10.2. The node-arc incident matrix matrix, $\boldsymbol{A}$ to represent the network topology is given by:

$$\boldsymbol{A} = \begin{bmatrix} -1 & -1 & 1 & 0 & 0 & 0 & 1 & 0 \\ 1 & 0 & -1 & -1 & 1 & 0 & 0 & 0 \\ 0 & 0 & 0 & 1 & -1 & -1 & 0 & 1 \\ 0 & 1 & 0 & 0 & 0 & 1 & -1 & -1 \end{bmatrix}$$

Gateway and link traffic:
In this example we arbitrarily define node 3 as the gateway for Internet access. Therefore the external traffic load in matrix form can be written as:

$$\Lambda = \begin{bmatrix} 0 & 0 & 0.1 & 0 \\ 0 & 0 & 0.1 & 0 \\ 1 & 1 & 0 & 1 \\ 0 & 0 & 0.1 & 0 \end{bmatrix} \lambda^{(DL)}$$

To express the traffic load in vector form we label only the (S,D) pairs with traffic load higher than zero as $p = 1 \ldots 6$ with the following labels:

Label p	1	2	3	4	5	6
(S,D)	(1,3)	(2,3)	(3,1)	(3,2)	(3,4)	(4,3)

Hence the traffic load in vector form is given by:

$$\boldsymbol{\Lambda} = \begin{bmatrix} 0.1 & 0.1 & 1 & 1 & 1 & 0.1 \end{bmatrix}^T \lambda^{(DL)}$$

Using the source-to-destination pairs in $\boldsymbol{\Lambda}$, we get the corresponding link-route incident matrix $\boldsymbol{R}$:

$$\boldsymbol{R} = \begin{bmatrix} 0 & 0 & 1 & 0 & 0 & 0 \\ 0 & 0 & 0 & 0 & 0 & 0 \\ 1 & 0 & 0 & 0 & 0 & 0 \\ 0 & 0 & 1 & 1 & 0 & 0 \\ 1 & 1 & 0 & 0 & 0 & 0 \\ 0 & 0 & 0 & 0 & 0 & 1 \\ 0 & 0 & 0 & 0 & 0 & 0 \\ 0 & 0 & 0 & 0 & 1 & 0 \end{bmatrix}.$$

Here we can see that for source-to-destination labeled 1, links 3 and 5 are utilized for routing (i.e. these link labels correspond to links (1,2) and (2,3)). Source-to-destination labeled 2 utilizes only link 5, etc.

From the routing and external traffic we can find the traffic load demand for each link by $\Pi = R\Lambda$. Note that in this case links 2 and 7 do not have traffic demand since links 1 and 3 are the ones selected for the downlink and uplink traffic for node 1. Since they are carrying no traffic they can be removed from been scheduled for transmission. In fact, in our implementation we redefine an equivalent link path routing matrix to account for the relative traffic load removing those links that are not carrying traffic. This equivalent matrix is defined as $R_{mesh} = (R * \mathrm{d}iag(\Lambda_{|\lambda^{(DL)}=1}})$ and removing links carrying no traffic) which results in:

$$R_{mesh} = \begin{bmatrix} 0 & 0 & 1 & 0 & 0 & 0 \\ 0.1 & 0 & 0 & 0 & 0 & 0 \\ 0 & 0 & 1 & 1 & 0 & 0 \\ 0.1 & 0.1 & 0 & 0 & 0 & 0 \\ 0 & 0 & 0 & 0 & 0 & 0.1 \\ 0 & 0 & 0 & 0 & 1 & 0 \end{bmatrix} .$$

Note that for this redefined matrix, the mesh-link labels are according to the order list of the set $\{(2,1),(1,2),(3,2),(2,3),(4,3),(3,4)\}$.

STDMA Scheduling and Capacity evaluation

To find the interference-based scheduling for constant transmission power and variable rate systems we follow a procedure similar to the one described in chapter 7 but with the redefined mesh equations derived in this chapter. That is, we find $\boldsymbol{S}$, $\boldsymbol{\alpha}$ and $\boldsymbol{\Lambda}_{mesh} = [\lambda_1 \dots \lambda_p]$ that solve the following optimization problem:

$$\begin{aligned} &\text{maximize } \lambda_{\min} \\ &\text{subject to } \lambda_i \geq \lambda_{\min} \forall i; \\ &\boldsymbol{R}_{\text{mesh}} \boldsymbol{\Lambda}_{mesh} \leq \boldsymbol{S}\boldsymbol{\alpha} \ ; \\ &\sum_k \alpha_k = 1 \ ; \\ &\lambda_{\min} \geq 0; \boldsymbol{\Lambda}_{mesh} \succeq \mathbf{0} \ ; \mathbf{0} \preceq \boldsymbol{\alpha} \preceq \mathbf{1} \ . \end{aligned}$$

By solving the above problem for our illustrative example, the following link capacity allocation is found:

$$\boldsymbol{C} = \boldsymbol{S}\boldsymbol{\alpha} = \begin{bmatrix} 1 & 0 & 0 & 0 & 0 & 0 \\ 0 & 1 & 0 & 0 & 0 & 0 \\ 0 & 0 & 1 & 0 & 0 & 0 \\ 0 & 0 & 0 & 1 & 0 & 0 \\ 0 & 0 & 0 & 0 & 1 & 0 \\ 0 & 0 & 0 & 0 & 0 & 1 \end{bmatrix} \begin{bmatrix} 0.2273 \\ 0.0227 \\ 0.4545 \\ 0.0455 \\ 0.0227 \\ 0.2273 \end{bmatrix} = \begin{bmatrix} 0.2273 \\ 0.0227 \\ 0.4545 \\ 0.0455 \\ 0.0227 \\ 0.2273 \end{bmatrix} \text{ [Mbps]}$$

The allocated end-to-end rate in matrix form can be written by:

$$\boldsymbol{\Lambda} = \begin{bmatrix} 0 & 0 & 0.0227 & 0 \\ 0 & 0 & 0.0227 & 0 \\ 0.227 & 0.227 & 0 & 0.227 \\ 0 & 0 & 0.0227 & 0 \end{bmatrix} \text{ [Mbps]}$$

In summary, by the transmission schedule, for this illustrative example the resulting end-to-end uplink transmission rate is 23kbps and for the downlink is 227kbps to each node. The total end-to-end network capacity is then 750kbps.

In the above example, if we reduce the distance between nodes to 10km and increase the interference margin to 5dB, the topology is maintained. In that case, the transmission rates in $\boldsymbol{S}$ increases from 1 to 12Mbps. That results in a throughput gain of 10 with respect to the previous case, i.e. the downlink to each user increases to 2.27Mbps and the uplink to 227kbps. ■

10.3 User-deployed and Capacity Evaluation for the Rural Communities of Nicaragua

Description of User-deployed approach

We assume a simple user-deployed behavior. The community starts by locating their own nodes at their locations (telecenters) and the shared Internet access node (Gateway) located at the closest land-based infrastructure. At the communities under consideration there are two municipalities head-end (towns) where it is possible to have access to land-based Internet services: San Juan de Limay and San Juan del Rio Coco. The geographical coordinates are shown in table 10.3. In San Juan de Limay the operator ENITEL has a 63-meter high tower, and we assume that a similar tower could be utilized (or is available) in San Juan del Rio Coco.

By utilizing these gateways we can group the communities into two potential user-deployed subnetworks as shown in Fig.10.3. We call the set of communities that are geographically closer to ENITEL in San Juan de Limay subnetwork 1, and the set of communities closer to San Juan del Rio Coco subnetwork 2.

The user-deployed approach corresponding to each subnetwork is then applied. The stages for connecting the communities in subnetwork 1 are illustrated in Fig.10.5 when utilizing 6dBi omnidirectional antennas (transmitter and receiver) and the parameters in table 10.1.

After stage 1 and its resulting connectivity, the users add a relaying node to connect node 5 (El Carrizo) and node 6 (El Angel 1) to ENITEL(San Juan de Limay). For that, they select an intermediate (high) point for the relaying node. We refer to relaying nodes that don't generate external traffic as Digipeater (Digi). On the next stage (stage 3), node 7 (El Mojon) has to be connected by also adding

Table 10.2: Geographical coordinates for Internet Gateways

Node name	Latitude	Longitude	Altitude
ENITEL (San Juan de Limay)	13° 10'23"N	086°36'23" W	948.6ft
San Juan del Rio Coco	13°33'00"N	086° 10' 00"W	2908.5ft

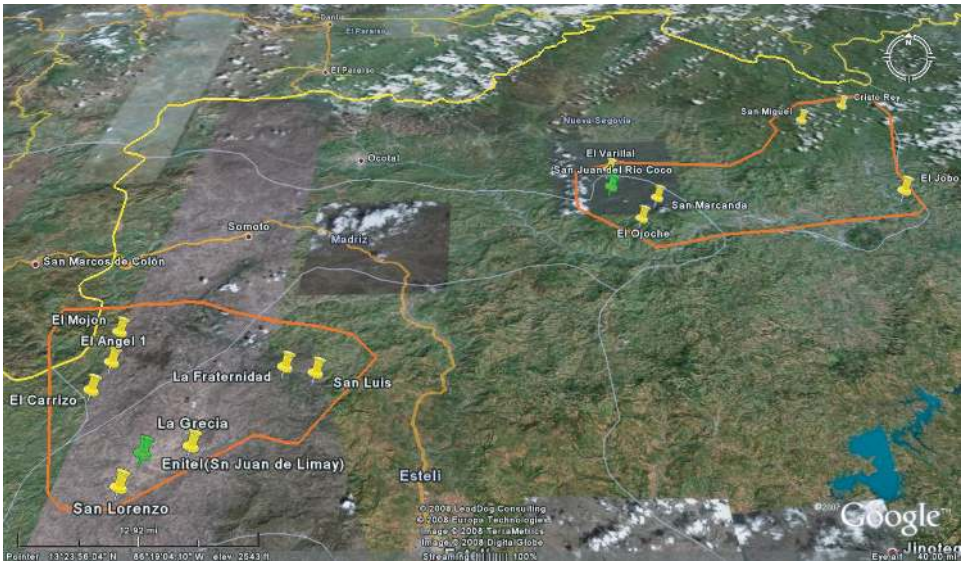

Figure 10.3: Subnetwork 1 and subnetwork 2.
Source: Map was derived using Google Earth™. © Google Inc.

another digipeater. One high point in the region can be located to connect node 5. The positions for the digipeaters are summarized in the table 10.3.

Capacity evaluation for subnetwork 1

We apply the previously described method together with the above user-deployed network and also utilizing beam-steering antenna systems. The capacity evaluations are summarized in table 10.4.

We can note that utilizing an interference margin of 5dB and Beam-steering antennas produces higher end-to-end data rate. This is because when utilizing IM=2dB with beam-steering antennas, the network topology changes with respect to the omnidirectional case, making link (3,5) feasible. Link (3,5) is a weak link utilized for routing traffic towards the gateway (node 8) and to satisfy its traffic demand its activation consumes a lot of network capacity.

In summary, by the simple user-deployed approach for the subnetwork 1, the (upper bound) allocated end-to-end downlink transmission rate was about up to 5.2Mbps per node (telecenter) and for the uplink was about up to 517kbps per node.

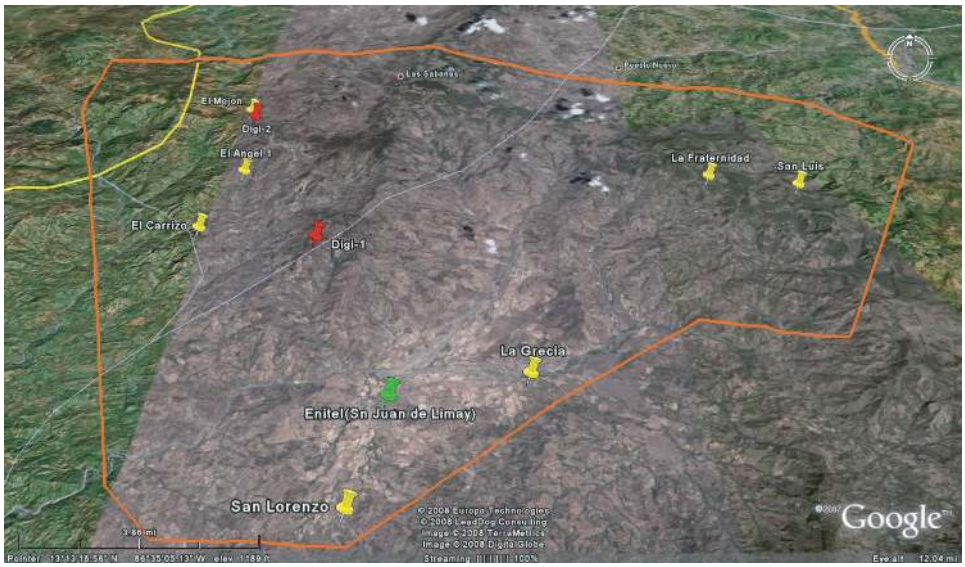

Figure 10.4: User-deployed (subnetwork 1).
Source: Map was derived using Google Earth™. © Google Inc.

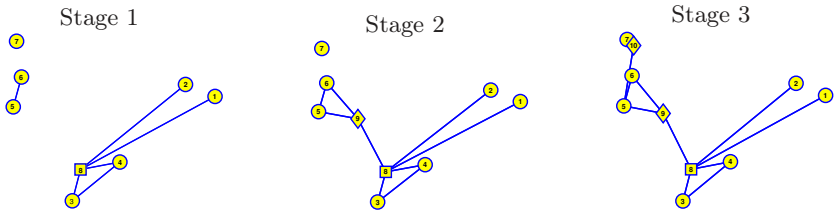

Figure 10.5: User-deployed stages for subnetwork 1. The gateway is indicated by a square (node 8) and digipeaters by rhombus (nodes 9 and 10).

Table 10.3: Geographical coordinates for digipeaters in subnetwork 1

Node name	**Latitude**	**Longitude**	**Altitude**
Digi-1(node 9)	13°01'56"N	086°38'23"W	3218.5ft
Digi-2(node 10)	13°18'15"N	086°40'24"W	3802.5ft

Table 10.4: Capacity evaluation for subnetwork 1

Antenna System	Interference Margin [dB]	Antenna Gain [dBi]	Uplink (rate/node)	Downlink (rate/node)	Total rate
Omni	2	6	115kbps	1.2Mbps	8.8Mbps
Beam-steering (HPBW=30)	2	12	233kbps	2.3Mbps	18Mbps
Beam-steering (HPBW=30)	5	12	517kbps	5.2Mbps	40Mbps

* Communities and digipeaters: San Luis, La Fraternidad, San Lorenzo, La Grecia, El Carrizo, El Angel 1, El Mojon, ENITEL (San Juan de Limay), Digi-1, Digi-2.

User-deployed subnetwork 2

To connect the remaining communities we assume that an Internet gateway can be installed at the municipality head-end called San Juan del Rio Coco. Next, following the user-deployed approach described before, we add two digipeaters in the locations summarized in table 10.5.

For the gateway at San Juan del Rio Coco we assume 63m tower height. As before, all nodes in the network are assumed to be installed utilizing 20m antenna height. Figure 10.6 shows the locations of the communities and the digipeaters needed for connectivity to the Internet gateway to be located in San Juan del Rio Coco.

When utilizing omnidirectional antennas with the selected points there is not fully connectivity for all nodes that comprises the network. The utilization of beam-steering antennas with an Interference margin of 2dB makes it possible to connect all the communities to the Internet gateway. The increment on the interference margin is done in order to allow more resistance to interference and this way we remove links with low transmission rate (we avoid them being used for routing traffic and being scheduled). However, when increasing the interference margin to

Table 10.5: Locations for digipeaters in subnetwork 2

Node name	**Latitude**	**Longitude**	**Altitude**
Digi-3	13°31'45.1"N	086°09'27.4"W	3438.3ft
Digi-4	13°34'59.6"N	086°59'02.8"W	3676.2ft

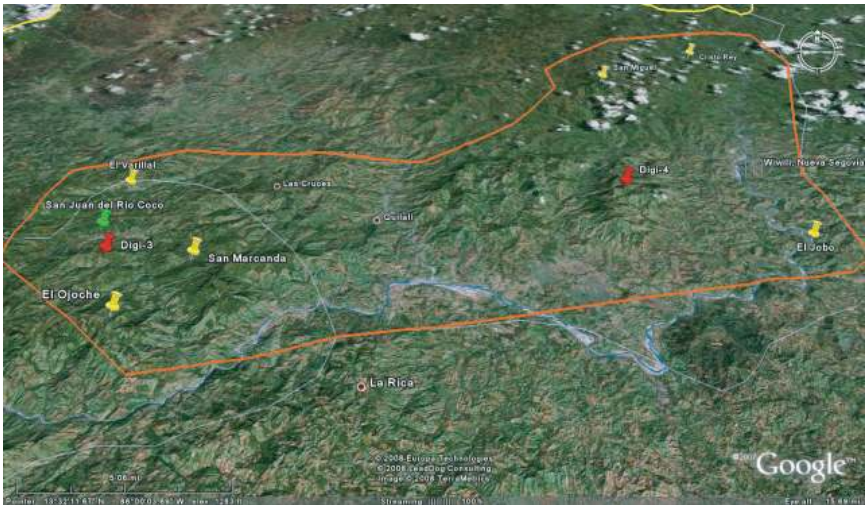

Figure 10.6: User-deployed (subnetwork 2).
Source: Map was derived using Google Earth™. © Google Inc.

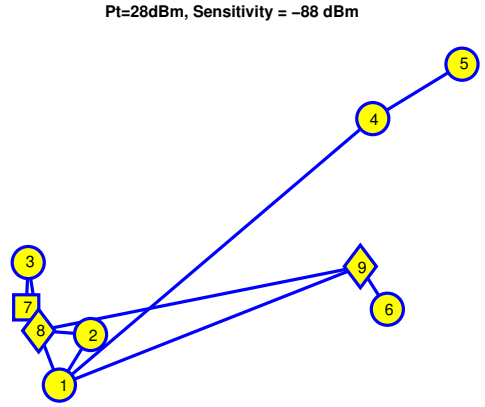

Figure 10.7: Network topology (subnetwork 2). Node 7 (San Juan del Rio Coco) is the Internet gateway and nodes 8 and 9 are the digipeaters.

5dB we found that the community called El Jobo gets disconnected. Fig.10.7 shows the network topology when utilizing beam-steering antennas with 2dB interference margin.

Note that there is a long-range connection of 36.2km from El Ojoche (node 1) to San Miguel (node 4). This is because there is line of sight between these two points as illustrated in Fig.10.8.

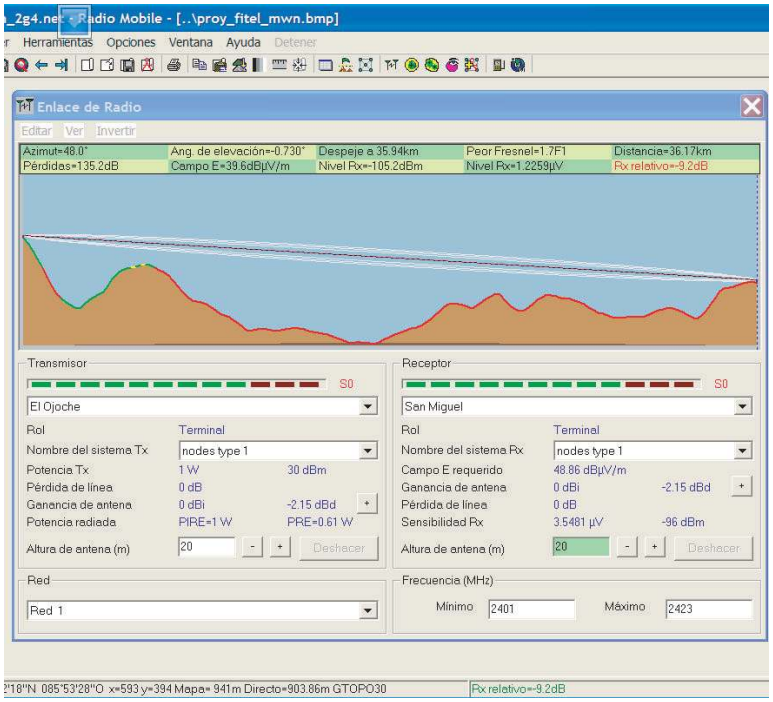

Figure 10.8: Terrain profile between El Ojoche and San Miguel.

The capacity evaluations for subnetwork 2

We again apply the previously described method before together with the above user-deployed network and also utilizing beam-steering antenna systems. The capacity evaluations are summarized in table 10.6.

Table 10.6: Capacity evaluation for subnetwork 2

Antenna System	Interference Margin [dB]	Antenna Gain [dBi]	Uplink (rate/node)	Downlink (rate/node)	Total rate
Omni	2	6	-	-	-
Beam-steering (HPBW=30)	2	12	388kbps	3.9Mbps	26Mbps
Beam-steering (HPBW=30)	5	12	-	-	-

* Communities and digipeaters: : El Ojoche, San Marcanda, El Varrillal, San Miguel, Cristo Rey, El Jobo , San Juan del Rio Coco, Digi-3, Digi-4.

Hence, for this user-deployed subnetwork, the resulting (upper bound) end-to-end downlink transmission rate is up to about 3.9Mbps per node (community) and 388.5kbps per node for the uplink.

10.4 Concluding Remarks

In this chapter we have introduced a methodology for capacity evaluation of user-deployed multihop wireless networks in rural areas. We have applied the methodology to evaluate a user-deployed scenario for Internet access in thirteen rural communities of Nicaragua. These communities are currently candidate sites to install telecenter by the regulatory body of Nicaragua.

In order to reduce the Internet service cost we have utilized shared common access points under asymmetric traffic demands. In our practical example, due to the terrain roughness and long distance, the communities were divided into two geographical sets conforming disjoint community subnetworks connected by two independent gateways. In order to overcome the high path losses due to the long distance and mountains, digital repeaters (relaying nodes) were assumed to be installed to progressively connect each community from the gateways.

To study the systems we have considered the utilization of 6dBi omnidirectional antennas and also beam-steering circular array antenna systems with half power beamwidth of 30^o (12 dBi).

The theoretical maximum end-to-end transmission rate (throughput) provided to each node by the user-deployed approach is found by link transmission scheduling applying nonlinear optimization considering the asymmetric traffic demands.

The utilization of AAS provided the benefit of radio range extension and reduction of multiple access interference yielding the need of fewer number digipeaters and therefore faster deployment. With the underlying assumptions and the radio parameters in table 10.1, the aggregated end-to-end data rate per user was higher than the typical ADSL connection when utilizing AAS and approximated to the typical ADSL connection when connectivity was possible using omnidirectional antennas (subnetwork 1). The maximum end-to-end rate per node i.e. from the gateway to the community telecenters (downlink) was about 1.2 Mbps when connectivity was possible using omnidirectional antennas and up to about 5 Mbps per node with beam-steering circular antennas. The results provide useful figures-of-merit under the hypothetical system and conditions assumed in our evaluations,and show that MWN is a feasible alternative to provide rural communication to those communities.

Chapter 11

Conclusions

This thesis has dealt with the analysis and design of Multihop Wireless Networks (MWN) with Advanced Antenna Systems (AAS) as a potential technology to provide access to telecommunication services in rural areas. The selection of this technology has been proposed as an appealing solution by analyzing the roll-out process of the telecommunication infrastructure in the developing country of Nicaragua. So far rural areas have been unattractive to private investors due to low population density, large coverage areas, in perhaps difficult and rough terrain together with the low income of potential users. In this context multihop wireless network has been considered a technology that could be utilized to extend the existing land-based infrastructure or in combination with satellite technologies.

Utilization of AAS has been studied with the centralized Spatial Time Division Multiple Access (STDMA) as well as with the distributed MAC protocol Carrier Sense Multiple Access (CSMA/CA) with handshaking. Centralized STDMA to some extent supports control of the relative capacity assigned to links, provides bounded packet-delay and some degree of service quality. One the other hand, one potential drawback with centralized STDMA may be the use of global network information to derive its control decisions. Therefore, STDMA may not support fast response to peak rate variations for bursty data traffic and its response time to adapt to topology changes, which can occur due to the variant channel conditions and occasional node failures, may be slower than a distributed MAC protocol. In rural communications networks the proposed technology has been considered to be deployed with only stationary nodes, and the environment in which these networks operate is expected to be slow time-varying.

A distributed approach is likely to react much faster to changes in traffic demands than a centralized approach. The Carrier Sense Multiple Access/ Collision Avoidance (CSMA/CA) with handshaking therefore has an ability to provide high peak data rates and may react faster than a centralized approach, since nodes make their own decisions based on partial information about the network.The problem with this protocol, as with any other random protocol in multihop networks, is the

issue of estimating packet delay, making it difficult to guarantee service quality [38].

The utilization of AAS with STDMA has been found to provide substantial gain in performance with respect to omnidirectional antenna deployed networks. The use of AAS using beam-steering always results in higher SINR. The improved link quality and reduced multiple access interference can be used to increase the reuse of slots in link assignment scheduling in fixed rate systems or to utilize higher transmission rate in variable rate systems.

The potential improvement provided by AAS can be further increased by route selections. To improve the network performance, a novel procedure to create the interference-based centralized link schedule called Reused Adaptive Minimum Hop Algorithm (RAMHA) was introduced and its performance evaluated. Substantial higher end-to-end throughput and lower end-to-end packet delay has been demonstrated.

Furthermore, investigations of the performance improvement generated by combining rate control and power control together with AAS in STDMA have been presented. The research question to be answered is posed as a nonlinear optimization problem solved by the column generation method proposed in [58] extended to include the use of AAS. The results have shown that variable rate systems provide a significant gain with respect to constant rate systems. The use of power control together with AAS produces an additional gain but this gain is not significant. This effect becomes even more pronounced when more narrow-beam antenna systems are used. These results suggest that advanced antenna systems without power control with centralized interference-based scheduling provide a good trade-off between performance and system complexity when the main objective is to maximize the end-to-end network throughput. Low-complexity interference-based link scheduling algorithms have also been proposed. Although simpler, these algorithms yield reasonable results close to the performance of the (variable slot-length) optimal schedule solution, which is very computational demanding.

The use of AAS with CSMA/CA reduces the overall multiple access interference, thus reducing the exposed terminal problem, but it likely also increases the hidden terminal problem. Four different beam selection policies have been proposed and their performance has been evaluated by discrete step simulation. Three of these policies (Policy I, II, and III) are well applied to static or nomadic networks while policy IV could be implemented for mobile networks where neither the transmitter nor the receiver knows in advance the exact location of its neighbors. The results show that the most aggressive policy, referred to as Policy II (Di-RTS), performs the best in terms of throughput-delay performance. Policy II (Di-RTS) utilizes directional antenna patterns whenever possible. An additional advantage of this policy is that it can be implemented without power control to keep the same radio range of RTS and data transmissions, which results in lower hardware cost. If mobile networks are being considered then policy IV is recommended.

Finally, an example of user-deployed multihop wireless networks for rural communities of Nicaragua together with the networks capacity evaluations has been presented. The methodology to find the upper bound on capacity for asymmetric

traffic requirement sharing Internet access points provides a useful figure of merit.

11.1 Further Research Work

This thesis has addressed aspects and issues regarding the use of advanced antenna systems, however there are still a number of further research questions considered relevant for future work. In particular all the algorithms proposed for interference-based scheduling have been centralized assuming that global information about the network and channel conditions are known. We believe that the centralized algorithms could be modified to be distributed; making nodes to make their own decisions based on partial information about the network is an interesting area for further research. In the literature we can find interesting distributed algorithms for link assignment and advanced antenna systems based on two hop neighborhood information exchange for fixed transmission rate systems [38, 43] that can be used as reference.

Further research on how to exchange relevant neighborhood information using the directional radiation pattern of advanced antenna systems is needed. The utilization of omnidirectional transmissions to propagate neighborhood information proposed in some studies may not be the best solution. For instance in [38], to maintain the same radio range they assume that the AAS and omnidirectional transmission operate on different frequencies and possibly use different power level. Beside the additional complexity, some practical issues related to this mechanism could be interesting to further investigate, such as the impact of the channel correlation due to the difference on frequencies that may affect the accuracy of the channel estimation. However, it is more desirable to utilize the same channel to exchange the relevant neighborhood information as in the case of CSMA/CA while at the same time maintaining the benefit of predictable end-to-end packet delay for QoS guarantee. It could be interesting, for instance, to utilize methods used for neighbors discovered with directional antennas to exchange the neighbor information. Another method to be used with AAS that seems to be interesting to further investigate is the algorithm originally defined by Lyui described in [120] that does not required a contention-based channel access protocol.

Finally, in our framework we have analyzed homogeneously configured nodes network deployment in which all nodes in the network utilize omnidirectional antennas or all nodes utilize AAS. As the technology advances and its cost is reduced there may be a smooth network evolution process in multihop wireless networks where nodes could utilize different AAS solutions. Despite this, it might not be possible or cost-effective to upgrade all nodes at once to be equipped with advanced antenna systems. Therefore during the evolution (migration) toward a total AAS there may exist legacy nodes in the network utilizing, for instance, omnidirectional antennas. Therefore networks composed by heterogeneous configured nodes are foreseen in the future and are an interesting area for further research.

Bibliography

[1] (2007) International telecommunications union. [Online]. Available: http://www.itu.int/AFRICA2001/forum/public_sessions.html

[2] R. G. Stephens, "Cellular telephony - new isntrument for universal access in latinamerica," L@tin.tel Magazine, No.1, Mar. 2004, (in Spanish).

[3] R. Pabst, B. H. Walke, D. C. Schultz, P. Herhold, S. Mukherjee, H. Viswanathan, M. Lott, W. Zirwas, D. D. Falconer, and G. P. Fettweis, "Relay-based deployment concepts for wireless and mobile broadband radio," *IEEE Commun. Mag.*, vol. 42, pp. 80–89, Sep. 2004.

[4] C. E. Perkins, Ed., *Ad Hoc Networking*. Addison-Wesley, 2001.

[5] J. Zheng and M. J. Lee, "Will IEEE 802.15.4 make ubiquitous networking a reality?: a discussion on a potential low power, low bit rate standard," *IEEE Commun. Mag.*, vol. 42, pp. 140–146, Jun. 2004.

[6] G. Saban and R. Braun, "Wireless local loop and packet radio technology for developing communities," in *Proceedings of the 1998 South African Symposium on Communications and Signal Processing, 1998 (COMSIG '98)*. Rondebosch, South Africa: IEEE, Sep. 1998, pp. 1–6.

[7] N. Abramson, "The Throughput of Packet Broadcasting Channels," *IEEE Trans. Commun.*, vol. 25, no. 1, pp. 117–128, 1977.

[8] M. Frodigh, P. Johansson, and P. Larsson, "Wireless ad hoc networking - the art of networking without a network," *Ericsson Review*, no. 4, 2000.

[9] *Wireless LAN Medium Access Control (MAC) and Physical Layer (PHY) Specification*, IEEE Std. 802.11, 1999.

[10] C. Fullmer and J. Garcia-Luna-Aceves, "Floor Acquisition of Multiple Access in Ad-Hoc Networks," in *Proc. ACM SIGCOMM95*, Cambridge, MA, 1995.

[11] C. L. Fullmer and J. Garcia-Luna-Aceves, "Completed Single-Channel Solutions to Hidden Terminal Problems in Wireless LANs," in *Proceedings of ICC '97*. Montreal, Canada: IEEE, 1997.

[12] V. Bhaghavan, A. Demers, S. Shenker, and L. Zhang, "MACAW: A Medium Access Protocol for Wireless LAN's," in *SIGCOMM95*. IEEE, 1995, pp. 262–273.

[13] J.Deng and Z. Hass, "Dual busy tone multiple access (DBTMA): A new access control for packet radio networks," in *Proc. Int. Conf. Universal Personal Comm.* IEEE, Oct. 1998.

[14] (2007) Mobile ad-hoc networks website. [Online]. Available: http://www.ietf.org/html.charters/manet-charter.html

[15] P. Gupta and P. Kumar, "The capacity of wireless networks," *IEEE Trans. Inf. Theory*, vol. 46, no. 2, pp. 388 – 404, Mar. 2000.

[16] P. Kumar, "A correction to the proof of a lemma in "the capacity of wireless networks," *IEEE Trans. Inf. Theory*, vol. 49, no. 11, p. 3117, Nov. 2003.

[17] S. Yi, Y. Pei, and S. Kalyanaraman, "On the capacity improvement of ad hoc wireless networks using directional antennas," in *the ACM Symposium on Mobile Adhoc Networking and Computing (MOBIHOC 2003)*, Annapolis, Maryland, USA., Jun. 2003, pp. 108 – 116.

[18] C. Peraki and S. D. Servetto, "On the maximum stable throughput problem in random networks with directional antennas," in *Proc. ACM Symposium on Mobile Adhoc Networking and Computing (MOBIHOC 2003)*, Annapolis, Maryland, USA., Jun. 2003.

[19] J. J. C. Liberti and T. S. Rappaport, *Smart Antennas For Wireless Communications: IS-95 and Third Generation CDMA Applications*, T. Rappaport, Ed. Prentice Hall, 1999.

[20] K. Gyoda and T. Ohira, "Design of electronically steerable passive array radiator (ESPAR) antennas," in *IEEE Antennas and Propagation Society International Symposium*, vol. 2, Salt Lake City, UT, USA., Jul. 2000, pp. 922 – 925.

[21] L. Godara, "Applications of antenna arrays to mobile communications, Part I: Performance improvement, feasibility, and system considerations," *Proc. IEEE*, vol. 85, no. 7, pp. 1031–1060, Jul. 1997.

[22] D. Gesbert, M. Shafi, D. Shiu, P. Smith, and A. Naguib, "From theory to practice: an overview of MIMO space-time coded wireless systems," *IEEE J. Sel. Areas Commun.*, vol. 21, no. 3, pp. 281 – 302, Apr. 2003.

[23] S. Hirata, A. Ohira, and T. Karmakar, "Fast beamforming of electronically steerable parasitic array radiator antennas: Theory and experiment," *IEEE Trans. Antennas Propag.*, vol. 52, no. 7, pp. 1819–1832, Jul. 2004.

[24] *IEEE Standard for Information technology-Telecommunications and information exchange between systems-Local and metropolitan area networks-Specific requirements - Part 11: Wireless LAN Medium Access Control (MAC) and Physical Layer (PHY) Specifications*, IEEE Std. 802.11, Jun. 2007.

[25] L. Berlemann, C. Hoymann, G. Hiertz, and B. Walk, "Unlicensed operation of IEEE 802.16: Coexistence with 802.11(A) in shared frequency bands," in *IEEE 17th International Symposium on Personal Indoor and Mobile Radio Communications 2006*. Helsinki, Finland: IEEE, Sep. 2006, pp. 1–5.

[26] T. Robertazzi and P. Sarachik, "Self-Organizing Communication Networks," *IEEE Commun. Mag.*, vol. 24, no. 1, pp. 28–33, Jan. 1986.

[27] A. Chou and V. Li, "Fair Spatial TDMA Channel Access Protocols for Multihop Radio Network," in *INFOCOM '91, Bal Harbour, FL*, Apr. 1991.

[28] A. Chandra, V. Gummalla, and J. O. Limb, "Wireless Medium Access Control Protocols," *IEEE Commun. Surveys Tuts.*, Second Quarter 2000 2000.

[29] R. Rom and M. Sidi, *Multiple Access Protocols*. Springer-Verlag, 1989.

[30] L. Kleinrock and F. A. Tobagi, "Packet Switching in Radio Channels: Part I - Carrier Sense Multiple-access modes and their throughput-delay characteristic," *IEEE Trans. Commun.*, vol. 23, pp. 1400–1416, Dec. 1975.

[31] F. A. Tobagi and L. Kleinrock, "Packet Switching in Radio Channels: Part II - the hidden terminal problem in carrier sense multiple-access modes and the busy tone solution," *IEEE Trans. Commun.*, vol. 23, pp. 1417 – 1433, Dec. 1975.

[32] P. Karn, "MACA - a new channel access method for packet radio," in *ARRL/CRRL Amateur Radio 9th Computer Networking Conference*. ARRL 1990, 1990.

[33] G. Lundy, M. Almquist, and T. Oruk, "Specification, Verification and Simulation of a Wireless LAN Protocol: MACAW," Available from http://www.argreenhouse.com/society/TacCom/papers98/17_02u.pdf.

[34] R. Nelson and L. Kleinrock, "Spatial- TDMA, a collision-free multihop channel access protocol," *IEEE Trans. Commun.*, vol. 33, no. 9, pp. 934–944, Sep. 1985.

[35] J. Zander, "Slotted ALOHA multihop packet radio networks with directional antennas," *Electronics Letters*, vol. 26, no. 25, pp. 2098 – 2100, Dec. 1990.

[36] T. Yum, "Design algorithms for multihop packet radio networks with multiple directional antennas stations," *IEEE Trans. Commun.*, vol. 40, no. 11, pp. 1716 –1724, Nov. 1992.

[37] J. Ward and R.T. Jr. Compton, "High throughput slotted ALOHA packet radio networks with adaptive arrays," *IEEE Trans. Commun.*, vol. 41, no. 3, pp. 460 – 470, Mar. 1993.

[38] L. Bao and J. Garcia-Luna-Aceves, "Transmission scheduling in ad hoc networks with directional antennas," 2002. [Online]. Available: citeseer.ist.psu.edu/bao02transmission.html

[39] Y. Ko, V. Shankarkumar, and N. Vaidya, "Medium Access Control Protocols Using Directional Antennas in Ad Hoc Networks," in *Proc. IEEE INFOCOM 2000*, vol. 1. Tel Aviv, Israel: IEEE, Mar. 2000, pp. 13–21.

[40] A. Nasipuri, J. Mandava, H. Manchala, and R. Hiromoto, "On-Demand Routing Using Directional Antennas in Mobile Ad Hoc Networks," in *Proc. Computer Comm. and Networks 2000*. Las Vegas, NV, USA: IEEE, Oct. 2000, pp. 535 – 541.

[41] S. Bandyopadhyay, K. Hasuike, S. Horisawa, and S. Tawara, "An adaptive mac and directional routing protocol for ad hoc wireless network using ESPAR antenna," in *Proc. ACM Symposium on Mobile Adhoc Networking and Computing (MOBIHOC 2001)*, Long Beach, CA, USA, Oct. 2001.

[42] R. Ramanathan, "On the performance of ad hoc networks with beamforming antennas," in *the ACM Symposium on Mobile Adhoc Networking and Computing (MOBIHOC 2001)*. Long Beach, CA, USA.: ACM, Oct. 2001.

[43] M. E. Steenstrup, "Exploiting directional antennas to provide quality of service and multipoint delivery in mobile wireless networks," in *Proc. IEEE Military Communications Conference, 2003 (MILCOM 2003)*. Boston, MS, USA: IEEE, Oct. 2003, pp. 987 – 992.

[44] R. Ramanathan, J. Redi, C. S. D. Wiggins, and S. Polit, "Ad hoc networking with directional antennas: a complete system solution," *IEEE J. Sel. Areas Commun.*, vol. 23, no. 3, pp. 496 – 506, Mar. 2005.

[45] T. Robertazzi and J. Shor, "Traffic sensitive algorithms and performance measures for the generation of self-organizing radio network schedules," *IEEE Trans. Commun.*, vol. 41, no. 1, Jan. 1993.

[46] A. Ephremides and T. Truong, "Scheduling broadcasts in multihop radio networks," *IEEE Trans. Commun.*, vol. 38, no. 4, pp. 456 – 460, Apr. 1990.

[47] S. Chandra and T. G. Robertazzi, "Heuristic scheduling strategies for multihop radio networks with regular structure," in *IEEE International Conference on Communications (ICC 88)*, vol. 1, Philadelphia, PA, USA., Jun. 1988, pp. 437 – 442.

[48] B. Hajek and G. Sasaki, "Link scheduling in polynomial time," *IEEE Trans. Inf. Theory*, vol. 34, no. 5, pp. 910 – 917, Sep. 1988.

[49] J. Wieselthier, C. Barnhart, and A. Ephremides, "A neural network approach to routing without interference in multihop radio networks," *IEEE Trans. Commun.*, vol. 42, no. 1, pp. 166 – 177, Jan. 1994.

[50] O. Somarriba, "Multihop Packet Radio Systems in Rough Terrain," Licenciate Thesis, Radio Communication Systems, Department of S3. Royal Institute of Technology, Stockholm, Sweden, Oct. 1995.

[51] J. Grönkvist, "Traffic Controlled Spatial TDMA in multihop radio networks," in *Proceedings of Personal, Indoor and Mobile Radio Communications*, vol. 3. IEEE, Sep. 1998, pp. 1203 – 1207.

[52] J. Grönkvist, E. Englund, A. Hansson, and C. Jönsson, "Spatial TDMA for Multi-hop Radio Networks," Defence Research Establishmen (FOA), Division of Command and Control Warfare Technology, Scientific report, Sep. 1999.

[53] O. Somarriba and T. Giles, "Transmission Power Control for Spatial TDMA in Wireless Radio Networks," in *Proc. of Mobile and Wireless Communications Networks (MWCN)2002*, Stockholm, Sweden, Sep. 2002, pp. 394 – 398.

[54] T. Grici and A. Ephremides, "Joint routing and scheduling metrics for ad hoc wireless networks," in *Conference Record of the Thirty-Sixth Asilomar Conference on Signals, Systems and Computers, 2002*, vol. 2. Pacific Grove, California, USA: IEEE, Nov. 2002, pp. 1155 – 1159.

[55] P. V. P. Bjorklund and D. Yuan, "Resource optimization of Spatial TDMA in ad hoc radio networks: a column generation approach," in *Proc. IEEE INFOCOM 2003*, San Francisco, USA, Apr. 2003, pp. 818–824.

[56] T. Elbatt and A. Ephremides, "Joint scheduling and power control for wireless ad hoc networks," *IEEE Trans. Wireless Commun.*, vol. 3, no. 1, pp. 74–85, Jan. 2004.

[57] J. Gronkvist, "Interference-based scheduling in spatial reuse TDMA," Ph.D. dissertation, Radio Communication Systems. Royal Institute of Technology, Stockholm, Sweden, Sep. 2005.

[58] M. Johansson and L. Xiao, "Cross-layer optimization of wireless networks using nonlinear column generation," *IEEE Trans. Wireless Commun.*, vol. 5, no. 2, pp. 435–444, Feb. 2006.

[59] D. Lal, T. Joshi, and D. Agrawal, "Localized transmission scheduling for spatial multiplexing using smart antennas in wireless adhoc networks," in *Proc. 13th IEEE Workshop on Local and Metropolitan Area Networks (LANMAN 2004)*, San Francisco, USA, Apr. 2004, pp. 175– 180.

[60] K. Dyberg, L. Farman, F. Eklof, J. Gronkvist, U. Stemer, and J. Rantakokko, "On the performance of antenna arrays in spatial reuse TDMA ad hoc networks," in *Proc. MILCOM 2002*, California, USA, Oct. 2002, pp. 270–275.

[61] S. Toumpis and A. J. Goldsmith, "Capacity regions for wireless ad hoc networks," *IEEE Trans. Wireless Commun.*, vol. 2, no. 4, pp. 736 – 748, Jul. 2003.

[62] L. Farman, U. Sterner, and O. Tronarp, "Analysis of capacity in ad hoc networks with variable data rates," in *IEEE 59th Vehicular Technology Conference, 2004. VTC 2004-Spring.*, vol. 4. Milan, Italy: IEEE, May 2004, pp. 2101 – 2105.

[63] D. Bertsekas and R. Gallager, *Data Networks*, 2nd ed. Prentice Hall, 1992.

[64] L. Xiao, M. Johansson, and S. Boyd, "Simultaneous routing and resource allocation via dual decomposition," *IEEE Trans. Commun.*, vol. 52, no. 7, pp. 1136 – 1144, Jul. 2004.

[65] S. G. Nash and A. Sofer, *Linear and Nonlinear Programming*, ser. Industrial Engineering. McGraw-Hill, 1996.

[66] M. Sánchez, J. Zander, and B. Hagerman, "On the performance of power and rate control in STDMA multihop networks with advanced antennas," in *Proc. International Conference on Networking (ICN2008).* Cancun, Mexico: IEEE, Apr. 2008.

[67] M. Sánchez, J. Zander, and B. Hagerman, "A Reuse-Greedy Algorithm for STDMA Multihop Networks with Advanced Antennas & Rate Control," in *Proc. International Symposium on Wireless Pervasive Computing 2008 (ISWPC2008).* Santorini, Greece: IEEE, May 2008.

[68] M. Sánchez, J. Zander, and B. Hagerman, "Radio Resource Allocation in Spatial TDMA Multihop Networks with Advanced Antennas," in *Proc. Wireless Rural and Emergency Communications Conference (WRECOM2007).* Rome, Italy: IEEE, Oct. 2007.

[69] M. Sanchez and M. Munguia, "On the Integration of Adaptive Antenna Systems in Mul-tihop Ad hoc Networks Utilizing Generalized TDMA as MAC protocol," in *Proc. XX Congreso Panamericano de Ingenieria Mecanica, Electrica, Industrial y Ramas Afines 2005 (COPIMERA 2005)*, Havana, Cuba, Nov. 2005, (in spanish).

[70] B. Shrader, M. Sanchez, and T. Giles, "Throughput-delay analysis of conflict-free scheduling in multihop ad-hoc networks," in *Proc. Swedish workshop on Wireless Ad hoc Networks 2003*, Stockholm, Sweden, May 2003.

[71] M. Sánchez, J. Zander, and T. Giles, "Combined routing and scheduling for spatial TDMA in multihop ad hoc networks," in *Proc. the 5th International Symposium on Wireless Personal Multimedia Communications, 2002 (WPMC2002)*, vol. 2. Honolulu, Hawaii, USA.: IEEE, Oct. 2002, pp. 781 – 785.

[72] M. Sanchez, J. Zander, and T. Giles, "Combined routing and scheduling for spatial TDMA in multihop ad hoc networks," in *Proc. Swedish workshop on Wireless Ad hoc Networks 2002*, Stockholm, Sweden, Mar. 2002.

[73] M. Sánchez, T. Giles, and J. Zander, "CSMA/CA with beam forming antennas in multihop packet radio," in *Proc. Swedish workshop on Wireless Ad hoc Networks 2001*, Stockholm, Sweden, Mar. 2001.

[74] M. Sanchez, O. Somarriba, and J. Zander, "User-deployed and capacity evaluation of multihop wireless networks: A case study for nicaragua," in *Proc. Swedish workshop on Wireless Ad hoc Networks 2008*, Stockholm, Sweden, May 2008.

[75] M. Sánchez and J. Zander, "Adaptive antennas in Spatial TDMA multihop packet radio network," in *Proc. Radio Scientific Conference , RVK99*, Karlskrona, Sweden, Jun. 1999.

[76] (2007, Dec.) Instituto Nicaraguense de Estudios Territoriales (INETER) . [Online]. Available: http://www.ineter.gob.ni/caracterizaciongeografica/caracterizaciongeografica.html

[77] B. Annis. (2007, Dec.) Nicaragua Diversification and Growth, 1945-77. The Library of Congress, December 1993. Retrieved on 2007-12-11. [Online]. Available: http://lcweb2.loc.gov/cgi-bin/query/r?frd/cstdy:\@field(DOCID+ni0047)

[78] (2007, Nov.) Fondo de Inversión de Telecomunicaciones (FITEL) . [Online]. Available: http://www.telcor.gob.ni/Desplegar.asp?PAG_ID=15

[79] "NIC-TMC-02-92: Beauty contest for the concession of cellular mobile telephony in nicaragua," May 1992, (in spanish).

[80] "Concession to exploit Cellular Mobile Telephony in Nicaragua by TCN," Nov. 1992, (in spanish).

[81] (2003, Dec.) Administrative resolution no. 136 - 2003. (in spanish). [Online]. Available: http://www.telcor.gob.ni/Descargar.asp?DOC_ID=1340

[82] "Concession contract of ENITEL," Dec. 2001, (in spanish).

[83] "Adendum No. TC-001-21/01/2004: Service area extension to the Center and Atlantic region of Nicaragua ," Jan. 2004, (in spanish).

[84] Japan International Cooperation Agency (JICA), "ICT policy reform and rural communications infrastructure," Mar. 2005. [Online]. Available: http://www.jica.go.jp/english/resources/publications/study/topical/ict/index.html

[85] (2007) The Constitution of the Republic of Nicaragua. [Online]. Available: http://www.asamblea.gob.ni/opciones/constituciones/Constitucion\\\%20Politica\%20y\%20sus\%20reformas.pdf

[86] C. E. Aichele, R. Flickenger, C. Fonda, J. Forster, I. Howard, T. Krag, and M. Zennaro, *Wireless Networking in the Developing World: A practical guide to planning and building low-cost telecommunications infrastructure*, 1st ed., R. Flickenger, Ed. Limehouse Book Sprint Team, January 2006. [Online]. Available: http://wndw.net/pdf/wndw-print.pdf

[87] G. Chouinard, "Bringing broadband access to rural and remote areas," ITU News Magazine, No.1, Jan. 2006. [Online]. Available: http://www.itu.int/itunews/manager/main.asp?lang=en\&iYear=2006\&iNumber=01

[88] (2005, Jan.) VIII census of population and IV of housing, 2005. (in spanish). [Online]. Available: http://www.inec.gob.ni/censos2005/ResumenCensal/Resumen2.pdf

[89] C. A. Balanis, *Antennas Theory: Analysis and Design*, 2nd ed. John Wiley & Sons, Inc., 1997.

[90] C. Roobol, "Multihop radio networks in random terrains: Connectivity and some terrain adaptive routing algorithms," in *Proc IEEE MILCOM 93*, vol. 2, Oct. 1993.

[91] L. Ladell, "Transmission Loss in Wooden Terrain," in *Proc. Nordic Radio Symposium, NRS96*, Stockholm, Sweden, Apr. 1986.

[92] T. S. Rappaport, *Wireless Communications: Principles and Practice*, 2nd ed. Prentice Hall, Inc., 2002.

[93] L. Ahlin and J. Zander, *Principles of Wireless Communications*, 2nd ed. Lund, Sweden: Studentlitteratur, 1998.

[94] A. Das, R. Marks, P. Arabshahi, and A. Gray, "Power controlled minimum frame length scheduling in TDMA wireless networks with sectored antennas," in *Proc. IEEE INFOCOM 2005)*, Miami, USA, Mar. 2005, pp. 1782 – 1793.

[95] H. L. Van Trees, *Optimum Array Processing*. John Wiley & Sons, 2002.

[96] R. K. Ahuja, T. L. Magnanti, and J. B. Orlin, *Network Flows: Theory, Algorithms, and Applications*. Prentice Hall, Inc, 1993.

[97] S. Basagni, M. Conti, S. Giordano, and I. Stojmenovic, Eds., *Mobile Ad Hoc Networking*, 1st ed. John Wiley & Sons, Inc., 2004.

[98] L. Kleinrock, *Queueing Systems*. John Wiley & Sons, 1975, vol. I.

[99] J. Grönkvist, "Assignment Strategies for Spatial Reuse STDMA," Licenciate Thesis, Radio Communication Systems, Department of S3. Royal Institute of Technology, Stockholm, Sweden, April 2002.

[100] M. Steenstrup, "Topology management in mobile networks with smart antennas," in *Proc. IEEE 3rd Scandinavian Workshop ADHOC Networks*, Stockholm, Sweden, May 2003.

[101] F. Tobagi, "Modeling and performance analysis of multihop packet radio networks," *Proc. IEEE*, vol. 75, Jan. 1987.

[102] M. Sánchez, "Multiple access protocols with smart antennas in multihop ad hoc rural-area networks," Technical Licentiate Thesis in Radio Communication Systems. Royal Institute of Technology, Stockholm, Sweden, Jun. 2002.

[103] D. Kim, C.-H. Min, and S. Kim, "On-demand SIR and bandwidth-guaranteed routing with transmit power assignment in ad hoc mobile networks," in *Proc. IEEE Transactions on Vehicular Technology*, vol. 53. Pacific Grove, California, USA: IEEE, Jul. 2004, pp. 1215 – 1223.

[104] O. Somarriba, "Heuristic Algorithms for Combined Scheduling and Routing in Spatial TDMA Wireless Ad hoc Networks," in *In Proceedings of the Fourth Scandinavian Workshop on Wireless Ad-hoc Networks*, Stockholm, Sweden, May 2004.

[105] "Cisco Aironet 1522 Lightweight Outdoor Mesh Access Point, Data Sheet," Cisco Systems Inc., California, USA. [Online]. Available: http://www.cisco.com/en/US/prod/collateral/wireless/ps5679/ps8368/product_data_sheet0900aecd8066a16c.pdf

[106] B. Radunovic and J. L. Boudec, "Rate performance objectives of multihop wireless networks," *IEEE Trans. Mobile Comput.*, vol. 3, no. 4, pp. 334–349, Oct./Dec. 2004.

[107] F. Kelly, A. Maulloo, and D. Tan, "Rate control in communication networks: shadow prices, proportional fairness and stability," *Journal of the Operational Research Society*, vol. 49, 1998.

[108] L. Tassiulas and S. Sarkar, "Maxmin fair scheduling in wireless ad hoc networks," *IEEE J. Sel. Areas Commun.*, vol. 23, no. 1, pp. 163 – 173, Jan. 2005.

[109] M. Johansson and L. Xiao, "Cross-layer optimization of wireless networks using nonlinear column generatio," Report IR-S3-REG-030302, Department of Signal, Sensors and Systems, Royal Institute of technology., Nov. 2003.

[110] S.-L. Kim, Z. Rosberg, and J. Zander, "Combined power control and transmission rate selection in cellular networks," in *Proc. IEEE VTS 50th Vehicular Technology Conference, 1999 (VTC 1999 - Fall)*, vol. 3. Amsterdam, Netherlands: IEEE, Sep. 1999, pp. 1653 – 1657.

[111] I. Martinez and J. Altuna, "A cross-layer design for ad hoc wireless networks with smart antennas and QoS support," in *15th IEEE International Symposium on Personal, Indoor and Mobile Radio Communications, 2004. PIMRC 2004*, vol. 1. Barcelona, Spain: IEEE, Sep. 2004, pp. 589 – 593.

[112] O. Somarriba, "Analysis of Capacity for Spatial TDMA in Wireless Ad Hoc Networks with Variable Power and Rate Control," in *Proc. IEEE 63rd Vehicular Technology Conference, 2006. VTC 2006-Spring.*, Melbourne, Australia, May 2006, pp. 906 – 910.

[113] D. Zwillinger, *Standard Mathematical Tables and Formulate*, 30th ed. CRC Press, 1996.

[114] S. Wu, Y.-C. Tseng, and J.-P. Sheu, "Intelligent Medium Access for Mobile Ad Hoc Networks with Busy Tones and Power Control," *IEEE J. Sel. Areas Commun.*, vol. 18, no. 9, Sep. 2000.

[115] (2008) Radio Mobile Freeware by VE2DBE. [Online]. Available: http://www.cplus.org/rmw/english1.html

[116] (2006, Jan.) AA 001-2006, Wireless Access System operation on the frequency bands: 900 MHZ, 2.4 GHZ, and 5 GHZ. Instituto Nicaragüense de Telecomunicaciones y Correos (TELCOR). In Spanish. [Online]. Available: http://www.telcor.gob.ni/Descargar.asp?DOC_ID=42024

[117] (2007) GTOPO30 - tile W100N40. [Online]. Available: http://edc.usgs.gov/products/elevation/gtopo30/w100n40.html

[118] G.A. Hufford, A.G. Longley, W.A. Kissick, "A Guide to the Use of the ITS Irregular Terrain Model in the Area Prediction Mode," National Telecommunications and Information Administration (NTIA) Report 82-100, Apr. 1982.

[119] J. E. Håkegård, B. Myhre, P. H. Lehne, T. Ormhaug, V. Bjugan, M. Mondin, M. Elkotob, and F. Steuer, "Open Broadband Access Network (OBAN): D8 scenarios and wireless performance and covegare," OBAN consortium, Mar. 2005. [Online]. Available: http://oban.prz.tu-berlin.de/D8_Scenarios_and_wireless_performance_and_coverage.pdf

[120] J. L. Hammond and H. B. Russell, "Properties of a transmission assignment algorithm for multiple-hop packet radio networks," *IEEE Trans. Commun.*, vol. 3, no. 4, pp. 1048 – 1052, Jul. 2004.

Appendix A

Routing Decision for Reuse Adaptive Minimum Hop Algorithm

In the following the *relative capacity* of the network $\boldsymbol{C}$ and the network topology are input parameters for routing decision. Each element in $\boldsymbol{C}$ denoted by C_{ij} represents the relative capacity assigned to link (i, j) and it is given by (5.7).

A.1 Algorithm

I. Using the network topology, collect the set of paths with shortest distance between all (S, D) pairs in the network.

II. Put the list of (S, D) pairs in ascending order according to the number of possible paths; i.e. (S, D) pairs with less number of choices are considered first. If several (S, D) pairs have equal number of possible paths, order then according to the number of hops in descending order.

III. Set the relative traffic load $T_{ij} = 0$; $\forall$ links (i, j).

IV. While there are elements in the list of (S, D) pairs:

   A. Take the first (S, D) pair in the list and take the first path as the best one.

   B. Store relative traffic load: $BestT_{ij} = T_{ij}$; $\forall$ links (i, j)

   C. Update the relative traffic load:

$$BestT_{ij} = (T_{ij} + 1);\ \forall \text{ links } (i, j) \text{ in the selected path.} \tag{A.1}$$

   D. Compute the relative flow vector:

$$BestFlow = \frac{C_{ij}}{BestT_{ij}};\ \forall \text{ links } (i, j) \text{in the selected path} \tag{A.2}$$

E. While there are paths not considered for this (S, D) pair:

1) Take the next path and store the relative traffic load:

$$NewT_{ij} = T_{ij} \ \forall \text{ links } (i, j) \tag{A.3}$$

2) Update traffic load:

$$NewT_{ij} = (T_{ij} + 1) \ \forall \text{ links } (i, j) \text{ in the new path.} \tag{A.4}$$

3) Compute the relative flow vector if we select this path:

$$NewFlow = \frac{C_{ij}}{NewT_{ij}}; \ \forall \text{ links } (i, j) \text{ in the selected path.} \tag{A.5}$$

4) If Better(NewFlow, BestFlow) /* See Fig A.1 */ then
- $BestT_{ij} = NewT_{ij}; \forall$ links (i, j)
- $BestFlow = NewFlow$

F. Update Traffic load and routing tables

1) $T_{ij} = BestT_{ij}; \forall$ links (i, j)
2) Update table of relaying nodes:

- put in routing table of node i, (S,D)=j , $\forall$ nodes i in lins (i, j) in the selected path.

G. Remove this (S, D) pair from the list.

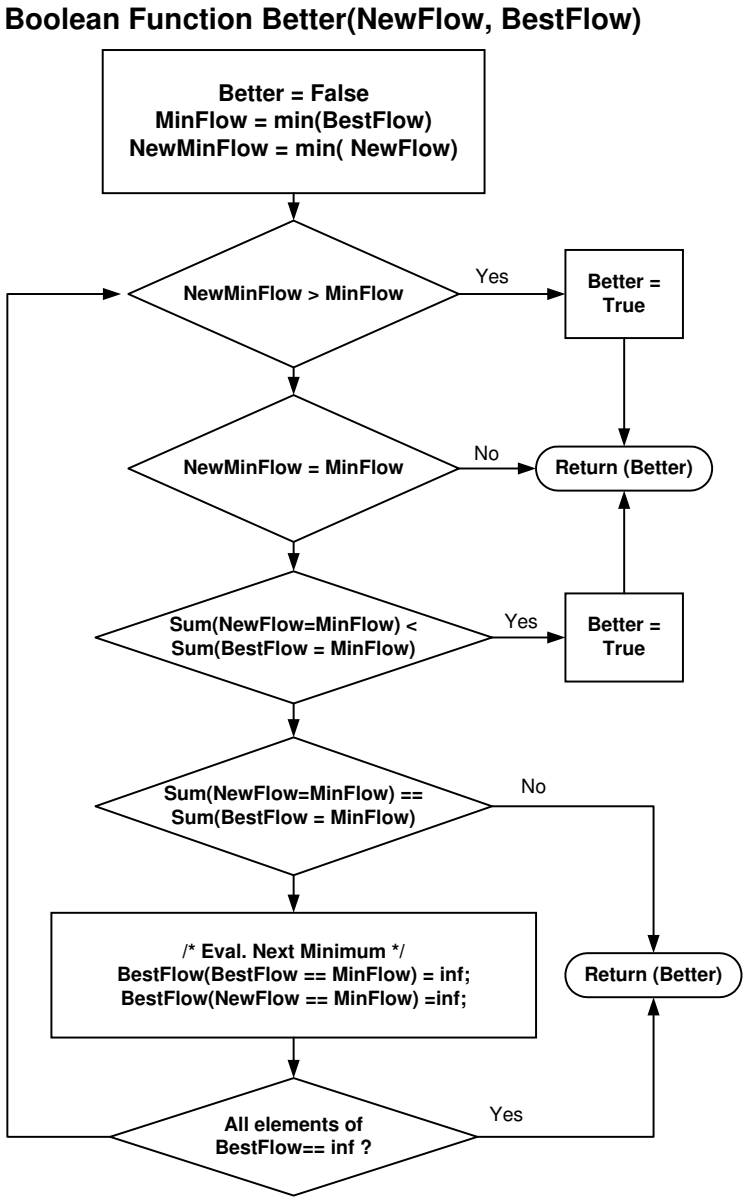

Figure A.1: Function to decide if the traffic flow over a selected path is better that the previously selected.

Appendix B

Rough Terrain Model and Radio Propagation

To analyze influence of mountains in a rural environment we use a (synthetic) terrain which is a modification to the one introduced in [90]. In this model, the terrain height variations are modelled by a stationary two-dimensional random process, $H(x, y)$, in the locations (x, y) given by

$$H(x,y) = \frac{1}{\sqrt{c}} \sum_{k=-\rho}^{k=\rho} \sum_{l=-\rho}^{\rho} \mid H^*(x-k, y-l) \mid p(k,l) \; , \tag{B.1}$$

where $H^*(x, y)$ is a two dimensional white Gaussian process with zero mean and variance σ^2, and $p(k, l)$ is the impulse response of a filter given by

$$p(x,y) = \begin{cases} 1 + \cos(\pi \frac{\sqrt{(x^2+y^2)}}{\rho}) & \mid x \mid \leq \rho, \mid y \mid \leq \rho \\ 0 & otherwise, \end{cases} \tag{B.2}$$

and

$$c = \sum_{k=-\rho}^{\rho} \sum_{l=-\rho}^{\rho} p^2(k,l) \; . \tag{B.3}$$

The parameters σ(m) correspond to the standard deviation of the terrain height and ρ(m) is an smoothness parameter that determines over which distance there exist correlation between heights. Fig. B.1 shows a typical terrain realization with $\sigma = 40$ m and $\rho = 5$ km used to simulate a hilly terrain. The maximum difference in terrain height was 70 m. In general, the terrain could be varied from relatively flat ($\sigma \approx 0$) to very mountainous terrain (high $\sigma > 40$).

The radio propagation properties of *m*ultihop ad hoc networks where analyzed using the diffraction model according to Epstein-Peterson refined by Ladell [91]. Using this model the over all propagation loss, L_T is a combination of the diffraction loss produced by mountains, L_{dif}, the flat-earth propagation loss, L_f and the free space propagation loss, L_{fs}, given by

$$L_T = L_{fs} + \sqrt{L_{dif}^2 + L_f^2} \text{ (dB)} \; , \tag{B.4}$$

These losses are calculated using the terrain model as described in [50]. Fig. B.2 shows the dominant received power level for a sample network deployed on the terrain of Fig. B.1.

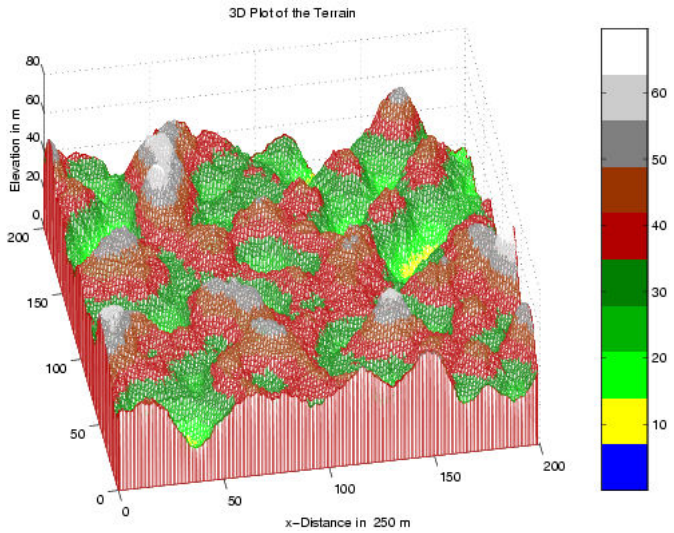

Figure B.1: Rough terrain realization with parameters $\sigma = 10m$ and $\rho = 5km$.

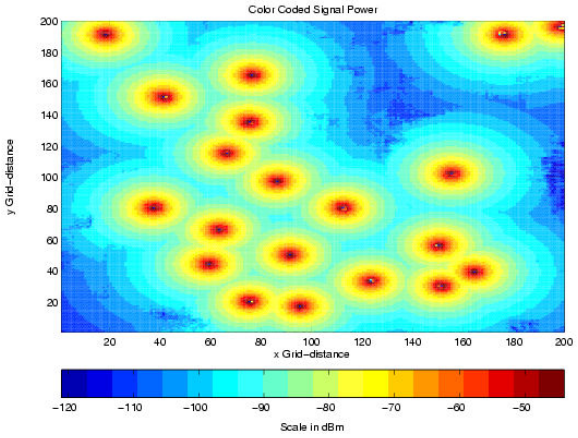

Figure B.2: Dominant (strongest) received power over rough terrain in Fig. B.1 with 20 nodes.

Appendix C

Simulation of CSMA/CA with RTS and CTS

In our implementation of CSMA/CA a node could be in one of 5 stages: PASSIVE, RECEIVE, HANDSHAKE, BACKOFF, and TxDATA. A TIMER control the time the node will be within a stage before changing to another stage. Transit between states is triggered by the occurrence of different events (e.g. packet arrival, carrier sensing, TIMER expired etc.). A node is in the stage PASSIVE while do not has packets to transmit and no carrier sense is detected. During this state the MAC sublayer order to the physical layer to utilized omnidirectional antennas. If while in this stage a packet arrives to the queue of the node, it transits to the HANDSHAKE stage and start transmitting an RTS packet to the relaying node (defined in its routing table) used to deliver the packet to its final destination, previous to start transmitting the packet the MAC sublayer order to the physical layer to use utilize either omnidirectional antenna or select the sector with best signal quality for the relaying node depending of the beam selection policy been used. Within this stage, after transmitting the RTS, the node waits for a CTS from the relaying node using the antenna type defined by the beam selection policy being used. If no CTS is received a collision is assumed and the node deferred its transmission switching to use omnidirectional antenna and passing to the RECEIVE stage for the period required to transmit a maximum size data packet aiming to prevent destroying an outgoing communication. On the other hand, if a CTS with the address field to this node is received, it is assumed that the channel is acquired passing to the TxDATA state initiating the data transmission utilizing the sector with best signal quality for the relaying node.

After transmitting the data packet the node order to the physical layer to switch to omnidirectional antennas and defers any other transmission for at least the period required to hear a CTS passing to the RECEIVE stage. If while in PASSIVE a carrier is detected, the node changes to the RECEIVE stage to receive the information coming into the receiver (using omnidirectional antenna). A node remains in

RECEIVE stage if no carrier is detected and if the TIMER set by any other stage does not expire. If carrier is detected the node starts receiving the packet from the physical layer and depending of the type of data received (RTS, CTS, DATA, or ERROR) it responds in different ways. If in this stage an RTS address to the node is received and the TIMER has not expired it do not answer to the RTS and remains in the RECEIVE stage. However, if the TIMER has expired it answers with a CTS to the requesting node using the antenna type defined by the beam selection policy being used and remaining in the RECEIVE stage afterwards using the sector with the best signal quality received from the transmitting node and setting the TIMER to the period of a packet. On the other hand, if a CTS is received while in RECEIVE stage, the node set the TIMER in this stage for at least the period of a packet to avoid a possible collision with a data packet from any other node. If in RECEIVE stage a Data packet is received with the address field the local node ID, this is passed to the network layer setting the TIMER to the period required to hear a CTS using omnidirectional antenna. Finally, if a data ERROR occurs, the node state in RECEIVE setting the TIMER to the period required to receive a data packet and using omnidirectional antenna. If the waiting time in RECEIVE expired while not carrier sense is detected and the node do not have packets in queue to be transmitted, it passes to the PASSIVE stage, otherwise it passes to the BACKOFF stage where omnidirectional antennas are used for carrier sensing.

In the BACKOFF stage an uniform distributed waiting time between 0 and 10 times the CTS period (contention windows) is generated. If the waiting time expire while not carrier is detected the node passes to the HANDSHAKE stage, otherwise it passes to the RECEIVE stage. To simulate the interaction with other nodes and the channel perceived at each node, we used discrete step simulation where at an instance of time t_i the channel state is passed to the node and its influence on the channel over the next time instants t_{i+1} is returned as illustrated in Fig. C.1. Each node was simulated as a state machine following the MAC-protocol described before. The channel radio propagation conditions between nodes were computed using the channel models described in chapter 3. The received power level in a given instance of time is modified to include the antenna radiation pattern utilized by the node within the current state.

Further it is assumed that:

- To hold a reliable link, the minimum required SNR is 10 dB.
- All nodes are assumed to know the location of their neighbors (nodes within it radio range).
- Each node uses the Minimum Hop Algorithm (MHA) to route packets through the network.
- Nodes use half-duplex transceivers with negligible turn around time from reception to transmission and vice versa.

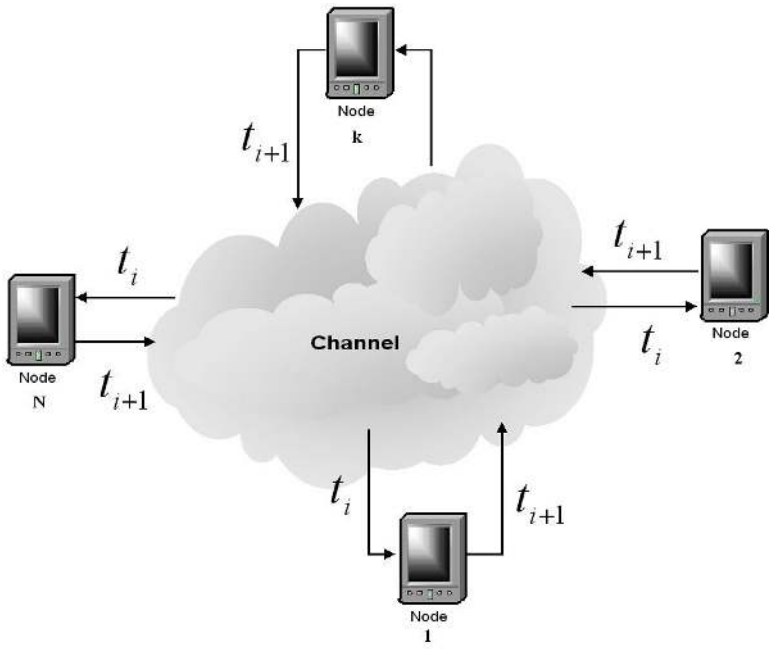

Figure C.1: The channel perceived by a node is given in time t_i and the node returns its influence on the channel at time instant t_{i+1}.

- The packet processing time is negligible.
- An SINR of at least 10 dB is required during the whole packet transmission period for correct reception.
- The channel radio propagation conditions do not change with time but the Multiple Access Interference does.
- No multipath arrival signals are considered.

The minimum value for SNR of 10 dB correspond to the use of the Binary Phase Shift Keying (BPSK) modulation scheme and a BER below 10^{-5} in the presence of White Additive Gaussian Noise (AWGN) [93]. In practice, the transmitter turn around time, the round-trip radio propagation delay, and packet processing time are critical parameters that have to be considered at the MAC sublayer. For instance, while sending an RTS packet, the MAC sublayer switches the transmitter to ON and has to wait the transceiver turn around time before starting to transmit the packet. The same is true while replying to an RTS packet or sending the DATA packet. On the other hand, the selection of the waiting time for an answer before assuming

that a conflict has occurred is a critical design parameter. The waiting time for an answer after sending an RTS or a CTS must be the sum of the transmitter turn around time, the round-trip radio propagation delay, and the packet processing time delay. The packet processing time delay must include the time required to detect (carrier sensing delay), receive, and decode the packet. For instance, after transmitting an RTS the packet processing time is the time needed for the receiving node to detect the RTS, decode the RTS and start to answer with a CTS. In the rural scenario, the radio range could be of several kilometers and the round-trip delay becomes significant. For instance, for a maximum radio range of 1km the round trip delay corresponds to $2(3.333) \approx 6.67\mu$s, while for 40 km corresponds to 266.67μs (0.267 ms). With 100 kbps the transmission time for a 500 Bytes packet is 40 ms, for 25 bytes RTS and CTS it is 2 ms. Therefore, with 100 kbps the round trip delay is negligible but is significant for 40 km (corresponding to 13% T_{RST}). In our simulation $t_{i+1} - t_i$ corresponds to a microslot and it was used to include the effect of the round trip delay selected to be $10\%T_{RTS}$.

Appendix D

Rural Communities for Case Study

Community	Latitude	Longitude	Altitude
San Luis	13°15.038'N	086°28.590'W	4128 ft
La Fraternidad	13°15.841'N	086°30.359'W	3861 ft
San Lorenzo	13°08.286'N	086°37.207'W	1106 ft
La Grecia	13°10.827'N	086°34.378'W	1098 ft
El Carrizo	13°14.411'N	086°40.783'W	2972 ft
El Angel 1	13°16.340'N	086°40.257'W	2745 ft
El Mojón	13°18.585'N	086°40.550'W	3777 ft
El Ojoche	13°29.123'N	086°08.454'W	4184 ft
San Marcanda	13°31.599'N	086°06.929'W	2726 ft
El Varillal	13°35.202'N	086°09.894'W	2500 ft
San Miguel	13°42.304'N	085°53.471'W	3061 ft
Cristo Rey	13°45.010'N	085°49.226'W	1790 ft
El Jobo	13°32.829'N	085°52.817'W	1400 ft

Appendix E

Notations

The notation utilized in the thesis are here defined.

E.1 Conventions

The following conventions have been used:

- Boldface roman denotes a vector or matrix
- Uppercase bold are used to denote a matrix
- $E[.]$ denotes the statistical expectation of the quantity in the bracket.
- The symbol $|.|$ means the magnitude of the scalar contained within.

E.2 Acronyms

AAS	Advanced Antenna Systems
ADSL	Asymmetric Digital Subscriber Line
BER	Bit Error Rate
BFA	Beam Forming Antenna
BFN	Beamforming Network
BPSK	Binary Phase Shift Keying
BSA	Beam-Steering Antenna System
BTMA	Busy Tone Multiple Access
BW	Antenna beamwidth
CDMA	Code Division Multiple Access
CR	Constant Rate
CS	Carrier Sense
CSMA	Carrier Sense Multiple Access

CSMA/CA	Carrier Sense Multiple Access/Collision Avoidance
CTS	Clear-To-Send
DBTMA	Dual Busy Tone Multiple Access
DSP	Digital Signal Processing
FAMA	Floor Acquisition Multiple Access
FBN	Fixed Beamforming Network
FDMA	Frequency Division Multiple Access
FIFO	First In First Out
GTDMA	Generalized Time Division Multiple Access
HPBW	Half-Power Beamwidth
ISM	Industrial, Scientific, Medical band
LAN	Local Area Network
LES	Linear Equally Spaced
MAC	Medium Access Control
MACA	Multiple Access Collision Avoidance
MACAW	Mutliple Access, Collision Avoidance for Wireless
MAI	Multiple Access Interference
MBAA	Multiple Beam Adaptive Array
MHA	Minimum Hop Algorithm
PAN	Personal Area Networking
PC	Power Control
PHY	Physical Layer
RA-MHA	Reuse Adaptive Minimum Hop Algorithm
RC	Rate Control
RF	Radio Frequency
RRM	Radio Resource Management
RS	Rate Selection
RTS	Request-To-Send
SBA	Switched-beam Antenna
SDMA	Spatial Division Multiple Access
SIR	Signal-to-Interference Ratio
SINR	Signal-to-Interference plus Noise Ratio
SNR	Signal-to-Noise Ratio
STDMA	Spatial Time Division Multiple Access
TCS	Traffic Controlled Schedule
TDMA	Time Division Multiple Access
VR	Variable Rate
VR+PC	Variable Rate and Power Control
VSAT	Very Small Aperture Terminal
WLAN	Wireless Local Area Network
WMAN	Wireless Metropolitan Area Networks

E.3 Symbols

$\mathcal{A}$	Set of feasible links in the network.
$\boldsymbol{A}$	node-arc incident matrix.
$A_i(.)$	Antenna pattern used by node i.
A_{max}	Antenna maximum gain.
A_{RTS}	RTS reception area.
a_{sl}	Antenna side lobe attenuation.
B	Effective noise bandwidth.
$\boldsymbol{C}$	Network capacity Matrix.
$\boldsymbol{c}$	Assigned link-capacity.
$\mathcal{C}$	Network connectivity.
C_{ij}	Capacity of link (i, j).
d_{ij}	Distance between node i and node j.
d_{cap}	Capture range.
d_{cs}	Maximum range of carrier sensing.
d_{RTS}	Maximum range of error free reception of RTS.
D_{ij}	Packet delay over link (i, j).
$E[\cdot]$	Statistical expectation.
F_{sys}	Receiver noise figure.
G	Path gain matrix.
G_{ij}	Path gain on link (i, j).
G_{ml}	Path gain between transmitter on link m (node r) and the receiver on link l (node j).
$\mathcal{G}$	Directed network.
h_{ij}	Number of hops from node i to node j.
i	Node identification number.
(i, j)	Unidirectional link from node i to node j.
K_f	Schedules's period.
K	Number of colums in $\boldsymbol{S}$.
k	Boltzmann constant ($k = 1.38 \cdot 10^{-}23$).
L	Number of feasible links.
L_{ij}	Radio propagation path loss on link (i, j).
L_{max}	Maximum propagation path loss for connectivity.
l	link label for directed link (i, j).
M	Number of antenna elements.
m	link label for directed link (r, k).
N	Number of nodes that form a particular network.
$\mathcal{N}$	Set of nodes.
n_{ij}	Number of slots assigned to link (i, j).
$\mathcal{N}_i$	Number of neighbors to node i.
P_i	Transmission power level used by node i.
P_{ij}	Received power level at node j from node i's transmission.
P_l	Transmission power level on link l.

P_{Noise}	Background noise power level at the receiver.
P_{omni}	Transmission power with omnidirectional antenna.
P_{Th}	Carrier detection power level threshold.
$\boldsymbol{R}$	link-route incident matrix.
$\boldsymbol{r}$	Routing table.
$\boldsymbol{S}$	Time schedule.
(S, D)	source to destination.
s	Antenna selected sector.
$\boldsymbol{s}_k$	Set of links assigned to transmit during slot k.
T_0	Reference temperature ($T_0 = 290$K).
T_{ij}	Relative traffic load on link (i, j).
T	Relative Traffic Load matrix.
$\boldsymbol{\alpha}$	Fraction of time columns of $\boldsymbol{S}$ are active.
α	Path loss exponent.
Γ_{ij}	Signal-to-Interference plus Noise Ratio for a packet transmitted from node i to node j.
γ_0	Minimum SINR required for correct reception.
γ_{cs}	SNR for carrier sensing.
λ	Average total external traffic load.
$\boldsymbol{\Lambda}$	Average external traffic load.
λ_{ij}	Average traffic load through link (i, j).
λ^*	Maximum End-to-end throughput.
λ^*_{ij}	Maximum throughput for link (i, j).
ρ	Terrain smoothness parameter.
σ	Terrain height standard deviation.
θ_{ij}	Angle to node j as seen from node i.
ϕ_h	Antenna beamwidth.